DISSERTATION

submitted to the

Combined Faculties for the Natural Sciences and for Mathematics

of the Ruperto-Carola University of Heidelberg, Germany

for the degree of

Doctor of Natural Sciences

Presented by

Diplom-Biologist Katrin Bartels

born in Heidelberg, Germany

Oral-examination: _____

Conditional Knockout of the L-Type Voltage-gated Calcium Channel Cav1.3 via the FLEX Switch

Referees: Prof. Dr. Hilmar Bading

Prof. Dr. Dusan Bartsch

Hiermit erkläre ich gemäß § 8 (3) b) und c) der Promotionsordnung, dass ich die vorgelegte Dissertation selbst verfasst und mich dabei keiner anderen als der von mir ausdrücklich bezeichneten Quellen und Hilfen bedient habe.

I hereby declare according to § 8 (3) b) and c) of the doctoral degree regulations that I have written the submitted dissertation myself and in this process I have used no other sources or materials than those expressly indicated.

Mannheim, 23. Juli 2009 _____

Katrin Bartels

Acknowledgements

This work was performed at the Central Institute of Mental Health Mannheim (ZI) in the laboratory and under supervision of Prof. Dr. Dusan Bartsch.

Foremost, I would like to express my special thanks to Prof. Dr. Dusan Bartsch for giving me the opportunity to work for my Ph.D. thesis in his laboratory under excellent working conditions and for providing me the interesting project, for his helpful suggestions and his encouragement.

I am very grateful to Hilmar Bading for the supervision and the evaluation of my thesis.

Furthermore I would like to thank:
Kai Schönig for his scientific support regarding theoretical and technical aspects during the thesis.
Tillmann Weber for his mentoring in the first years, the introduction in the lab work and his ongoing scientific support.
Vera Baier for her helpful remarks concerning the immunofluorescence techniques and for her moral support.
Ariana Frömmig for generating the knockout animals.
Thorsten Lau for his scientific support in ES cell differentiation and microscopy.
Claus Beck and Uwe Leimer for the introduction in ES cell culturing.
Celine Lentrodt for her help during the cloning of the targeting construct.
All former and recent lab members for the scientific support, continuous help and for the nice time in the lab.
All animal care takers at the ZI, especially Peter Siegel, taking care of the transgenic mice.
All members of the graduate college 791 for their support in technical or scientific questions.
The graduate college 791 for the financial support.

Summary

L-type voltage-gated calcium channels (VGCCs) play a central role in regulating intracellular calcium (Ca^{2+}) concentrations, thereby contributing to signal transduction in many electrically excitable cells. The L-type channel $Ca_V1.3$ is expressed in neurons, in hair cells of the inner ear, in heart tissue and in pancreatic ß-cells. Mice with a ubiquitous deletion of the pore-forming α1-subunit ($Ca_V1.3^{-/-}$) showed that $Ca_V1.3$ has cardiac pace maker activity and controls the neurotransmitter release in the cochlea. Furthermore, Ca^{2+} influx through this channel was proposed to be involved in anxiety-related behaviour and in consolidation of contextually conditioned fear. Aim of my work was to gain more insight into the physiological role of $Ca_V1.3$ in different cell types and tissues, especially in neurons. To circumvent the phenotypes of the conventional knockout mice like deafness and heart insufficiency which may interfere with behavioural analysis, we decided to generate a conditional $Ca_V1.3\alpha1$ knockout mouse using the *Cre/loxP*-based FLEX switch system. By a *Cre*-mediated inversion of the targeted locus, this strategy coupled the ablation of the $Ca_V1.3\alpha1$ gene to the expression of the reporter gene eGFP, thereby mirroring the exact expression pattern of the endogenous $Ca_V1.3$ gene in all tissues. Heterozygous $Ca_V1.3$-GFP^{flex} mice were bred with "Cre-deleter" mice in which the *Cre* recombinase is ubiquitously expressed. We could show that, after *Cre* expression, the FLEX switch occurred efficiently *in vitro* and *in vivo* and that the reporter gene was driven by the endogenous $Ca_V1.3\alpha1$ promoter. Immunohistochemical analysis revealed eGFP expression in heart tissue as well as in many brain areas like the olfactory bulb, the cerebellum, superior colliculus, brain regions associated with emotional behaviour and sensory processing. In contrast to previously reported $Ca_V1.3$ expression, only moderate eGFP staining was found in hippocampal regions. An unexpected observation was the intense eGFP expression in the peri- and subventricular zone, suggesting a role of $Ca_V1.3\alpha1$ in adult neurogenesis and neural stem cell proliferation. In parallel, we crossed $Ca_V1.3$-GFP^{flex} mice to CaMKIIa-mice, thereby obtaining specific eGFP expression in the forebrain according to the expression of the CaMKIIa promoter.

This mouse model offers a great potential to further investigate the distribution and function of the L-type Ca^{2+} channel $Ca_V1.3$ in various tissues.

Zusammenfassung

L-typ spannungsgesteuerte Calciumkanäle (VGCC) spielen eine zentrale Rolle in der Regulierung der intrazellulären Ca^{2+} Konzentration und tragen somit zur Signalverarbeitung in vielen elektrisch erregbaren Zellen bei. Der L-typ Kanal Cav1.3 wird in Neuronen, in Haarzellen des Innenohrs, im Herzgewebe und in ß-Zellen des Pankreas exprimiert. Mäuse mit einer ubiquitären Deletion der porenbildenden α1-Untereinheit ($Cav1.3^{-/-}$) zeigten, dass der Cav1.3 Kanal Herzschrittmacher-Funktionen besitzt und die Neurotransmitter-Ausschüttung in der Cochlea kontrolliert. Des Weiteren wird dieser Kanal mit dem Ängstlichkeitsverhalten und Konsolidierung von kontextabhängig konditionierter Angst in Verbindung gebracht. Ziel dieser Arbeit war es, weitere Einblicke in die physiologische Rolle von Cav1.3 in verschieden Zelltypen und Geweben, im Besonderen in Neuronen, zu erhalten. Da konventionelle Knockout-Mäuse Phänotypen wie Taubheit und Herzinsuffizienz zeigen, die Verhaltensanalysen beeinträchtigen können, haben wir uns entschlossen, diese zu umgehen und eine konditionale Cav1.3α1 Knockout-Maus mithilfe des *Cre/loxP*-basierten „FLEX switch“ Systems zu generieren. Durch ein *Cre*-vermitteltes Invertieren des „gefloxten“ Allels koppelt diese Strategie die Inaktivierung des Cav1.3α1 Gens an die Expression des Reportergens eGFP, wodurch das exakte Expressionsmuster des endogenen Cav1.3α1 Gens in allen Geweben gespiegelt wird. Heterozygote Cav1.3-GFP^{flex} Mäuse wurden mit “Cre-Deleter”-Mäusen verpaart, welche die *Cre*-Rekombinase ubiquitär exprimieren. Wir konnten zeigen, dass nach *Cre*-Expression der FLEX „switch“ *in vitro* und *in vivo* effizient erfolgte und dass das Reportergen von dem endogenen Cav1.3α1 Promotor getrieben wurde. Immunhistochemische Analysen ließen eGFP-Expression im Herzgewebe und vielen Hirnarealen erkennen, wie dem olfaktorischen Bulbus, Cerebellum, Superior Colliculus und Regionen, die mit emotionalem Verhalten und sensorischer Verarbeitung assoziiert sind. Im Gegensatz zu der bekannten Cav1.3 Expression, zeigte sich in den hippokampalen Hirnregionen nur eine gemäßigte eGFP-Färbung. Eine unerwartete Beobachtung war die intensive eGFP-Expression in der peri- und subventrikulären Zone, was auf eine Funktion von Cav1.3 in adulter Neurogenese und neuronaler Stammzellproliferation hinweisen könnte. Parallel verpaarten wir Cav1.3-GFP^{flex} Mäuse mit CaMKIIa-Mäusen, wobei wir eine spezifische eGFP-Expression im Vorderhirn in Übereinstimmung mit der Expression des CamKIIa-Promoters ausmachen konnten.

Das Cav1.3-GFP^{flex} Mausmodel stellt somit ein großes Potential dar, die Funktion and Verbreitung des L-typ Kalziumkanals Cav1.3 weiter aufzuklären.

Contents

1 Introduction

1.1 Calcium as Second Messenger

Cytosolic calcium (Ca^{2+}) is a ubiquitous intracellular signal which is essential in many signal transduction pathways, controlling a wide range of cellular activities. The significance of Ca^{2+} in cell biology was recognized in 1883 by Sydney Ringer. He demonstrated that the presence of Ca^{2+} in the bathing solution was necessary to maintain contraction of frog heart muscles (Ringer, 1883). This observation opened an entire field of studies regarding the role of calcium in molecular, cellular and organismal function. By the end of the 19th century the list of described functions for calcium included its role in egg fertilization and development of tissues (Ringer, 1890) and conduction of nerve impulse to muscle, cell adhesion and plant growth. An important discovery in the 20th century was the identification of change in the concentration of free Ca^{2+} ions in response to hormone treatment. In 1947 Lewis Victor Heilbrunn demonstrated by injecting various cations into frog muscle cells that only calcium caused muscle fibre to contract (Heilbrunn and Wiercinski, 1947). Later, Sandow proposed the term excitation-contraction coupling for this phenomenon (Sandow, 1965).

Calcium ions play a major role in controlling the function of all cells in the body by acting as carriers of intracellular messages. Cells receive external signals through neurotransmitters and hormones which bind to receptors on their surface. These signals are transferred to the inside of the cell by opening channels in the cell membrane, allowing external Ca^{2+} ions to enter the cell, or by releasing Ca^{2+} ions from internal stores (endoplasmic reticulum, ER) into the cytoplasm. Calcium ions as second messenger mediate a wide range of cellular functions as muscle contraction, neurotransmitter and hormone release, metabolism, cell division and differentiation.

In the evolution of eukaryotic cells, the calcium ion has been selected as a second messenger in preference to other intracellular ions like sodium, potassium, chloride or magnesium ions (Carafoli and Penniston, 1985). As a double charged ion, Ca^{2+} binds more tightly to the protein binding sites than single charged ions of sodium, potassium and chlorine (Hardingham and Bading, 1998). Furthermore, it is energetically favourable for the cell to utilise calcium as a second messenger. The concentration of free calcium ions in the cytoplasm of a resting cell is extremely low (~100 nM), several orders of magnitude below the

extracellular Ca^{2+} concentration. For this reason a relatively small amount of calcium needs to pass into the cell to increase significantly the intercellular Ca^{2+} concentration. Consequently, to return the ion concentration to the basal level, relatively little energy is required to pump calcium ions either out of the cell or into internal stores like the ER.

Many different cell types rely on an elevation of intracellular Ca^{2+} to activate essential biological function. Calcium is, for example, immensely important in the earliest stages of development – in fertilization. When the sperm enters the egg, it causes a local increase in cytosolic Ca^{2+}, which spreads through the cell in a wave. This oscillation activates the egg to start development (Shen, 1995). Ca^{2+} is also required for acute cellular responses, such as contraction or secretion. Released by internal stores, Ca^{2+} mediates the contraction of muscles by interacting with troponin and tropomyosin (Eisenberg and Hill, 1985). Ca^{2+} is the major component of the signalling pathways that regulate epithelial cell secretion, including both discharge of proteins and regulation of transepithelial secretion of salts and water, and carbohydrate metabolism in the liver, including glycogenolysis and gluconeogenesis (Siegel et al., 1999). Furthermore, Ca^{2+} ions play a role in necrosis and apoptosis. The earliest change in cells undergoing apoptosis is a rapid, sustained increase in intracellular calcium concentrations (Schwartzman and Cidlowski, 1993). Inhibition of this increase prevents stimulus-induced cell death in various cell types. Ca^{2+} influx through extrasynaptic NMDA receptors causes a loss of mitochondrial membrane potential and cell death in neurons (Hardingham et al., 2002). Also T-lymphocytes rely on an elevation of intracellular calcium to trigger their activation in response to antigen presentation to the T-cell receptor (Cardenas and Heitman, 1995). In neurons, Ca^{2+} plays a pivotal role in the reception of signals (input), signal transmission (output), the regulation of neuronal excitability as well as the cellular changes that underlie synaptic plasticity and learning and memory. To support long-term cellular changes, calcium signalling has a central role in regulation of activity-dependent gene expression. Calcium-mediated gene expression can lead to a variety of enduring changes in cell functions, as modifications of protein synthesis underlie such diverse processes like cell survival, differentiation and synaptic plasticity (Ghosh et al., 1994).

1.1.1 Ca^{2+} Signalling

Calcium signalling comprises molecular and physiological events that link an external stimulus to the expression of intracellular response through an increase in cytoplasmic Ca^{2+} concentration. The external stimulus can be neurotransmitters, growth factors or hormones. It is known that increase in cytosolic Ca^{2+} concentration is temporally and spatially complex. Depending on cell type and nature of stimulation, Ca^{2+} signals can be transient or oscillatory, and can occur as localised or global event (Bootman et al., 2001b).

1.1.1.1 Release of Ca^{2+} from Internal Stores

Ca^{2+} is stored intracellularly in specialised compartments such as the endoplasmic reticulum (ER) and the sarcoplasmic reticulum (SR). The binding of many hormones and growth factors to specific receptors on the plasma membrane leads to the activation of phospholipase C (PLC) which catalyses the hydrolysis of phosphatidylinositol 4,5-biphosphate (PIP_2) to produce the intracellular messengers inositol 1,4,5-triphosphate (IP_3) and diacylglycerol (DAG) (Bootman et al., 2001a). IP_3 diffuses into the cell interior and binds to specific IP_3 receptors (IP_3Rs) in the ER/SR. After conformational change the receptors are opened, allowing the Ca^{2+} that is stored in the ER/SR at high concentrations to enter the cytoplasm.
Beside IP_3, a variety of established intracellular messengers exist which increase intracellular Ca^{2+} concentration: cyclic adenosine 5′-diphosphoribose (cADPR) which activates ryanodine receptors (RyRs), nitric oxide (NO), hydrogen peroxide (H_2O_2), diacylglycerol (DAG), arachidonic acid (AA), sphingolipids and Ca^{2+} itself (Bootman et al., 2002). Similar to the IP_3R are the ryanodine receptors (RyRs), a class of intracellular Ca^{2+} release channels found in excitable tissues as neurons and muscles. These receptors are named after the plant alkaloid ryanodine that binds to the channel with high affinity. RyRs mediate the calcium release from internal Ca^{2+} stores, which is an essential step in muscle contraction. In cardiac muscles, channel activation occurs via calcium-induced calcium release (CICR), a mechanism by which local elevations of intracellular Ca^{2+} are amplified by Ca^{2+} release from ryanodine-sensitive Ca^{2+} stores (Fabiato, 1983). A recent study pointed out that the ryanodine receptor type 2 (RyR2) even interacts with the L-type calcium channel $Ca_V1.3$ with implications in translating synaptic activity into alterations in gene expression (Kim et al., 2007).

1.1.1.2 Calcium Influx through Voltage- or Ligand-Gated Ion Channels

Extracellular Ca^{2+} can enter the cell via several different types of Ca^{2+} influx channels, which can be grouped on the basis of their activation mechanism. Voltage-gated Ca^{2+} channels (VGCC) are found in a variety of excitable cell types, including neurons, muscles and endocrine and neuroendocrine cells (Miller, 1992). Five different types of voltage-gated Ca^{2+} channels could be classified, based on their electrophysiological and pharmacological properties, as L-, T-, N-, P-, Q- and R-type (Catterall, 2000). These channels can be activated by membrane depolarization, either by a propagated action potential or by the opening of other ligand-gated channels. Calcium influx through VGCC is linked to many Ca^{2+} dependent processes like contraction of smooth muscles, secretion, neurotransmitter release and gene expression.

Besides VGCC, Ca^{2+} ions enter the cell through ligand-gated receptors, such as N-methyl-D-aspartate (NMDA) and α-amino-3-hydroxy-5-methyl-4-isoxazolepropionic acid (AMPA) glutamate receptors. Upon binding glutamate the NMDA receptor allows the influx of divalent cations as Ca^{2+} and Na^{+}. The elevation of cytoplasmic Ca^{2+} may lead to the transient activation of a variety of Ca^{2+}-activated enzymes, including Ca^{2+}/calmodulin-dependent protein kinase II, calcineurin, PKC and phospholipase A_2. The Ca^{2+} influx through these receptors is thought to be a necessary first step for long-term potentiation (LTP), a form of synaptic plasticity (Ghosh et al., 1994). Also AMPA glutamate receptors can contribute to Ca^{2+} influx. The permeability of the AMPA receptor to calcium is governed by the GluR2 subunit; AMPA receptors lacking this subunit are permeable to Ca^{2+}, Na^{+} and K^{+} (Geiger et al., 1995).

1.1.2 Ca^{2+} Signalling in Neuronal Cells

Calcium plays an important role in regulating a variety of neuronal processes like neurotransmitter release, generation of dendritic Ca^{2+} spikes, neuronal plasticity or regulation of activity-dependent gene expression. Like in other cells, neurons use multiple mechanisms to increase the intracellular calcium concentration.

One function of calcium in neurons is the propagation of an electrical signal from one neuron to another. An action potential, which travels through the neuron, will arrive the axon where it triggers calcium-mediated neurotransmitter release. This neurotransmitter release is

mediated by N-type ($Ca_v2.2$) and P/Q-type ($Ca_v2.1$) VGCCs, which are primarily located in the presynaptic terminals (Dunlap et al., 1995). Strong depolarization by an action potential causes these channels to open and allow influx of Ca^{2+}, initiating vesicle fusion with the presynaptic membrane and releasing their contents into the synaptic cleft. The neurotransmitter causes again an electrical change in the postsynaptic neuron through the activation of neurotransmitter-gated ion channels. Thus, calcium is involved in coupling action potentials to neurotransmitter release and enables information to be passed from neuron to neuron.

Calcium is a critical component in signalling processes from synapse to nucleus. Increase in intracellular calcium concentration activates various signalling pathways that lead to the expression of genes essential for dendritic development, neuronal survival and synaptic plasticity. It is well established that in response to physiological synaptic activity Ca^{2+} entry through both glutamate-gated NMDA receptors and L-type Ca^{2+} channels initiates nuclear signalling to the transcription factor CREB (cAMP response-element binding protein) (Bito et al., 1996; Deisseroth et al., 1996). CREB is strongly implicated in synaptic plasticity, long term memory and long-lasting, protein synthesis dependent LTP (Kandel, 2001). CREB is activated by phosphorylation on its Ser 133 residue, which allows recruitment of CREB binding protein (CBP) and initiation of transcription (Chrivia et al., 1993). The synapse-to-nuclear signalling involves different pathways, including CREB activation through the CaM-CaMKIV, the Ras/MAPK and the CaM/AC/PKA pathway (Deisseroth et al., 2003). Additionally, Ca^{2+} itself may enter the nucleus and activate nuclear kinases that lead to CREB phosphorylation in the nucleus (Hardingham et al., 2001).

The mode of calcium entry determines which signalling pathways are activated and thus specifies the cellular response. Calcium influx specifically through L-type VGCCs triggered by KCl (50-90 mM) depolarization or high-frequency (50 Hz) stimulation appears crucial for stimulating CREB phosphorylation and subsequent expression of the immediate early gene *c-fos* (Hardingham et al., 1999; Zhao et al., 2007). Furthermore, blocking the L-type channels by dihydropyridine (DHP) selectively eliminates CREB phosphorylation (Dolmetsch et al., 2001). Among the L-type VGCCs, $Ca_v1.2$ and $Ca_v1.3$ are the most widely expressed L-type channels in neurons (Lipscombe et al., 2004). However, little is known about the neuronal function of $Ca_v1.3$, as most molecular studies of L-type calcium channels concentrate on

$Ca_V1.2$. Due to the lack of pharmacological tools to distinguish $Ca_V1.2$ and $Ca_V1.3$ subtypes it is difficult to dissect their specific roles. Here we want to elucidate the neuronal function and distribution of $Ca_V1.3$ in the CNS using a transgenic mouse model.

1.2 The L-type Voltage-gated Calcium Channel $Ca_V1.3$

Voltage-gated calcium channels (VGCCs) are transmembrane proteins in electrically excitable cells, which play a key role in the regulation of intracellular Ca^{2+} concentration. Their activity is essential to couple electrical signals on the cell surface to physiological events in the cell. They are activated upon membrane depolarization and mediate calcium influx down an electrical gradient in response to action potentials and sub-threshold depolarization signals. Ca^{2+} entering the cell through VGCCs serves as second messenger of electrical signalling, initiating a number of intracellular processes such as muscle contraction, secretion, neurotransmitter and hormone release and gene expression. VGCCs are members of a gene superfamily of transmembrane ion channel proteins that also include Na^+ and K^+ channels (Yu and Catterall, 2004). They are multi-subunit complexes, comprising a α_1, a α_2-δ, a β and, in some cases, a γ subunit. The Ca^{2+} channels can be classified according to their electrophysiological and pharmacological properties.

1.2.1 Calcium Channel Diversity

The pharmacological and electrophysiological diversity arises primarily from the existence of multiple forms of α_1 subunits. Mammalian α_1 subunits are encoded by at least ten distinct genes, nine expressed in the nervous system. In 1994, Birnbaumer et al. proposed a unified nomenclature in which the α_1 subunit was referred to as α_{1S} for the original skeletal muscle isoform and α_{1A} to α_{1I} for those discovered subsequently (Birnbaumer et al., 1994). More recently, a rational nomenclature was adopted, defining the calcium channels into three structurally and functionally related subfamilies Ca_V1, Ca_V2 and Ca_V3 (Ertel et al., 2000). Based on their electrophysiological properties, voltage-gated calcium channels can be divided into high voltage-activated (HVA) and low voltage-activated (LVA) channels (Fig. 1). Among the HVA channels there are two groups (L-type and non-L-type channels) based on the sensitivity to dihydropyridines (DHPs). L-type ("Long-lasting") VGCCs are formed

by the Cav1 family, which comprise the isoforms Cav1.1, Cav1.2, Cav1.3 and Cav1.4, containing α1S, α1C, α1D and α1F subunits, respectively. The first L-type Ca^{2+} currents were measured in cardiac myocytes (Reuter, 1967). They require a strong depolarization and are long-lasting which contributed to their name L-type (Nowycky et al., 1985). Furthermore, they can be characterized by large single-channel conductance, slow voltage-dependent inactivation and regulation by cAMP-dependent protein phosphorylation pathways. One special property of L-type currents is their high sensitivity to calcium antagonist drugs as dihydropyridines (DHPs), phenylalkylamines and benzodiazepines (Reuter, 1983), even though there are differences among the L-type channel isoforms in their affinity for DHPs (Lipscombe et al., 2004). L-type VGCCs display a broad expression profile. Whereas Cav1.1 and Cav1.4 expression is restricted to skeletal muscles and the retina, respectively, the other two channels are found in a variety of tissues. Cav1.2 and Cav1.3 channels are expressed in neurons, neuroendocrine cells (including pancreatic ß-cells), sensory cells such as retinal neurons and cochlear hair cells, in the cardiovascular system and in smooth muscle cells (Striessnig et al., 2006).

Non-L-type HVA channels belong to the Cav2 family (Cav2.1 – Cav2.3) containing the subunits α_{1A}, α_{1B} and α_{1E}. They mediate P/Q-type, N-type and R-type calcium currents, respectively. P-type ("Purkinje") currents were first recorded in Purkinje neurons (Llinas et al., 1989) and can be distinguished by high sensitivity to the spider toxin ω-agatoxin IVA. N-type ("non-L-type" or "Neural") currents were distinguished by their intermediate voltage dependence and rate of inactivation – more negative and faster than L-type but more positive and slower than T-type (Nowycky et al., 1985). They are primarily found in presynaptic terminals and are involved in neurotransmitter release. R-type ("Residual") currents in cerebellar granule cells are resistant to the subtype-specific organic and peptide Ca^{2+} channel blockers (Randall and Tsien, 1995). Non-L-type currents also require strong depolarization for activation. Unlike L-type channels they are relatively unaffected by dihydropyridines and other L-type channel specific drugs but are blocked by specific polypeptide toxins from snail and spider venoms (Catterall et al., 2005). They are mainly expressed in neurons where they initiate neurotransmitter release and mediate Ca^{2+} entry into dendrites and cell bodies.

Low-voltage activated channels include the Cav3 subfamily (Cav3.1–Cav3.3), which contains channels with the subunits α_{1G}, α_{1H} and α_{1I}, mediating T-type ("Transient") currents. T-type currents have transient kinetics and are activated at much more negative potential than L-type currents. They inactivate rapidly, deactivate slowly and have small single-channel conductance (Nowycky et al., 1985). They are resistant to both organic antagonist drugs like DHPs and to snake and spider toxins. T-type currents are expressed in a variety of cells, mainly in neurons and cardiac myocytes, where they are involved in pacemaking and controlling patterns of repetitive firing.

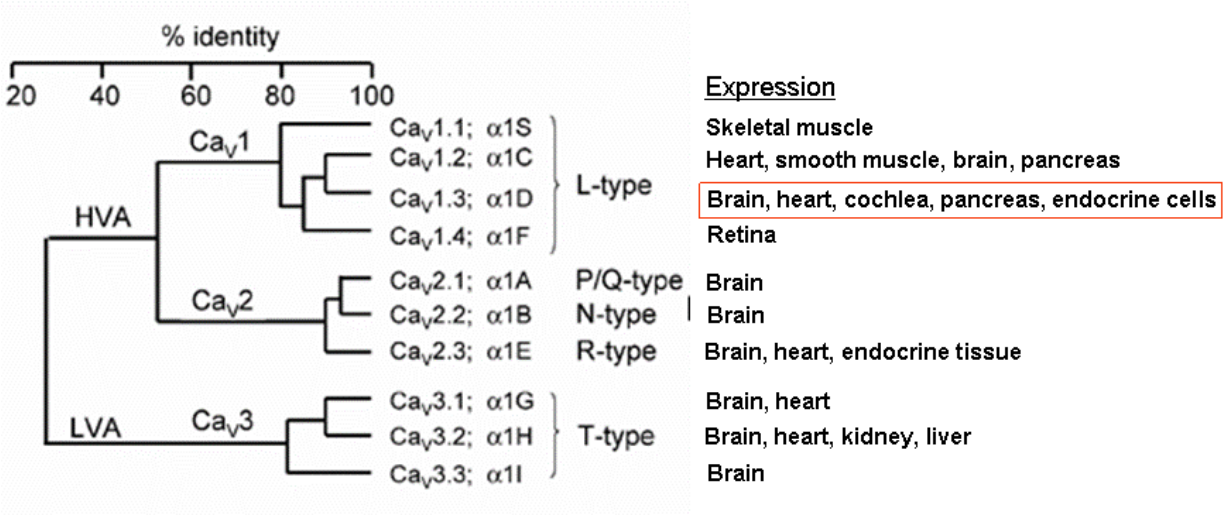

Fig. 1: Phylogenic tree of voltage-gated calcium channel α1 subunit, showing the per cent identity between the different cloned calcium channels.

1.2.2 Structural Organization of L-type Cav1.3 Channels

L-type VGCCs have been first purified from the transverse tubule membrane of skeletal muscle (Curtis and Catterall, 1984). Biochemical analyses have characterized them as heteromeric proteins composed of 4-5 subunits encoded by multiple genes: the pore forming, transmembrane α1 subunit of ~ 190-250 kDA, a transmembrane, disulfide-linked dimer of α2 and δ subunits, an intracellular β subunit and, in some tissues, a transmembrane γ subunit. The pore-forming α1 subunit consists of four homologous repeats (I-IV), each of which composed of six transmembrane segments (S1-S6) (Catterall, 2000) (Fig. 2). The S4 segments of each homologous domain serve as voltage sensors. Positively charged residues on one side of each S4 α-helix initiate voltage-dependent conformational changes from non-conducting to conducting states of the channel (Bezanilla, 2002). The asymmetric channel

pore is formed by the segments S5 and S6 together with the hydrophobic linker sequence in between which is called pore (P-) loop. Each of these loops contains a conserved glutamate residue (EEEE) as selectivity filter and for permeation of Ca^{2+} ions (Yang et al., 1993). The P-loop can either bind one Ca^{2+} ion with high affinity or two ions with low affinity. Thus, monoligand binding with high affinity for Ca^{2+} provides the molecular basis for selectivity. Permeation, in contrast, requires at least two ions in the pore, since double occupancy destabilizes the complex and allows one of the bound Ca^{2+} ion to dissociate into the cytoplasm (Striessnig, 1999). The L-type specific drugs dihydropyridines, phenylalkylamines and benzodiazepines bind to three separate sites of the α1 subunit, namely the IIIS5, IIIS6 and IVS6 transmembrane segments (Hockerman et al., 1997). Consequently, drug binding occurs near the pore and close to the calcium selectivity filter.

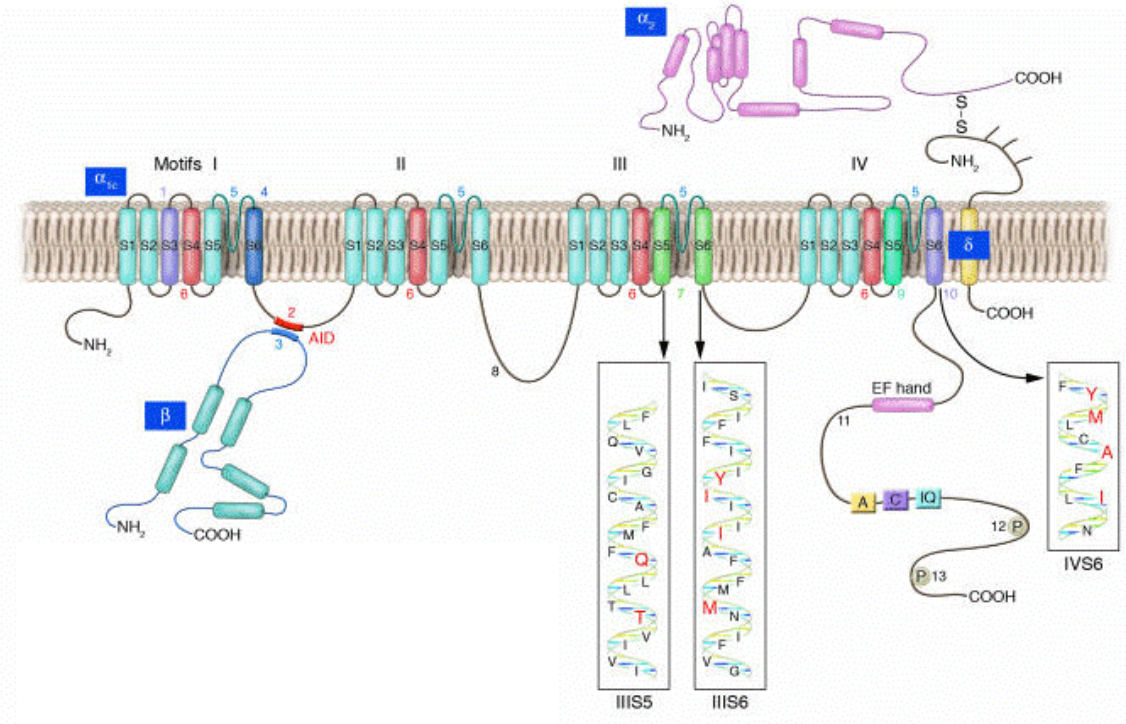

Fig. 2: Structural organisation of L-type VGCCs. The primary structure of the α1 subunit is composed of four homologous repeats (motifs I – IV), each of which consists of six transmembrane segments (S1-S6). Adopted from Bodi I. et al., JCI, 2005

Expression of the α_1 subunit is sufficient for the functionality of the channels, but co-expression of α_2-δ and especially the β subunit enhances the level of expression, kinetics and voltage dependence of Ca^{2+} channel current (Miller, 1992). The α_2-δ subunit is closely

associated with the α_1 subunit by surface interaction. The α_2-δ subunit is a glycosylated protein which is highly conserved in most tissues. The transmembrane δ subunit anchors the extracellular α_2 protein by disulfide bridges to the plasma membrane (Hofmann et al., 1994). The δ peptide is sufficient to stabilize the gating properties of the channels, whereas α_2 is required to stabilize DHP binding to the α_1 subunit (Gurnett et al., 1997). The intracellular β subunit is the most important subunit for fine-tuning of L-type VGCC activity. It also stabilizes the pore region and facilitates conformational changes which open the channel once the voltage-sensor movement is completed. Moreover, all four isoforms of the β subunit (β_{1b}, β_{2a}, β_4, and β_4) increase L-VGCC membrane density by modulating α1 subunit expression (Neely et al., 1993). The γ subunit was first found only in skeletal muscle calcium channels. However, recently also a neuronal γ subunit isoform has been identified (Striessnig, 1999). Although these auxiliary subunits modulate the properties of the channel complex, the pharmacological and electrophysiological diversity of calcium channels arises primarily from the existence of multiple α_1 subunits.

1.2.3 L-type Cav1.3 Channel Properties

1.2.3.1 Ca_V1.3 Gene

The human Cav1.3α1 gene *CACNA1D* is located at chromosome 3p14.3 and spans approximately 400 kb of human genomic sequence (Seino et al., 1992). It is encoded by up to 52 exons, and at least seven of these exons can be alternatively spliced. Sites of alternative splicing are the exons 8a/8b in transmembrane IS6, exon 11 in the intracellular loop I-II, exons 31a/31b of transmembrane IVS3, exon 32 in the IVS3-IVS4 extracellular linker, and exon 42a in the C-terminus (Lipscombe et al., 2002). The murine gene (*Cacna1d*) for the Cav1.3α1 subunit is mapped to a position 7.5 cM proximal to Np-1 of mouse chromosome 14 (Chin et al., 1991). Depending on the transcript variant, the murine Cav1.3α1 gene comprises 47-49 exons and spans over 311-450 kb. Two forms of exon 1 are known, an adult exon 1a and an embryonic exon 1b (Klugbauer et al., 2002). Alternative splicing of rodent Cav1.3α1 has been described in hair cells, the rat heart, rat neurons, and endocrine cells (Kollmar et al., 1997; Koschak et al., 2001; Safa et al., 2001; Takimoto et al., 1997). Presently, only a limited number of studies address the functional significance of alternative splicing of Cav1.3α1. The

splice variant α1-D_{8A}, containing exon 8a sequence in repeat I, yielded α1-D protein and L-type currents, whereas no intact protein and L-type currents were observed when exon 8b was expressed (Koschak et al., 2001). The splice variant Ca_V1.3a with the long C-terminal contains PDZ-binding motifs which are required for interaction with the PDZ domain of the scaffolding protein Shank and Erbin (Calin-Jageman et al., 2007; Zhang et al., 2005a).

1.2.3.2 Ca_V1.3 Expression and Localization

The expression pattern of each $Ca_V\alpha$1 gene is tightly regulated, depending on cell-specific and developmental factors that, together with characteristic structural features, permit coupling to specific effector proteins and second messenger systems. Ca_V1.3 is expressed in neurons (Hell et al., 1993), the cardiac atrial myocytes and pacemaker cells (Takimoto et al., 1997), pancreatic ß-cells (Iwashima et al., 1993), in cochlear hair cells (Green et al., 1996) and, possibly, even in immune cells (Gomes et al., 2004). This expression pattern is very similar to the α1-C subunit containing Ca_V1.2 VGCC; the two isoforms are expressed even in the same cells. In the brain, Ca_V1.3 is less abundant than Ca_V1.2, as in a study by Hell et al. antibodies against the α1-D subunit immunoprecipitated 20% and antibodies against the α1-C subunit immunoprecipitated 75% of all L-type Ca^{2+} channels solubilised from rat cortex and hippocampus. Nevertheless, the presence of Ca_V1.3/α1-D L-type Ca^{2+} channels was demonstrated in most brain regions, including cortical neurons, hippocampal pyramidal cells, dentate granule neurons, cerebellar Purkinje cells, many interneurons and several other classes of central neurons (Hell et al., 1993). Within individual neurons, Ca_V1.3 channels are distributed over the surface of the somata with accumulation at the base of major dendrites and a diminishing density on more distal regions of dendrites. The relatively high concentration of Ca_V1.3 L-type channels in cell bodies and proximal dendrites suggests an involvement of these channels in general cellular functions like regulation of cellular signalling pathways and gene function.

1.2.3.3 Ca_V1.3 Pharmacological Properties and Kinetics

The traditional view of L-type calcium channels is that they are high-voltage activating and have slow activation kinetics. Their unique high sensitivity to dihydropyridine agonists and

antagonists has proved critical for their identification in physiological assays and for their biochemical isolation. Contrary to the general characteristics of L-type channels, Cav1.3 channels start to activate at about -55 mV, a voltage that is approximately 20-25 mV more hyperpolarized as compared to Cav1.2. This low-threshold activation is a prominent feature of all Cav1.3 clones isolated, independent of tissue of origin and of auxiliary subunits (Koschak et al., 2001; Xu and Lipscombe, 2001). Also the activation kinetics differs from the prevalent textbook view, as Cav1.3 L-type currents open with rapid kinetics. In addition to biophysical criteria, L-type calcium channels are defined by their high sensitivity to dihydropyridine (DHP) agonists and antagonists. However, Cav1.3α1 currents are ~ 20-fold less sensitive to inhibition by nimodipine compared to Cav1.2α1 (Xu and Lipscombe, 2001). Inhibition of Cav1.3 channels by DHPs seems to be state-dependent: the inhibition is enhanced at depolarized membrane potentials that open the channel, and reduced at hyperpolarized membrane potentials (Berjukow et al., 2000).

These properties of fast, sub-threshold calcium signalling strongly implicate Cav1.3 L-type channels in driving oscillatory activity. Cav1.3 channels could also mediate sustained calcium entry during action potential plateaus, as calcium-dependent and voltage-dependent inactivation is minimal at depolarized voltages (Lipscombe et al., 2004). These characteristics make Cav1.3 Ca^{2+} channels to be activated in response to physiological stimuli that do not open other L-type channels.

1.2.3.4 $Ca_V1.3$ Interactions

In recent years diverse studies revealed the existence of binding motifs in the Cav1.2α1 and Cav1.3α1 subunit which can associate with adaptor proteins. These interactions play an important role for Ca^{2+} signalling mediated by L-type calcium channels.

First interaction studies were done on Cav1.2 channels. The α1C subunit contains an isoleucin-glutamine ("IQ") motif in the C-terminus that binds Ca^{2+}/calmodulin which is critical for MAPK-dependent CREB phosphorylation and CRE-dependent transcription (Dolmetsch et al., 2001). In addition to the IQ motif, the C-termini of both Cav1.2 (α1C) or Cav1.3 (α1D) channels contain unique class I PDZ [postsynaptic density-95 (PSD-95)/Discs large/zona occludens-1 (ZO-1)] interaction sequences, that have been shown to associate with various scaffolding proteins that contain PDZ domains (Kurschner et al., 1998; Kurschner

and Yuzaki, 1999). Association with PDZ proteins plays an important role in coupling L-type VGCCs to phosphorylation of nuclear CREB (Weick et al., 2003). It has been shown that L-type channels containing the $Ca_V1.3$ subunit regulate CREB activation via association with the Shank PDZ domain (Zhang et al., 2005a). $Ca_V1.3$ channels exist in two splice variants that differ at their C-terminus (Safa et al., 2001): a short isoform ($Ca_V1.3b$) that terminates immediately after the calmodulin-binding IQ (isoleucin-glutamine) motif, and a long splice variant ($Ca_V1.3a$) that extends additional 512 amino acids containing a PDZ binding motif. Zhang et al. demonstrated that $Ca_V1.3a$ interacts with the postsynaptic adapter protein Shank via the PDZ interaction sequence ITTL as well as a proline-rich region in the C-terminus that bind to the Src homology 3 (SH3) domain of Shank. In cultured hippocampal neurons, the presence of the Shank-binding motifs in $Ca_V1.3a$ sequence is both necessary and sufficient for synaptic clustering of $Ca_V1.3$ L-type VGCCs. The association of $Ca_V1.3$ and Shank plays also an important role in $Ca_V1.3$-mediated signalling to CREB especially at low levels of stimulation. Compared to $Ca_V1.2$ Ca^{2+} channels, $Ca_V1.3$ channels activate at significantly more hyperpolarized membrane potential (Koschak et al., 2001; Xu and Lipscombe, 2001). This unique voltage dependence of activation implies that $Ca_V1.3$ L-type Ca^{2+} channels mediate cellular processes that depend on calcium influx in response to relatively small membrane depolarization.

Moreover, a recent study indicated that interactions of $Ca_V1.3$ may also be critical to inner hair cell functions in the cochlea. A Ca^{2+}-dependent association of the II-III cytoplasmic loop of $Ca_V1.3$ and the C2 domain of otoferlin may mediate the regulation of hair cell synaptic exocytosis by otoferlin (Ramakrishnan et al., 2009). This could be of great importance, since a mutation in the C2D domain that causes deafness in humans ablates the binding to $Ca_V1.3$.

1.2.3.5 Physiological Functions of $Ca_V1.3$

$Ca_V1.3$ and $Ca_V1.2$ L-type channels display a very similar expression pattern. Even though $Ca_V1.3$ channels are less sensitive to dihydropyridine agonists and antagonists than $Ca_V1.2$, currently available L-type calcium channels blockers are unsuitable pharmacological tools for dissecting the functions of $Ca_V1.3$ and $Ca_V1.2$. The physiological properties of $Ca_V1.3$ could be first revealed by conventional knockout mice ($Ca_V1.3^{-/-}$) lacking the α1D subunit (Platzer et al., 2000). The knockout indicates that $Ca_V1.3$ channels control neurotransmitter

release in the cochlea, since Cav1.3$^{-/-}$ mice are deaf due to the complete absence of L-type currents in cochlear inner hair cells (IHCs) and degeneration of outer (OHCs) and inner hair cells between postnatal days 14 and 35 (Michna et al., 2003). Patch clamp analysis of IHCs revealed that Cav1.3α1 contributes more than 90% of VGCC currents. Electrocardiogram recordings in these mice exhibited sinoatrial node (SAN) dysfunction with bradycardia and arrhythmia which shows that Cav1.3 L-type channels are required for generation of cardiac pacemaking activity (Mangoni et al., 2003). The role of Cav1.3 in pancreatic ß-cells for Ca^{2+} currents and insulin secretion has been discussed controversially. Three different mouse models as well as biochemical data have provided evidence both for a role of Cav1.3 in ß-cells (Namkung et al., 2001; Yang et al., 1999) as well as against it (Barg et al., 2001). Nevertheless, more recent data support the view that Ca^{2+} entry involved in insulin secretion is mediated by Cav1.2 channels (Schulla et al., 2003; Sinnegger-Brauns et al., 2004).

1.2.3.6 Role of $Ca_V1.3$ in Brain Function and Behaviour

The most abundant L-type calcium channel subtypes expressed in the brain are encoded by the Cav1.2 and Cav1.3 subunit. As mentioned above, L-type calcium channels are important in translating synaptic activity into alteration in gene expression and neuronal function by mediating the activation of the transcription factor CREB. CREB is involved in learning and memory in general and formation of long-term fear memories in particular. In addition, its role was implied in depression-like states and the long-term effects of antidepressants (Blendy, 2006). The role of Cav1.3 in signalling to CREB could be directly confirmed in primary cultures of cortical, hippocampal and striatal medium spiny neurons of Cav1.3$^{-/-}$ mice. Cav1.3 channels preferentially mediate nuclear CREB signalling in hippocampal neurons at low, but not at high, levels of stimulation which reflects the ability of these channels to open at lower levels of depolarization (Zhang et al., 2006).

L-type channels affect neuronal resting potential and stabilise plateau potentials in many neurons. Direct evidence that such upstate potentials and the subsequent spontaneous firing activity are mediated by Cav1.3 channels has been obtained in striatal spiny neurons of Cav1.3 knockout mice, where this activity was completely absent (Olson et al., 2005). This correlates well with the observation made by Chan et al. who showed that Cav1.3 channels are required for pacemaking activity especially in dopaminergic neurons which could be

possibly connected to Parkinson's disease (Chan et al., 2007). The reliance on $Ca_V1.3$ increases with age, as juvenile dopaminergic neurons use pacemaking mechanisms common to other neurons, mediated by Na^+ and HCN channels. DHP-mediated blocking of $Ca_V1.3$ channels in adult neurons induced a reversion to the juvenile form of pacemaking. This "rejuvenation" protects dopaminergic neurons in both *in vitro* and *in vivo* animal models of Parkinson's disease.

By conducting low-voltage activated L-type Ca^{2+} currents $Ca_V1.3$ channels can shape neuronal firing patterns. This reveals a key role of $Ca_V1.3$ in neuronal activity and plasticity, and prompts questions about the physiological role of this channel for neuronal function and animal behaviour *in vivo*. An interesting approach to study and dissect the *in vivo* function of $Ca_V1.2$ and $Ca_V1.3$ is a transgenic mouse model ($Ca_V1.2DHP^{-/-}$), whose $Ca_V1.2\alpha1$ subunit lacks high sensitivity to DHP agonists and antagonists (Sinnegger-Brauns et al., 2004). This model allows investigating the direct DHP effect on $Ca_V1.3$ channels. By using c-fos activation as a marker for neuronal activation, the neuronal circuits stimulated by $Ca_V1.3$ activation could be displayed. Significant Fos expression induced by DHP agonist BayK 8644 was detectable only in a small subset of brain regions, particularly in the central amygdala, the BNST (bed nucleus of the stria terminalis), the PVN (paraventricular hypothalamic nucleus), the lateral preoptic area, in the locus coeruleus and in the nucleus of solitary tract (Hetzenauer et al., 2006). This indicates that selective stimulation of $Ca_V1.3$ restricts neuronal activation to a specific set of limbic, hypothalamic and brainstem areas, which are associated with brain functions concerning integration of emotion-related behaviour and processing of stress. Some of these regions, such as the amygdala, the PVN, the BNST or the ventral striatum, are part of anatomical circuits associated with depression-related behaviour (Manji et al., 2001). These findings are supported by behavioural experiments with $Ca_V1.3^{-/-}$ knockout mice which show a significantly suppressed anxiety- and depression-related behaviour (Nguyen et al., 2005).

A recent study also indicates a role of $Ca_V1.3$ channels in Pavlovian fear conditioning in mice. McKinney et al. used $Ca_V1.3$ knockout mice to elucidate the contribution of the channel in consolidation and extinction of conditioned fear (McKinney and Murphy, 2006). They found that these mice exhibit significant impairments in consolidation of contextually conditioned

fear, whereas their extinction of contextually conditioned fear was not altered compared to wildtype mice.

Ca^{2+} influx through postsynaptic L-type VGCCs and NMDA receptors (NMDAR) can lead to long-term potentiation (LTP), which is an activity-dependent enhancement in synaptic efficacy and a favoured candidate for a cellular mechanism of hippocampus-dependent forms of memory (Bauer et al., 2002). Induction of NMDAR-independent LTP seems to require activation of the L-type channel isoform $Ca_V1.2$ (Moosmang et al., 2005) and $Ca_V1.3$ channels are likely to play a role in working memory impairment in aging. In aged rats the increased expression of $Ca_V1.3$ channels correlates with age-related working memory decline in the area CA1 in the hippocampus and chronic treatment with nimodipine ameliorates the memory deficits (Veng et al., 2003).

These summarised data support an important role of the $Ca_V1.3$ channel in various brain functions and in behaviour. However, since conventional $Ca_V1.3\alpha1$ knockout mice ablate the $Ca_V1.3\alpha1$ subunit in all tissues and thus show phenotypes like deafness and heart insufficiency which might interfere with behavioural analysis, it would be important to investigate its function selectively in different types of neurons and brain areas required for learning and memory and mood.

1.3 Conditional Knockout of the $Ca_V1.3$ α1 Subunit Gene

The development of gene knockout technologies in mammals was crucial for the investigation of physiological functions of a gene. The mouse has become an important model for studying genetics and disease as it shares genomic, anatomical and physiological similarities with humans. In the early 1980s the isolation of embryonic stem (ES) cells from mouse embryos and their undifferentiated maintenance in cell culture (Evans and Kaufman, 1981; Martin, 1981) presented the first prerequisites for targeted gene inactivation in mice. The appearance of gene targeting technology – the replacement of endogenous genomic DNA with a mutant version of this DNA sequence based on homologous recombination – in mouse ES cells has led to a first generation of so-called knockout (KO) animals (Capecchi, 1989) and presents a powerful approach to introduce a variety of mutations in many different loci. Phenotyping of these null mutant mice has provided valuable information

about gene function and a variety of these knockout mice serves as animal models of human diseases.

The conventional knockout technology, however, has limited utility in several situations. The gene of interest could be essential for development and survival, and the gene knockout may lead to a lethal phenotype. Furthermore, the targeted gene could be important for normal development and share functional redundancy with other genes. In this case the phenotype could be hardly detectable and would likely result from compensatory mechanisms that may be difficult to elucidate.

1.3.1 The *Cre-loxP* Recombination System

To circumvent the difficulties associated with the complete deletion of a specific gene, sequence-specific recombination systems have been developed. These systems made it possible to obtain spatial and temporal control of the gene knockout, which is referred to as conditional knockout. Several such recombinase systems have been established in mice, two most common provide the basic tools for *in vivo* genetic engineering: the *Cre/loxP* system derived from the bacteriophage P1 (Sauer and Henderson, 1989) and the *Flp/FRT* system from the yeast *Saccharomyces cerevisiae* (O'Gorman et al., 1991). Both *Cre* and *Flp* recombinases belong to the λ integrase superfamily of site-specific recombinases that recognise a minimal target site of 34 bp where the recombination reaction takes place. The recombination reaction is carried out with absolute fidelity, such that not a single nucleotide is gained or lost, and no cofactors are required, making these recombination systems quite adaptable for use in a variety of heterologous organisms.

The *Cre/loxP* technology, which is the most established and popular approach to control targeted genetic inactivation in mice, was first reported by Rajewski et al. to knock out the DNA polymerase beta gene specifically in T-lymphocytes. The *Cre* (Causes recombination) recombinase catalyses the site-specific recombination between two recognition sites called *loxP* (*lo*cus of cross-over (*x*) in *P*1). The 34 bp long *loxP* site consists of two 13 bp inverted repeats and an 8 bp asymmetrical core spacer sequence, which determines the orientation of the site (Fig. 3 A). Depending on the orientation of the flanking *loxP* sites, a DNA fragment is excised (*loxP* sites oriented head-to-tail) (Fig. 3B) or inverted (*loxP* sites oriented head-to-head) (Fig. 3C) by the *Cre*-recombinase (Rajewsky et al., 1996). *Cre* catalyses the exchange

between the pair of *loxP* sites in the core spacer region by combined cleavage, exchange and rejoining reaction. A *cis* recombination event between two sites will lead to excision or inversion of the *loxP*-flanked ("floxed") DNA sequence. Recombination between two *loxP* sites *in trans* will lead to the reciprocal exchange of the regions that flank the *loxP* sites. *Cre* can also induce these recombination events when the *loxP* sites are located several megabases apart on the same chromosome, or on two homologous or non-homologous chromosomes (Ramirez-Solis et al., 1995). The equilibrium of the reactions of the deletion, inversion, exchange and integration of *loxP*-flanked DNA sequences can be pushed in the desired direction by using suitable selection markers. The mechanism of *Cre*-mediated recombination is as follows: after one recombinase monomer binds each palindromic 13 bp repeat, two such target sites are brought together in a synaptic complex. The subsequent events occur in the core spacer region where the DNA strands are cleaved, exchanged and ligated via a Holliday intermediate. In the final recovered product, the symmetry arms of the two target sites have been exchanged and the core regions of the two recombinants are heteroduplex.

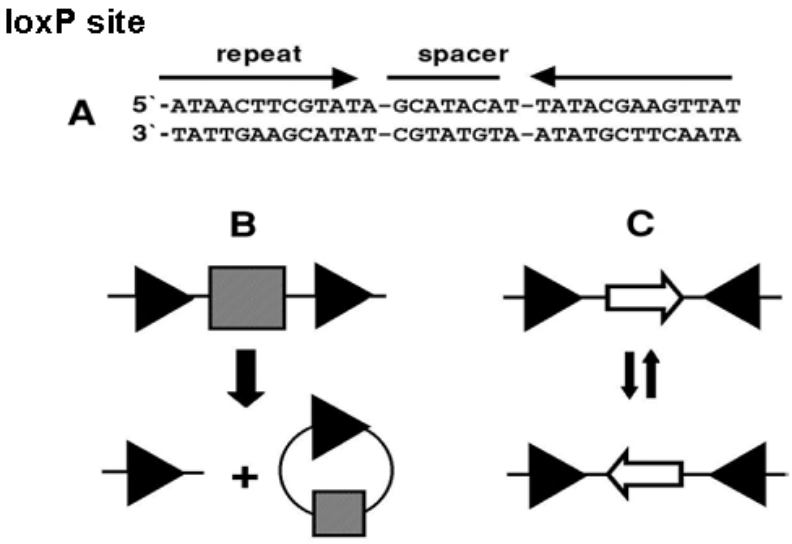

Fig. 3: The *loxP* site consists of an asymmetrical 8 bp spacer and two 13 bp inverted repeats **(A)**. Depending on the orientation of the *loxP* sites the flanked region is excised **(B)** or inverted **(C)**. Adopted from Hofker MH, van Deursen J, Methods in Mol. Biology, vol.209

Conditional targeting of *loxP*-flanked genes or gene segments can be achieved by crossing the mouse with *loxP*-flanked ("floxed") alleles with a "Cre" mouse expressing *Cre*-recombinase in a cell-type-specific or inducible manner. The floxed mouse is obtained by

homologous recombination in ES cells and displays wildtype phenotype since the *loxP* sites should not disturb gene transcription. The "Cre" mouse classically is a transgenic mouse, produced by pronuclear injection of a cDNA encoding *Cre*-recombinase under the control of a specific promoter. The transgene integrates randomly into the genome, and distribution of *Cre* activity requires careful characterization. In offspring derived from intercross between these two lines, *Cre*/*loxP* site dependent recombination will occur only in *Cre*-expressing cells, leading to an excision or inversion and consequently inactivation of the gene. In contrast, the target gene should remain functional in cells of all other tissues where the *Cre* transgene is not expressed as the promoter controlling the recombinase is inactive. The DNA excising capability of *Cre*-recombinase can also be used to turn on a gene by cutting out an intervening *loxP*-stop-*loxP* cassette between the promoter and the coding region of the transgene (Tsien et al., 1996). An elegant way to achieve temporal control of *Cre*-mediated recombination is by using an inducible *Cre* version. This *Cre-ERT2* recombinase, fused to an estrogen-mutated ligand binding site, is inactive at first. At time of experiment, *Cre* activity is induced by the systemic administration of the synthetic steroid ligand tamoxifen (Metzger and Chambon, 2001). All these features make the *Cre*/*loxP* system a valuable tool for molecular biology in that it allows the isolation of individual genes and their functions by establishing tissue specific gene ablation.

1.3.2 Conditional Gene Inactivation via the FLEX Switch

The development of the *Cre*/*loxP* system presents an opportunity to induce gene alterations both at precise time points and in specific cell types. Unfortunately, a frequent problem in transgenic mice expressing *Cre*-recombinase is position effect variegation that leads to a mosaic expression of the transgene. To address this problem, a so called reporter mouse line is used whose expression of a reporter gene (e.g. ß-galactosidase) is dependent on a *Cre*-mediated event excising a functionally silencing cassette (Branda and Dymecki, 2004). However, the excision pattern for a conditional allele cannot be accurately concluded from that of a reporter transgene. Moreover, their use to monitor gene ablation at the level of individual cells is often limited, as in some tissues the reporter gene may be silenced or reside in a chromatin configuration inaccessible for recombination. Therefore a direct

approach that allows to identify individual cells that are recombined at a given gene locus was required.

An elegant way is to directly couple reporter expression to gene ablation, thereby permitting a clear identification of each cell in which site-specific recombination has taken place. This is accomplished by the FLEX (Flip Excision) switch, through which the expression of a gene of interest is turned off, while the expression of another (e.g. reporter gene) is simultaneously turned on (Schnutgen et al., 2003). The FLEX switch is based on the ability of the *Cre*-recombinase to invert or excise a DNA fragment, depending on the orientation of the flanked *loxP* sites, and the availability of wildtype (WT) and mutated *loxP* sites. A FLEX allele contains two pairs of heterotypic *loxP* sites (e.g. *loxP* and *loxP257*) which are alternately arranged in head-to-head orientation. The mutated *loxP* site differs from the WT *loxP* site by one to three nucleotides in the core spacer sequence but is still recognized by the *Cre* recombinase. Thus, the two different *loxP* sites are incompatible to each other, indicating that for example the *loxP* sites cannot recombine with the *loxP257* sites but efficiently with themselves. By now various mutated *loxP* sites are available. Whereas *loxP511* differs from the WT *loxP* site in only one nucleotide and *loxP2272* and *loxP5171* in two nucleotides in the 8bp spacer region (Siegel et al., 2001), the *loxP257* or here referred to as *L3* site contains aberrant nucleotides at three positions in the core region (Fig. 4).

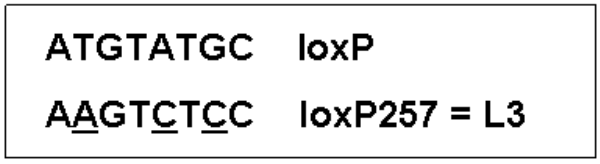

Fig. 4: Sequence of the 8 bp spacer region within the *loxP* site. Underlined nucleotides represent the base changes that differ from the original *loxP* sequence. Changes in the spacer sequence generate *loxP* sites that recombine with themselves but not with other *loxP* sites.

The combination of WT *loxP* and *L3* has been successfully used with high efficiency and without detection of any *Cre*-recombination between the two heterotypic *loxP* sites (Wong et al., 2005). For this strategy the application of heterotypic *loxP* sites is fundamental, since flanking an exon of the gene of interest by only one pair of homotypic *loxP* sites in head-to-head orientation would result in repeated rounds of recombination and inversions. In living cells, this would finally result in equilibrium, with half of the *loxP*-flanked DNA being in sense, the other half in antisense orientation (Abremski et al., 1983).

Beside the heterotypic *loxP* sites the FLEX switch allele contains an exon of a gene to be inactivated and a promoterless reporter gene with a universal splice acceptor and a polyadenylation (polyA) site in antisense orientation (Fig. 5). After Cre expression, each pair of *loxP* sites recombines with the corresponding pair, thereby inverting the floxed cassette in an irreversible way. By inverting, the expression of the reporter gene eGFP is switched on, while the exon of interest is inactivated. The cassette is now transcribed from the endogenous promoter in form of a fusion transcript in which the exon upstream of the insertion locus is spliced in frame to eGFP. This fusion transcript forms a nonfunctional and truncated version of the gene, since transcription is terminated by the polyadenylation site. Thus the FLEX switch presents a strategy to simultaneously inactivate the gene of interest and visualises the inactivation by expression of a "knock-in" reporter gene driven by the endogenous promoter.

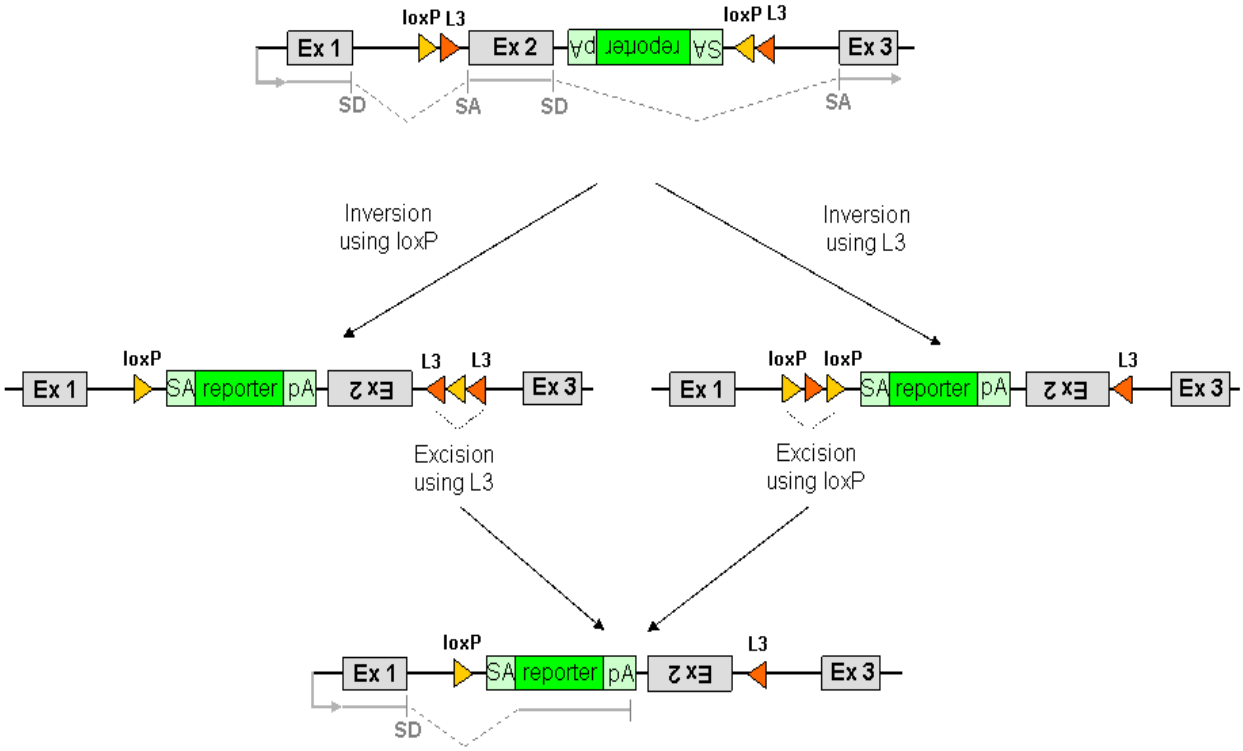

Fig. 5: Schematic drawing of the FLEX switch. The FLEX switch uses two pairs of heterotypic, antiparallel *loxP* recombination sites, which first undergo a *Cre*-mediated inversion of the coding sequence (exon 2), followed by excision of two sites, leading to one of each heterotypic recombination site oppositely orientated and incapable of further recombination. Note that it does not make any difference for the stable end product whether the inversion occurs at *loxP* and the excision at *L3* sites or the other way round. After the switch the exon of interest is inactivated whereas the reporter gene is driven by the endogenous promoter in form of a fusion transcript.

1.4 Aim of the Thesis

$Ca_V1.3$ voltage-gated calcium channels are widely expressed in the brain where they are involved in activity-dependent gene activation in neurons, CREB-signalling and behaviour. They have been also detected in many non-neuronal tissues like the heart atria, pancreatic ß-cells and cochlear hair cells. Conventional knockout mice of $Ca_V1.3\alpha1$ with a deleted channel in all tissues displayed important phenotypes. The mice were deaf due to the complete loss of cochlear hair cells and they exhibited sinoatrial dysfunction with bradycardia and arrhythmia. Furthermore, Ca^{2+} influx through $Ca_V1.3$ was proposed to be involved in memory formation, impairments in anxiety-related behaviour and in consolidation of contextually conditioned fear.

Here, we are interested to gain more insights into the role of $Ca_V1.3$ channels in neuronal tissues. We want to analyse the neurological functions and distribution of the L-type voltage-gated Ca^{2+} channel (VGCC) isoform $Ca_V1.3\alpha1$ in the brain using genetically modified mice. Since conventional $Ca_V1.3\alpha1$ knockout mice ablate the $Ca_V1.3\alpha1$ subunit in all tissues and thus show phenotypes like deafness and heart insufficiency which interfere with behavioural analysis, we generate conditional knockout mice via *Cre/loxP* mediated recombination with a tissue-specific deletion of the channel in brain areas required for learning and memory and mood. Furthermore, the knockout can be temporally controlled to rule out the possibility that genetic compensation could affect the neural phenotype in the $Ca_V1.3\alpha1$ knockout.

Aim of this study was to generate a conditional $Ca_V1.3\alpha1$ KO mouse line. This $Ca_V1.3$-GFP^{flex} mouse line is generated using a special knockout strategy, the *Cre*-mediated FLEX switch system, by which the $Ca_V1.3\alpha1$ gene is turned off while the reporter gene eGFP is switched on. With this knockout-strategy the expression pattern of the channel and the extent and time course of its ablation can be monitored, since so far no reliable working antibodies against $Ca_V1.3$ are available for immunohistochemical detection. The eGFP labelled neurons allow performing single cell electrophysiological recording and molecular studies within all $Ca_V1.3$ tissues. Furthermore, crossed by the germline "*Cre*-deleter" mouse, replacing by eGFP will reveal the exact expression pattern of $Ca_V1.3\alpha1$ in all tissues. With this floxed $Ca_V1.3\alpha1$ mouse line, crossed with animals expressing *Cre* under the control of a tissue-specific promoter, we can produce conditional-null mutants for a wide range of tissues with the possibility of direct cellular monitoring of the gene ablation.

2 Material

2.1 Laboratory Equipment

Accurate scales	BP210S, Satorius
Autoclave	Fritz Gössner
Incubator	Heraeus
Centrifuge Tubes	Beckman-Coulter
Electroporator	ECM630, BTX
Magnetic stirrer	MR3001, Heidolph
Thermal Cycler	I-cycler, BioRad
	Primus 96, MWG Biotech
	UNO II Biometra
Pipetting controller	Pipetus akku, Hirschmann Laborgeräte
pH-meter	pH537, WTW
Refrigerator	Liebherr
-80°C freezer	Sanyo
Shaker	Duomax 1030, Pharmacia Biotech
Spectrophotometer	Ultrospec 200, Pharmacia Biotech
	NanoDrop ND-1000, MWG Biotech
Vacuum concentrator	Speed Vac SC110, Savant
Tabletop centrifuge	Centrifuge 5415D, Eppendorff
	Centrifuge 5415R, Eppendorff
	Multifuge 3 S-R, Heraeus
	CS-6, Beckman-Coulter
Thermo block	Thermomixer comfort, Eppendorff
Ultracentrifuge	Optima L-70, Beckman-Coulter
	J2 MC, Beckman-Coulter
Vortexer	MS1 Minishaker, IKA
Vacuum pump	Mini-Vac E1, Axon Labs
Water purifier	Milli-Q RG, Millipore

2.1.1 Microscopy

Microscopes	A1R 4 laser line confocal microscope, Nikon
	Axiovert 2 plus, Zeiss
	Stemi 2000-C, Zeiss

2.1.2 Agarose Gelelectrophoresis

Electrophoresis chamber	B1A, B2 ;B3, Owl Scientific
Power supply	Poer Pac 300, BioRad
Gel photo imager	Gene Flash, Syngene

2.1.3 Cell Culture

Hood	Nuair class II
Cell culture incubator	Nuaire US autoflow
Vacuum pump	IBS Integra Biosciences
Cell culture water bath	GFL

2.2 Consumables

Electroporation cuvettes	*E.coli* Pulser Cuvette, Bio-Rad, Munich
Laboratory film	Parafilm M, American Can Company
Pasteur-Capillary- Pipettes	WU, Mainz
Plastic syringes	Discardit II, Becton Dickinson GmbH
Petri dishes	Greiner-Bio-One GmbH
Plastic material for cell culture	Sarstedt GmbH, Nümbrecht
Plastic material for cell culture	Falcon, Becton Dickinson GmbH, Heidelberg
Pipette Tips	Easy load, Greiner-Bio-One GmbH, Frickenhausen
Reaction tubes 1,5ml, 2ml, 15ml, 50ml	Sarstedt GmbH, Nümbrecht
PCR tubes	Sarstedt GmbH, Nümbrecht

2.3 Chemicals

The commonly used chemicals had analysis quality (p.A.) and have been sourced by the companies listed below:

Acros Organics, Geel (Belgien)

AppliChem GmbH, Darmstadt

Biomol Feinchemikalien GmbH, Hamburg

Bio Rad GmbH, Munich

Carl Roth KG, Karlsruhe

Difco Laboratories, Detroit Michigan (USA)

Fluka Feinchemikalien GmbH, Neu-Ulm

Gerbu Biotechnik GmbH, Gaiberg

Invitrogen (Gibco) GmbH, Karlsruhe

J.T. Baker, Deventer (Holland)

Merck AG, Darmstadt

Pharmacia Chemikalien GmbH, Dübendorf

Promega, Mannheim

Riedel de Haen Laborchemikalien AG, Seelze

Roche Diagnostics GmbH, Mannheim

Roth Chemikalien, Karlsruhe

Serva Feinbiochemika GmbH & Co., Heidelberg

Sigma-Aldrich GmbH, Seelze

2.4 Antibiotics

Ampicillin	Sigma-Aldrich GmbH, Seelze
Carbenicillin	Roth Chemikalien, Karlsruhe
Kanamycin	Invitrogen (Gibco) GmbH, Karlsruhe
Chloramphenicol	Sigma-Aldrich GmbH, Seelze
Neomycin G418	Calbiochem by Merck KGaA, Darmstadt
Ganciclovir	Sigma-Aldrich GmbH, Seelze

2.5 Enzymes and Recommended Buffers

ß-Agarase	Fermentas, St. Leon-Roth
DNA Ligase T4	Fermentas, St. Leon-Roth
	10 x T4 DNA Ligation buffer:
	400 mM Tris-HCl (pH 7,8 at 25°C), 100 mM $MgCl_2$,
	100 mM DTT, 5 mM dATP
DNA Polymerase T4	Fermentas, St. Leon-Roth
	5 x Reaction Buffer:
	335mM Tris-HCl (pH 8.8 at 25°C), 33mM $MgCl_2$
	5mM DTT, 84mM $(NH_4)_2SO_4$
DNA Polymerase *Taq*	Bioron, Ludwigshafen
	PCR-Buffer (10x): 160 mM $(NH_4)_2SO_4$, 670 mM Tris-HCl (pH 8.8), 0.1% Tween-20, 25 mM $MgCl_2$
	dNTP-Mix: 10 mM dATP, 10 mM dCTP , 10 mM dGTP, 10 mM dTTP in ddH_2O

DNA Polymerase *Pwo* (proofreading Taq)	Roche Diagnostics, Mannheim
	PCR-Buffer (10x) with $MgSO_4$:
	100 mM Tris-HCl (pH 8.85, 20°C), 250 mM KCl,
	50 mM $(NH_4)_2SO_4$, 20 mM $MgSO_4$
Expand Long Range dNTPack, Enzyme Mix	Roche Diagnostics, Mannheim
	PCR-Buffer (5x) with 12.5 mM $MgCl_2$:
Proteinase K	Qiagen, Hilden
Reverse Transcriptase	Qiagen, Hilden
	Invitrogen, Karlsruhe
Restriction enzymes	Fermentas, St. Leon-Roth
	New England Biolabs, Frankfurt
RNase A	Roche Diagnostics, Mannheim
Shrimp Alkaline Phosphatase	Promega, Mannheim
	10X Reaction Buffer:
	100mM $MgCl_2$, 0.5M Tris-HCl (pH 9.0)
	New England Biolabs, Frankfurt

2.6 Reaction buffers for restriction endonucleases

2.6.1 Fermentas Buffers

1X Buffer B (blue)	1X Buffer R (red)
10mM Tris-HCl (pH 7.5 at 37°C)	Tris-HCl (pH 8.5 at 37°C
10mM MgCl2	10mM MgCl2
0.1mg/ml BSA	100mM KCl
	0,1mg/ml BSA
1X Buffer G (green)	1X Buffer Tango™ (yellow)
10mM Tris-HCl (pH 7.5 at 37°C)	33mM Tris-acetate (pH 7.9 at 37°C)
10mM MgCl2	10mM magnesium acetate
50mM NaCl	66mM potassium acetate
0.1mg/ml BSA	0.1mg/ml BSA
1X Buffer O (orange)	
50mM Tris-HCl (pH 7.5 at 37°C)	
10mM MgCl2	
100mM NaCl	
0.1mg/ml BSA	

2.6.2 New England Biolabs Buffers

1X NEBuffer 1
10 mM Bis-Tris-Propane-HCl
10mM MgCl2
1 mM DTT
pH 7.0 at 25°C

1X NEBuffer 2
50 mM NaCl
10mM MgCl2
10 mM Tris-HCl
1 mM DTT
pH 7.9 at 25°C

1X NEBuffer 3
100 mM NaCl
50 mM Tris-HCl
10mM MgCl2
1 mM DTT
pH 7.9 at 25°C

1X NEBuffer 4
50 mM potassium acetate
20 mM Tris-acetate
10 mM magnesium acetate
1 mM DTT
pH 7.9 at 25°C

2.7 Antibody Staining

2.7.1 Antibodies

1. Antibody	Source	Dilution	Supplier
Anti-eGFP	rabbit	1:8000	Molecular Probes Invitrogen, # A11122
Anti-eGFP	chicken	1:1000	Chemicon, # AB16901
Anti-Doublecortin (C-18)	goat	1:500	Santa Cruz Biotechnology, # sc-8066
Anti-GFAP	mouse	1:2000	Sigma-Aldrich GmbH, # G3893
Anti-TPH1	mouse	1:2000	Sigma-Aldrich GmbH, # T0678
Anti-NeuN	mouse	1:4000	Chemicon, # MAB377
Anti-Sox2	rabbit	1:1500	Chemicon, # AB5603
Anti-GAD67	mouse	1:100	Chemicon, # MAB5406
2. Antibody			
Alexa Fluor® 488 anti-rabbit IgG (H+L)	donkey	1:500	Molecular Probes Invitrogen
Alexa Fluor® 555 anti-goat IgG (H+L)	donkey	1:500	Molecular Probes Invitrogen
Cy™ 3-conjugated anti-mouse IgG (H+L)	donkey	1:200	Jackson Immuno Research Laboratories
Cy™ 5-conjugated anti-mouse IgG (H+L)	donkey	1:500	Jackson Immuno Research Laboratories
Hoechst 33258	-	1:2000	Invitrogene

2.7.2 Compounds for Antibody Staining

Normal Donkey Serum	Jackson Immuno Research Laboratories, Inc.
Albumin Fraktion V	Carl Roth GmbH, Karlsruhe
Triton X100	Sigma-Aldrich GmbH, Seelze
Vectastain ABC Kit	Vector Laboratories, Inc., California
DAB (3,3`- Diaminobenzidine tetrahydrochloride)	Sigma-Aldrich GmbH, Seelze
Eukitt	O. Kindler GmbH & Co., Freiburg
Dako Fluorescent Mounting Medium	Dako Deutschland GmbH, Hamburg

2.8 Nucleic Acids

2.8.1 Nucleotids

Deoxyribonucleotids (dNTPs)	Fermentas, St. Leon-Roth

2.8.2 DNA Markers

PFGE Low Range	New England Biolabs, Frankfurt
PFGE Mid Range I & II	New England Biolabs, Frankfurt
λ/2 HindIII ladder	Fermentas, St. Leon-Roth
1 Kb DNA-ladder	Fermentas, St. Leon-Roth
100bp ladder	Fermentas, St. Leon-Roth

2.8.3 Primers

All primers are ordered from MWG Biotech and are used in a concentration of 100 pmol/µl.

L3 sense	ATAACTTCGTATAAAGTCTCCTATACGAAGTTATGGATCCCG
L3 antisense	ATAACTTCGTATAGGAGACTTTATACGAAGTTATGGATCCCG
HA-C_for	ACGCGTCGACTACTGAATTATTGGTTGAG
HA-D_rev	GGAATTCCTGACTTTGAAAACACATG
HA-E_for	ATAAGAATGCGGCCGCCTCAGTTTGTCAGAAG
HA-F_rev	TCCCCGCGGCCATTGTTGTGCCACACC
HA-G_for	GGGGTACCTTAGCAGTCTGGAATGTGAG
HA-H_rev	TTAGGGCCCGTGGCTAAATATACTCATGGACAC
HA-I_for	ATTTGCGGCCGCAACTTCATAGTGGTAGG
HA-J_rev	ATTCCGCGGCAGCATACCAAATTTTCAAC
GFP_for	CGCACCATCTTCTTCAAGGACGAC
GFP_rev	AACTCCAGCAGGACCATGTGATCG

Neo_for	TGCTCCTGCCGAGAAAGTATCCATCATGGC
Neo_rev	CGCCAAGCTCTTCAGCAATATCACGGGTAG
NeoES_for	CCGGTAGAATTTCGACGACCTG
3'HAext_rev2	TGACCATCCAAGTGAGAGCAAGAC
3'HAint_rev	AAGGCCGGCCACGCTAATC
Neo_Xho-FRT-Xho	TGAGGCGGAAAGAACCAG
Ex2 ES_rev	GCTGTTGGGCTGAGAAGTTGGT
ES3'_for	GGACGTAAACTCCTCTTCAGACCTG
5`HA_end_for	GGAGTTGTGTATATCTGTTAAGCCATG
3'HAvorne_rev	CCAGAAGATTCCACTAAAGGTCAT
eGFP(GATC)_rev	CCGTCCAGCTCGACCAG
CaV1.3-FRT_for	CGATAAGCTTGATATCGAATTCCGAAGTTCC
CaV_Ex3rev	AGCTAAGGCCACACAATTGGC

2.8.4 Plasmids

Name	Origin	Resistance
J14279Q4	RZPD	Kan???
pBelo.BAC HD	Kai Schönig	Cm
pL253	N. Copeland, Frederick, USA	Amp
pL451	N. Copeland, Frederick, USA	Amp/Kan
pL452	N. Copleand, Frederick, USA	Amp/Kan
pUC 18	Stratagene, Heidelberg	Amp
pMCS5	Molecular Probes	Amp
pBlueskript II SK (+)	Stratagene, USA	Amp
pMC1-Cre	D. Bartsch	Amp
pCaggsFlpE	F. Stewart, TU Dresden	Amp/Puro
SA.eGFP.pA+2	Frank Schnütgen, Frankfurt	Amp

2.9 Bacteria Strains

DH5a	Invitrogen, Karlsruhe	Δ(lac)U169, endA1, gyrA46, hsdR17(r_K-m_K+), phi80, Δ(lacZ)M15, recA1, relA1, supE44, thi-1.
DH10B	Invitrogen, Karlsruhe	F- *mcr*A Δ(*mrr-hsd*RMS-*mcr*BC)

		φ80*lac*ZΔM15; Δ*lac*X74; *rec*A1 *end*A1 *ara*D139 Δ(*ara, leu*)7697 *gal*U *gal*K λ- *rps*L *nup*G
EL250	Neil G. Copeland, National Cancer Institute, Frederick, USA	DH10B [_cl857 (*cro-bioA* < > *araC-*P_{BAD}*flpe*]
EL350	Neil G. Copeland, National Cancer Institute, Frederick, USA	DH10B [_cl857 (*cro-bioA* < > *araC-*P_{BAD}*cre*]

2.10 Cell Lines

HeLa	Human cervix carcinoma cells	ATCC-LGC Promochem
R1	Mouse embryonic stem cells from 129/SvJ mouse strain	From A. Nagy, Toronto, Canada

2.11 Mouse Lines

TgN(EIIa-Cre)C5379Lmgd	Adenovirus EIIa promoter directs expression of Cre recombinase in preimplantation mouse embryos. This transgene expresses Cre recombinase in nearly all tissues	H.Westphal, NIH Bethesda, USA
Tg(ACTFLPe)9205Dym/J	Human ACTB promoter drives the expression of FLPe also in the germline	S.Dymecki, Harvard, USA
B6D2F1/Crl	C57BL6/N and DBA2 F1-hybrids for ES cell injection foster mothers and vasectomised males	Charles River, Sulzfeld
C57BL6/NCrl		Charles River, Sulzfeld
Camkcre4 mice (TgCre4)	Cre recombinase expressed postnatally under control of the CamKIIα gene present in a BAC expression vector (8.5 kb promoter fragment)	Günther Schütz, DKFZ, Heidelberg

2.12 Buffers, Media and Solutions

Antibiotics stock solutions:	
Ampicillin (1000x)	100mg/ml in H_2O
Carbenicillin (1000x)	100mg/ml in EtOH
Doxycyclin-hydrochloride (1000x)	1mg/ml in H_2O
Kanamycin (2000x)	25mg/ml in H_2O
Chloramphenicol (2000x)	25mg/ml in H_2O
D-MEM	Dulbecco´s modified Eagle Medium, Invitrogen GmbH, Karlsruhe with GlutaMAX I4500 mg/L D-Glucose Sodium-pyruvate
10xDNA-loading buffer	30 % (w/v) Glycerol 0.3 % (w/v) bromine phenol blue 0.3 % (w/v) xylene-cyanole 10 mM Tris-HCl; pH 7.5
Ethidium bromide	10 mg/ml in H_2O
FCS	Fetal calw serum, Invitrogen GmbH, Karlsruhe
In situ ß-Gal-staining solution	1 mg/ml X-Gal 2 mM $MgCl_2$ 5 mM $K4(Fe(CN)_6)$ 5 mM $K3(Fe(CN)_6)$
IPTG stock	400mM in H_2O
LB-agar	1.5 % (w/v) Bacto-Agar (Difco-Laboratories, Detroit, USA) in LB-medium
LB-medium	10 g Bacto-Trypton (Difco-Laboratories) 5 g yeast-extract (Difco-Laboratories) 10 g NaCl adjusted with NaOH to pH 7.5 ddH_2O ad 1000 ml
Mini-prep solutions	solution I: 50 mM tris-HCl, pH 8.0 10 mM EDTA 100µg/ml RNAse solution II: 0.2 M NaOH 1% SDS

	solution III:
	2.8 M potassium acetate, pH 5.1
	(adjusted with glacial acetic acid)
Opti-MEM	Serum reduced medium, Invitrogen GmbH, Karlsruhe
	with GlutaMAX I
	2400 mg/L sodium carbonat, HEPES, Sodium
	pyruvate, Hypoxathine, Thymidin, Growthfactors, 1.1
	mg/L Phenolred
PBS(1x), pH 7.4	140 mM NaCl
	2.7 mM KCl
	1.5 mM K_2PO_4
	8.1 mM Na_2HPO_4 x $2H_2O$
Sörensen Buffer 0.1M pH 7.3	350 ml Na_2HPO_4 0.2M
	650 ml NaH_2PO_4 0.2M
	1000 ml H_2O
	0.5 ml Heparin/l
TAE(1x)	Tris acetate EDTA:
	40 mM Tris-HCl, pH 8.3
	20 mM Sodium acetate
	2 mM EDTA
TBE(1x)	Tris borate/EDTA:
	90 mM Tris-HCl, pH7.8
	90 mM Boric acid
	3 mM EDTA
TE	Tris/EDTA:
	10 mM Tris-HCl pH 7.5
	1 mM EDTA
Trypsin-EDTA	Invitrogen GmbH, Karlsruhe
	0.05% Trypsin
	0.53 mM EDTA x 4Na
YENB	0.75% Bacto yeast extract
	0.8% Bacto nutrient broth

2.12.1 Cell Culture Media

ES Medium	KnockOut DMEM (Invitrogen)
	0.1 mM non-essential amino acids (100x stock, Invitrogen)
	0.1 mM ß-mercaptoethanol (Sigma Aldrich)
	2 mM Glutamax (100x stock, Invitrogen)
	1x Penicillin/Streptomycin (100xstock, Invitrogen)
	15 % Fetal bovine serum (FBS), ES qualified (Invitrogen)
	1000U/ml ESGRO LIF (Chemicon)
Trypsin/EDTA	0.05 % trypsin in saline/EDTA (Invitrogen)
1x Freezing Medium	25 % FBS
	10 % DMSO
	In DMEM
Feeder Medium	DMEM high glucose
	10 % Fetal calf serum (FCS)
	1x Penicillin/streptomycin
	2 mM Glutamax
Gelatine solution	0.1 % Gelatine in water, autoclaved (Sigma)
Gancyclovir	2 µM (5000x stock , 10mM in PBS, sterile filtered)
G418	200µg/ml (1000x stock, 200mg/ml in PBS, sterile filtered)
ES Lysis buffer	10 mM Tris-HCl, pH 7.5
	10 mM EDTA
	10 mM NaCl
	1 mg/ml Proteinase K (Qiagen)
	0.5 % SDS
Mineral oil	Sigma Aldrich
NaCl/EtOH mix	15µl of 5M NaCl per 1ml of cold 100 % EtOH(.made fresh)
Mitomycin C	1 mg/ml stock

3 Methods

3.1 Microbiological Methods

3.1.1 Transformation of Bacteria

There are two methods to transform *E. coli* cells with plasmid DNA - chemical transformation and electroporation. Chemical competence is conferred to *E.coli* by re-suspension in $CaCl_2$ solution. The Ca^{2+} ion is thought to create pores in the membrane, assist binding of the DNA to the cell membrane and mask the negative charge on the DNA, facilitating its passage through the hydrophobic cell membrane. Here electroporation is used to introduce DNA into bacteria. Electroporation involves the application of an electric pulse of several hundred volts across the cell, which creates momentary "pores" in the cell membranes and forces the negatively charged DNA into the cells by an electrophoresis-type effect.

3.1.1.1 Generation of electrocompetent E. coli Cells

The uptake of DNA by *E.coli* cells can be increased by making cells electrocompetent. 5 ml YENB-medium are inoculated with a -80°C single colony stock solution and incubated overnight at 37°C. This overnight culture is used to inoculate 1 litre of pre-warmed YENB-Medium and incubated at 37°C on a shaker until an OD_{600} of 0.7 to 0.8. The cells are cooled on ice for 10 min and centrifuged for 10 min at 4000 x g at 4°C. The bacteria are washed twice with 100 ml ice cold ddH_2O and centrifuged as described above. The cells are resuspended in 20 ml ice cold ddH_2O with 10% glycerol and centrifuged. Finally the bacteria pellet is resuspended in 5ml cold ddH_2O containing 10% glycerol. Aliquots of 50µl are pipetted in pre chilled tubes, frozen in liquid nitrogen and stored at – 80°C. The transformation efficiency ought to be 10^8-10^9 colonies/µg plasmid used for the transformation reaction.

3.1.1.2 Electroporation of competent E.coli cells

50µl of the electrocompetent *E.coli* cells are thawed on ice and mixed with 1-2 µl DNA (ligation-) solution. This mixture is transferred into a pre-chilled electroporation cuvette with a 0.1 cm electrode gap. The electroporation settings are 1250 V, 125 Ω, 50 µF. Immediately after the electroporation 900 µl LB-medium without antibiotics is added and the mixture is

incubated for 1 hour at 37°C to ensure that the resistance gene expression can take place. Following a certain volume of the bacteria solution is plated on LB-agar plates containing the corresponding antibiotic.

3.2 Isolation and Purification of DNA

3.2.1 Isolation of Plasmid DNA (Miniprep)

This purification method is based on alkaline lysis. Bacteria containing the plasmid are lysed by a strong alkaline buffer (S2-buffer) containing detergent and a strong base, which breaks the cell membrane and denatures the proteins. Subsequent the pH-value is decreased (as a result of S3-buffer) to renature the nucleic acid. Within this process the chromosomal *E.coli* DNA renatures intermolecular by forming a highly complex structure while the plasmid DNA renatures intramolecular. Proteins are denatured via SDS in S2-buffer. Membrane particles, denatured proteins and chromosomal DNA are separated from plasmid DNA and RNA by centrifugation and the plasmid DNA is precipitated and isolated.

The procedure is performed as followed:

- 5 ml LB-medium containing the appropriate antibiotic is inoculated by a single colony and incubated in a shaker at 37°C over night.
- 2 ml overnight culture is transferred into a 2 ml reaction tube and centrifuged for 5 min in a table centrifuge at 9000 rpm. The supernatant is carefully discarded.
- The pellet is resuspended in 100 ml S1-buffer (100 ng/ml RNAseA) and incubated at room temperature for 5 min.
- 200 µl S2-buffer is added, mixed gently by inverting the tube and incubated for 2-3 min.
- 150 µl cold S3-buffer is added, mixed by inverting the tube and incubated on ice for 5 min.
- The sample is centrifuged in a table centrifuge for 15 min at maximum speed.
- The supernatant is transferred to a fresh microcentrifuge tube and the DNA is precipitated with 1 ml 100% ethanol and incubated for 20 min at -20°C.
- The precipitated DNA is centrifuged for 20 min at maximum speed at 4°C and washed twice with 0.5 ml 70% ethanol.
- The supernatant is carefully removed and the dried pellet resolved in 50 µl Tris-HCl buffer.

3.2.2 Isolation of Plasmid DNA on a large scale (Maxiprep)

For preparation of plasmid DNA in large quantities the Plasmid DNA Purification Kit NucleoBond PC 500 (MACHEREY-NAGEL GmbH) is used. This method is based on a modified alkaline/SDS lysis procedure followed by binding of plasmid DNA to a silica-based anion-exchange resin.

Both chromosomal and plasmid DNA are denatured under alkaline conditions. Potassium acetate is then added to the denatured lysate, which causes the formation of a precipitate containing chromosomal DNA and other cellular compounds. The potassium acetate buffer also neutralizes the lysate. Plasmid DNA, which remains in solution, can revert to its native supercoiled structure. After equilibrating the NucleoBond column with equilibration buffer, plasmid DNA is bound to the anion-exchange resin and finally eluted after efficient washing of the column. After precipitation of the eluted DNA it can easily be dissolved in TE buffer for further use.

Below the protocol of high-copy plasmid preparation is illustrated:

- Centrifuge up to 500 ml overnight culture at 4,500 - 6,000 x g for 15 min at 4°C.
- Carefully resuspend the pellet of bacterial cells in 12 ml buffer S1 + RNase A.
- Add 12 ml buffer S2 to the suspension. Mix gently by inverting the tube 6-8 times. Incubate the mixture at room-temperature (20-25°C) for 2–3 min (max. 5 min). Do not vortex, as this will release contaminating chromosomal DNA from cellular debris into the suspension.
- Add 12 ml pre-cooled buffer S3 (4°C) to the suspension. Immediately mix the lysate gently by inverting the flask 6-8 times until a homogeneous suspension containing an off-white flocculate is formed. Incubate the suspension on ice for 5 min.
- Place a NucleoBond folded filter in a small funnel for support, and pre-wet the filter with a few drops of buffer N2 or sterile deionised H_2O. Load the lysate onto the wet filter and collect the flow-through.
- Equilibrate a NucleoBond column with 6 ml buffer N2. Allow the column to empty by gravity flow. Discard flow-through.
- Load the cleared lysate from onto the column. Allow the column to empty by gravity flow.
- Wash the column with 32 ml buffer N3. Discard flow-through
- Elute the plasmid DNA with 15 ml buffer N5.

- Add 11 ml room-temperature isopropanol to precipitate the eluted plasmid DNA. Mix carefully and centrifuge at ≥ 15,000 x g for 30 min at 12°C. Carefully discard the supernatant.
- Add 5ml room-temperature 70% ethanol to the pellet. Vortex briefly and centrifuge at ≥ 15,000 x g for 10 min at room-temperature (20-25°C).
- Carefully remove ethanol from the tube with a pipette tip. Allow the pellet to dry at room-temperature (20-25°C), at least for the indicated time.
- Resolve pellet in an appropriate volume of buffer TE.

3.2.3 Isolation of genomic DNA from tail tissue of the mouse

The Qiagen DNeasy 96 Tissue Kit provides a fast and easy procedure for high-throughput purification of total genomic DNA from rodent tails and animal tissues. The DNeasy 96 procedure is ideal for simultaneous processing of 96 samples. The eluted DNA is ready for use in any downstream application, including PCR, Southern blotting, and other enzymatic reactions. DNA can be safely stored at –20°C for later use. The purified DNA is free of proteins, nucleases, and other contaminants and enzyme inhibitors. Routinely a 0.5 cm long tail biopsy of 3-4 weeks old mice is cut by a kauter to purify the whole genomic DNA.

The general procedure is performed as follows:

- A 0.5 cm mouse tail sample is cut with a kauter and placed into a collection microtube.
- 180µl Buffer ATL and 20µl Proteinase K solution are added and mixed by vortexing.
- The sample is incubated at 55°C overnight or until the sample is completely lysed.
- The collection tube is shaken vigorously and spun shortly down in a microfuge.
- 400µl buffer AL/E is added, mixed well and spun shortly down.
- The supernatant is carefully transferred to the DNeasy 96 Plate and centrifuged for 10min at 6000rpm.
- 500µl Buffer AW1 is added to each well and centrifuged for 5min at 6000rpm.
- 500µl buffer AW2 is added to each well and centrifuged for 5min at 6000rpm.
- The DNeasy 96 plate is dried at 70°C for 15 min.
- The genomic DNA is eluted with 200µl of pre-warmed elution buffer AE.
- The eluted DNA can be stored at -20°C.

3.2.4 Phenol-Chloroform extraction of DNA

To remove proteins from a liquid nucleic acid solution the same volume of equilibrated phenol:chloroform:isoamil alcohol (at a ration of 25:24:1 v/v, equilibrated with 100 mM Tris-HCl to pH8) is added to the sample. The phases are mixed thoroughly for 1 min and centrifuged for 4 min (table centrifuge, 13,000 rpm). The mixture is separated into a lower phenol phase, an interphase of white, denatured proteins and an upper aqueous phase, which contains the nucleic acids. The upper phase is transferred to a new tube and if required the phenol extraction can be repeated. The purified DNA is precipitated by isopropanol or 100% ethanol.

3.2.5 Photometric analysis of concentration and purity of nucleic acids

The nucleic acid concentration of an aqueous solution is due to the Beer-Lambert law directly proportional to its extinction and absorption, respectively (indicated as the optical density OD value). This relation is utilized to quantify the nucleic acid concentration spectrophotometrically. The maximum absorption of nucleic acid is at 260 nm whereas proteins have their maximum absorption at 280 nm. The absorption/concentration relations are:

- 1 OD_{260} = 50 µg/µl ds DNA
- 1 OD_{260} = 40 µg/µl ss RNA
- 1 OD_{260} = 30 µg/µl ss oligo nucleotides

The purity of a DNA solution is given by the OD_{260}/OD_{280} ratio, which is supposed to be between 1.8 and 2.0 for a pure DNA without protein-contamination.

By using the NanoDrop ND-1000 Spectrophotometer technology there is no need for cuvettes and other sample containing devices. To quantify the nucleic acid concentration, a 1µl sample is pipetted directly onto the measurement pedestal. The measurement is initiated using the NanoDrop software on the PC. A concentration from 2 to 3700 ng/µl is measurable without dilution.

3.2.6 DNA Extraction from Agarose Gel

3.2.6.1 Extraction by Silica-Gel Particles

For DNA extraction of 40-bp to 15-kb DNA fragments from 0.3-2% standard agarose gels in TAE buffers the Qiaex II Kit (Qiagen), was used according to the manufacturer's instructions listed below. Purification of DNA fragments with the QIAEX II system is based on solubilisation of agarose and selective adsorption of nucleic acids onto QIAEX II silica-gel particles in the presence of chaotropic salt. QIAEX II separates DNA from salts, agarose, PAA, dyes, proteins, and nucleotides.

User manuel:

- The DNA band from the agarose gel is excised with a clean, sharp scalpel. A 1.5-ml microfuge tube is used for processing up to 250 mg agarose.
- The gel slice is weighed in a colourless tube. 3 volumes of Buffer QX1 are added to 1 volume of gel for DNA fragments 100 bp - 4 kb; otherwise:

DNA fragments < 100 bp	Add 6 volumes of Buffer QX1
DNA fragments > 4 kb	Add 3 volumes of Buffer QX1 plus 2 volumes of H2O
> 2% or Metaphor agarose gels	Add 6 volumes of Buffer QX1

- QIAEX II is resuspended by vortexing for 30 sec. QIAEX II is added to the sample according to the table below and mixed.

< 2 μg DNA	Add 10 μl of QIAEX II
2-10 μg DNA	Add 30 μl of QIAEX II
Each additional 10 μg DNA	Add additional 30 μl of QIAEX II

- The sample is incubated at 50°C for 10 min to solubilise the agarose and bind the DNA. It is mixed by vortexing every 2 min to keep QIAEX II in suspension.
- If the colour of the mixture is orange or purple, 10 μl 3M sodium acetate, pH 5.0 is added, and mixed. The incubation is then continued for an additional 5 min at least.
- The adsorption of DNA to QIAEX II particles is only efficient at pH 7.5. Buffer QX1 contains a pH indicator which is yellow at pH 7.5, and orange or violet at higher pH, allowing easy determination of the optimal pH for DNA binding.
- The sample is centrifuged for 30 sec and the supernatant is carefully removed with a pipette.

- The pellet is washed with 500 µl of Buffer QX1 and the pellet is resuspended by vortexing. The sample is centrifuged for 30 sec and all traces of supernatant are removed with a pipette. This wash step removes residual agarose contaminants.
- The pellet is washed twice with 500 µl of Buffer PE to remove residual salt contaminants.
- The pellet is air-dried for 10-15 min or until the pellet becomes white. If 30 µl of QIAEX II suspension is used, the pellet is air-dried for approximately 30 min. Do not vacuum dry, as this may cause overdrying. Overdrying the QIAEX II pellet may result in decreased elution efficiency.
- To elute DNA, 20 µl of 10 mM Tris-HCl, pH 8.5 or H_2O is added and the pellet is resuspended by vortexing. The sample is incubated according to the table below.

DNA fragments < 4 kb	Incubate at room temp. for 5 min
DNA fragments 4-10 kb	Incubate at 50°C for 5 min
DNA fragments > 10 kb	Incubate at 50°C for 10 min

- Elution efficiency is dependent on pH. The maximum elution efficiency is achieved between pH 7.0 and 8.5. When using water for elution, the pH should also be within this range and the DNA is stored at -20°C as DNA may degrade in the absence of a buffering agent. The purified DNA can also be eluted in TE buffer (10 mM Tris-HCl, 1 mM EDTA, pH 8.0) but the EDTA may inhibit subsequent enzymatic reactions.
- The sample is centrifuged for 30 sec and the supernatant is carefully pipetted into a clean tube. The supernatant now contains the purified DNA.
- For fragments larger than 10 kb, the pellet is resuspended by inverting and flicking the tube because vortexing can cause shearing of large DNA fragments.

3.2.7 Extraction of DNA by Agarose Digestion

For recovery of DNA fragments larger than 15 kb from low-melting agarose gels, the enzyme Agarase is used. One unit of Agarase completely digests 100 µl (approx. 100 mg) of melted 1% low melting point agarose in 30 min at 42°C. The recovered nucleic acids can be subjected to further manipulations as restriction endonuclease digestion, ligation or sequencing.

The protocol is as following:

- The DNA is cut out from a 1% low melting point agarose gel prepared in TAE buffer

- The gel slice is placed into a 1.5 ml microcentrifuge tube and incubated for ~ 10 min at 70°C until the agarose is completely melted.
- The tube is transferred to 42°C and equilibrated for 5 min prior to adding Agarase.
- 1 unit of Agarase per 100 mg (~100 µl) of 1% agarose is added, gently mixed and incubated for 30 min- 1h at 42°C.
- If a higher percentage agarose is used, the amount of Agarase should be proportionally increased.

3.3 Purification of DNA

To clean DNA fragments from primers, nucleotides, enzymes or salts of PCR and other enzymatic reactions, the PeqLab E.Z.N.A. Cycle-Pure kit was used.

The corresponding protocol is listed below:

- Add 4-5 volumes of CP-buffer to the reaction batch and mix (for DNA fragments <200 bp add 6 volumes CP-buffer, for DNA fragments > 4 kb add 3 volumes CP-buffer plus 1 volume of ddH_2O).
- Place a HiBind-centrifuge column in a 2 ml collection tube and apply the mixture (reaction batch plus CP-buffer) to the column.
- Centrifuge collection tube with the column for 1 min at 10.000 x g and room temperature. Discard the flow-through and place the column back in the same collection tube.
- To wash, add 750 µl of completed DNA-wash buffer (buffer concentrate plus 1.5 x volumes absolute ethanol) to the column and centrifuge 1 min at 10.000 x g and room temperature. Discard the flow-through and place the column back in the same collection tube. Repeat the washing step once.
- To dry the column completely, centrifuge the column for an additional 1 min at maximum speed.
- To elute DNA place the column in a clean 1.5 ml microcentrifuge tube, add 50-100 µl ddH_2O or TE- buffer to the centre of the matrix and centrifuge the column for 1 min at 10.000 x g and room temperature.

3.4 Analysis of DNA

3.4.1 Fragmentation of DNA with Restriction Enzymes

Restriction endonucleases are enzymes, which recognize specific dsDNA sequences and cut both DNA strands. These sequences usually cover four to eight base pairs, which are characteristic for each enzyme. Hydrolysis of the phosphodiester bond occurs in the recognition site whereby the DNA fragment is cleaved at this particular position. Depending on the restriction endonuclease, this enzymatic reaction generates blunt end or cohesive end termini. Every restriction enzyme requires individual condition for hydrolysis. The enzymatic activity is indicated in units (u), whereby 1 u corresponds to the amount of enzyme needed for the digestion of 1 µg DNA (depending on the assay: λ phage DNA or adenovirus DNA) in one hour. In general these enzymes are used to linearize circular DNA, to cut out specific fragment from larger molecules or to cut genomic DNA. The restriction reactions are conducted in the recommended buffer and incubated for at least two hours at 37°C. In addition it is recommended, that the volumetric content of enzyme does not exceed 10% of the final volume since glycerine is major component of the enzyme solution and inhibits the enzymatic activity if its concentration is higher then 5%. If restriction endonucleases are used under extreme non-standard conditions (such as to many units, to long incubation time or eventually the use of a not recommended buffer), they might be capable of cleaving sequences which are similar but not identical to their defined recognition sequence, termed "star activity".

A typical analytical restriction digest reaction is composed as follows:

1 µg DNA in x µl TE
2 µl 10x restriction buffer
1-10 U restriction endonuclease
dd$H_2$0 ad 20 µl

After an appropriate incubation-time the generated DNA fragments can be separated via agarose-gel-electrophoresis.

3.4.2 Agarose Gel Electrophoresis

Agarose gel electrophoresis is used to separate DNA or RNA molecules by size. DNA has a negative charge in solution, so it will migrate to the positive pole in an electric field. In

agarose gel electrophoresis the DNA is forced to move through a sieve of molecular proportions that is made of agarose. Large pieces of DNA move slower through the gel matrix than small pieces of DNA. The DNA fragments in the gel can be visualized by staining with ethidium bromide (EtBr). EtBr is a fluorescent dye which intercalates between bases of the DNA and is excited by light of a wavelength around 300 nm. It is often incorporated into the gel but the gel can also be stained after electrophoresis by soaking in a solution of ethidium bromide.

3.4.2.1 Separation of DNA on Agarose gels

In this thesis agarose gels are used to analyse the size of restriction fragments or PCR products. The concentration of the gel ranges from 0.7-2%, depending on the expected size of the fragments. The agarose is dissolved in 1 x TAE buffer and boiled in a microwave oven until the agarose completely dissolves. After the solution cools down to 50-60°C, ethidium bromide is added to a final concentration of 0.5 µg/ml. The agarose solution is poured into a horizontal gel-electrophoresis device containing a gel-comb with pockets of appropriated size. Upon the gel becomes solid the comb is removed and the gel chamber is filled with TAE (1X) buffer. Subsequently the lanes are loaded with the DNA sample together with loading buffer. Alternatively 1x TBE buffer can be used.

The negatively charged DNA is separated according to its size in an electric field (~120 V; 45 min). The agarose gel electrophoresis allows DNA separation from about 100 bp to several 1000 bp, depending on the agarose concentration of the gel. In order to determine weight and size of the DNA sample it is necessary to apply a molecular DNA marker (100 bp / 1 kb DNA ladder, Fermentas GmbH) on a separate lane in the same gel. The ethidium bromide in the gel is used to visualize the DNA fragments via ultraviolet irradiation (wavelength 302nm).

3.4.2.2 Separation of High-Molecular DNA by PFGE (Pulse Field Gel Electrophoresis)

Pulse field gel electrophoresis is used for DNA fragments larger than 15-20 kb. Molecules of that size migrate through a conventional agarose gel in a size-independent manner. Therefore, in pulsed field electrophoresis, DNA molecules are subjected to alternating electric fields imposed for a period of time called the switch time. Each time the field is

switched, the DNA molecules must change direction or reorient in the gel matrix. Larger molecules take longer to reorient and have less time to move during each pulse, so they migrate slower than smaller molecules. Resolution will be optimal for DNA molecules with reorientation times comparable to the pulse time. So, as the DNA size increases, the pulse time needs to increase to resolve the molecules.

Voltage (Field Strength):

DNA migration increases with increases in voltage or field strength. However, greater migration is accompanied by decreased band sharpness. In general, as the size of the DNA molecules increases, the field strength should decrease. At high field strengths (6 V/cm) some very large DNA (>3 Mb) cannot be resolved on the gel and the field strength must be reduced. Moreover, some large DNA molecules will not enter the gels at high field strengths. Therefore, in selecting the field strength for an experiment, a compromise between run time and resolution has to be made.

Switch interval:

The larger the fragment, the longer the intervals in between two electric fields should be chosen. In general, a switch interval gradient is used, with short interval in the beginning and a longer interval in the end.

Field Angle:

The system allows separations to be carried out with electric field vectors oriented in any direction in the plane of the gel (90°–120°). With two field vectors, resolution of DNA molecules up to 1 mb is independent of the angle between them. It has been shown that decreasing the included angle from 120° to 94° increases the velocity of the DNA, with the mobility of large DNAs (>1 mb) affected to a greater degree by the change in angle than are smaller DNAs (<1 mb). Decreasing the included angle will decrease the resolution of smaller DNAs by causing them to pile up on each other. This same effect on small DNA can be seen with long switch times. It is recommended that the included angle be decreased (<120°) when separating large DNA molecules greater than 2 mb.

For routine separation of BAC mini-preps the following settings are used:

- Run time: 15h
- Voltage: 6V/cm
- Field angle: 120°

- Switch interval: 1-15 sec
- Temperature: 14°C

3.4.3 Staining of Nucleic Acid Agarose Gels with Ethidium Bromide

Nucleic acids in agarose gels can be visualized by staining with ethidium bromide (EtBr). EtBr intercalates in nucleic acids and emits light after excitation with ultraviolet light (optimal excitation wavelength is 254nm). The gel is stained for 10-30 min in an EtBr solution (1µg/ml). Unspecific bound EtBr should be removed by washing the gel twice for 10min in 1x TBE. The nucleic acids can then be visualized on a UV gel documentation system.

3.4.4 Oligonucleotide Annealing

Annealed oligonucleotides are often used to insert short DNA sequences of 10-60 bp into a plasmid. Single stranded DNA oligonucleotides with complementary DNA sequences can hybridize to double stranded DNA. For this purpose a 2 µl aliquot of each oligonucleotide (100 mM) is added to 10 µl 1x TE, 2 µl KCl (3M), and 24 µl dH_2O. The sample is vortexed and incubated at 95°C in a thermo block or water bath for 3 minutes. The thermo block/water bath is then switched off, so that the block/water cools slowly down to room temperature (takes about 1 hour), allowing the oligonucleotides to anneal. The sample can be used immediately for a ligation reaction (see below), or stored at -20°C for future use. Since the 5′termini of synthesized oligonucleotides are not phosphorylated, consequently the 5′ termini of a vector used in a ligation reaction together with the synthetic oligonucleotide should not be dephosphorylated since otherwise ligation can not occur.

3.4.5 Dephosphorylation of 5′-Ends from DNA by Alkaline Phosphatase

To prevent linearized DNA plasmids from relegation and recirculation, both phosphate groups of the 5′ termini are removed by the shrimp alkaline phosphatase (SAP). One unit of enzyme is the amount required to catalyze the hydrolysis of 1 µmol 4-nitrophenyl phosphate per minute at 37°C. SAP is completely and irreversibly inactivated by heating at 65°C for 15 minutes. For a "dephosphorylation reaction" 1 µg DNA is incubated with 3µl 1x SAP buffer and 1U SAP for 15 min at 37°C. The reaction is stopped by incubation for 15 min at 37°C.

3.4.6 Blunting of DNA Fragments with 5′- or 3′ – Protruding Ends

For ligation of two DNA fragments with non-compatible ends, it might be necessary to blunt the 5′- or 3′ -protruding termini by the enzyme DNA-polymerase of the bacteriophage T4. The T4 DNA polymerase catalyzes 5′→3′synthesis of a primed single-stranded DNA template and has a 3′→5′ exonuclease activity. It can therefore, in the presence of dNTPs, be used to fill 5′ protruding ends with dNTPs. Alternatively due to its exonuclease activity the T4 DNA polymerase can be used for the generation of blunt ends from DNA molecules with 3′ overhangs. To degrade a single-stranded 3′overhang, 1 µf DNA is incubated with 4 µl of 5x T4 DNA polymerase buffer and 1U of T4 DNA polymerase for 5 min at room temperature (or for 20 min at 11°C). The reaction is stopped by incubation for 10 min at 65°C. To fill-in a 5′-overhang, 1 µl of dNTPs (2mM) is added.

3.4.7 Ligation of DNA Fragments

The enzyme DNA ligase of the bacteriophage T4 can catalyze the formation of a phosphodiester bond between 5' phosphate and 3' hydroxyl termini in double stranded DNA. T4 DNA ligase is able to join blunt end and cohesive ends. The enzymatic activity is indicated in Weiss units (u), whereupon 1 u is equivalent to approximately 200 cohesive-end ligation units. One cohesive–end ligation unit corresponds to the amount of enzyme required to ligate 50% of *Hind*III fragments of λ DNA in 30 min at 16°C in 20 µl of the assay mixture and a 5′-DNA termini concentration of 0.12 µM. For a general standard cloning ligation purified vector and insert are combined in a molar ratio of 1: 3 (for sticky ends) or 1:5 (for blunt ends), using the following equation:

ng vector x 3 – 5 x bp insert / bp vector = ng insert

A typical ligation reaction was composed as follows:

60 ng of a 1 kb insert DNA-fragment

60 ng of a 3 kb vector-DNA fragment (backbone)

2 µl 10 x ligation buffer

1 µl T4-DNA-Ligase (1 Weiss unit / µl)

ddH_2O ad 20 µl

The reaction is incubated either for one hour at 22°C or overnight at 16°C. Subsequently the enzymatic reaction is stopped by 10 min incubation at 65°C.

3.4.8 Polymerase Chain Reaction

Polymerase chain reaction (PCR) is a method for amplification of specific DNA *in vitro.* The DNA region to be amplified is specified by selected primers. Primers are short oligonucleotides complementary to the DNA regions of the 5′ and 3′ ends of the DNA region. The length of the primers and their melting temperature is depended on various conditions (such as the C/G content within the sequence of the primer).Thermostable DNA-polymerase binds to the primed single-stranded DNA template and catalyzes the 5′→3′ synthesis of the new DNA strand.

The PCR process consists of a series of twenty to thirty five cycles; each cycle typically consists of 3 discrete temperature steps. In the *denaturation step*, the dsDNA is heated to 94°C for 20-30 sec to separate the complementary bases of the DNA strands, resulting in single strands of DNA. In the *annealing step* the temperature is lowered to 50-65°C allowing annealing to the ssDNA template. The annealing temperature is typically 3-5°C below the melting temperature of the primers. Finally, in the *elongation step* the DNA polymerase synthesizes a new DNA strand complementary to the DNA template strand by adding dNTPs that are complementary to the template in 5' to 3' direction. The elongation temperature depends on the DNA-polymerase (68-72°C). The extension time depends both on the DNA polymerase used and on the length of the DNA fragment to be amplified. At optimum temperature, the DNA polymerase will polymerize a thousand bases in one minute. The PCR run is completed by a single incubation of 3-7 min at elongation temperature.

A typical PCR reaction is composed as follows:

50-200 µg template DNA

5 µl 10 x PCR buffer complete (+ 25mM MgCl2)

0.5 µl dNTP-mix (10mM each)

0.25 µl 5′ Primer forward (100pM)

0.25 µl 3′ Primer reverse (100pM)

0.5-1.5 units Taq-Polymerase

Ad 50 µl with ddH_2O

The reaction is mixed together on ice in special PCR reaction tubes. Following the PCR an aliquot of the reaction is analyzed in respect of size and amount via agarose gel electrophoresis.

3.4.9 Colony PCR

In most PCR reactions purified DNA is used as template. However, it is possible to amplify specific DNA sequences without DNA purification by starting with a single living *E.coli* colony. This technique is known as colony PCR and provides a powerful and reliable method for the rapid detection of transformation success when primers are available which allow determination of correct ligation products by size or hybridization.

For this method, the PCR reaction mix (PCR-buffer, dNTPs, primers and *Taq*-DNA polymerase) is similar to the standard protocol. To inoculate the PCR reaction, a colony is picked with a sterile pipette tip and dabbed into the PCR tube and then placed in a correspondingly labeled culture tube. Subsequently the PCR reaction mix is added to the reaction tube and the PCR is carried out with appropriate conditions for the used primers and expected product. It is required to begin the PCR protocol with an extended time at 95°C, (e.g. 5 minutes) to ensure that complete lysis of the bacterial cells has occurred.

3.4.10 Sequencing of DNA

The sequencing method is based on a principle of Frederik Sanger according to which randomly incorporated dideoxinucleotids (ddNTPs) lead to a termination of the polymerase reaction. The four ddNTPs are coupled to dyes fluorescent in different wave length. This method is divided into two steps. First the **labeling-reaction** in order to produce a labeled source sample and second the **termination-reaction** where the synthesis of the fragments produced in the first reaction is ended by incorporation of fluorescence-labeled dideoyxnucleotides (ddNTPs). The sequencing reaction products are ethanol precipitated and the sequencing analysis is carried out with an ABI Prism 3130 xl Sequencer (Applied Biosystems). The laser detects the sequence of the fluorescence-labeled DNA fragments which are separated by capillary gel electrophoresis.

The sequencing of plasmid DNA or PCR product takes places according to the "BigDye Terminator v3.1 Cycle Sequencing Kit" protocol (Applied Biosystems):

Terminator Ready Reaction mix	8µl
Template	150ng Plasmid or BAC DNA; 10-50ng PCR product
Primer	3.2 pmol
ddH2O	Ad 20µl

The reaction occurs in analogy to a PCR, however only one primer is added. After the reaction the DNA is precipitated, ethanol washed and dried. The DNA is resuspended in 15 µl HiDi formamide and then ready to use for sequencing.

3.5 In vitro Modification and Recombination in Bacteria

One major limitation for engineering of large genomic DNA fragments in BACs or PACs is that restriction sites for endonucleases are often not located on required positions in the gene. A newer and much simpler approach is to use homologous recombination to construct the targeting vector. This new form of chromosome engineering is termed "recombineering". Efficient homologous recombineering in *E.coli* is obtained by the use of phage-encoded proteins. These so called *Red* genes of bacteriophage λ permit linear ds DNA fragments to be inserted into DNA cloned on plasmids, BACs or PACs via homologous recombination. Two *Red* genes are required for the recombination: *exo*, which encodes a 5′–3′ exonuclease (Exo) that acts on the 5′ ends of the linear dsDNA fragment to produce 3′ single-strand DNA (ssDNA) overhangs, and *bet*, which encodes a pairing protein (Beta) that binds to the 3′ssDNA overhangs created by Exo and promotes annealing to its complementary DNA strand on the cloned DNA. The recombination functions of Exo and Beta are further assisted by λ-encoded Gam protein, which inhibits the RecBCD exonuclease activity of *E.coli*. In the defective prophage expression system the expression of the recombination genes is under control a temperature-sensitive repressor. At 32°C, expression of *exo*, *bet*, and *gam* is undetectable. However, by shifting the culture temperature to 42°C for 15 minutes, expression of *exo*, *bet*, and *gam* can be induced to very high levels.

In this work the bacterial strains EL 250 and EL 350 are used, which harbour the *Red* genes for homologous recombination and the Cre recombinase (EL 350) or the Flpe recombinase (EL250).

3.5.1 Transformation of BAC DNA into Recombinant Strains

5 ml YENB media are inoculated by a single colony of the EL250 or EL350 *E.coli* strain and grown over night at 32°C to suppress the expression of the *Red* genes. The culture is centrifuged at 5000 rpm at 4°C for 5 min, resuspended in 1 ml of ice-cold water and transferred in a 1.5 ml microcentrifuge tube. The cells are washed three times with ice-cold water by centrifugation in a 4°C benchtop centrifuge for 20 seconds at 13000 x g. Finally the bacterial pellet is resuspended in ~50 µl ice-cold water and transferred to a pre-cooled 1 mm gap electroporation cuvette. Subsequently ~100 ng of BAC DNA or 1-10 ng of plasmid DNA is added and mixed by pipetting. The electroporation conditions are: 1800 V, 25 µF and 200 Ω. After the electroporation 1ml of LB medium is added, the cells are transferred to a microcentrifuge tube and incubated for 1 hour at 32°C. The bacteria are spread on LB plates with the appropriate antibiotics.

3.5.2 Recombination through Temperature Control

Before recombination, EL250 or EL350 bacteria cells are transformed (as described before) with the template plasmid or BAC, in which the targeting cassette is to be integrated within the following recombination. After successful transformation, 20 ml of YENB medium are inoculated with 2 ml overnight bacteria culture containing the template DNA. The culture is grown at 32°C until the OD_{600} reaches 0.6 (2-3h). Half of the culture is transferred into a new Erlenmeyer flask and incubated at 42°C for 15 min to activate the expression of the *Red* genes. The other Erlenmeyer flask containing the rest of the culture serves as 32°C control. After 15 min the bacteria are immediately cooled down by shaking the flasks in an ice-water bath for 2 min. The induced (at 42°C) and the control (at 32°C) bacteria are transferred into a 15 ml falcon tube, respectively and centrifuged at 4°C for 5 min at 5000 rpm. The pellet is resuspended in 1 ml of ice-cold sterile water and transferred to a 1.5 ml microcentrifuge tube. The bacteria are washed three times with ice cold water as described above. Finally the bacterial cells are resuspended in ~50 µl ice-cold water and mixed with 100 ng of the purified targeting cassette and electroporated as described above. After electroporation the cells are incubated in 900 µl LB medium for 1 h at 32 °C. The The bacteria were spread on LB plates which contained the appropriate antibiotics. The expression of these single site specific recombinases can be used to excise loxP or FRT site flanked selection markers.

3.5.3 Excision through Arabinose Induction

The bacterial strains EL350 and EL250 express the Cre recombinase and the Flpe recombinase, respectively, under the tight control of an arabinose-inducible promoter.

1 ml over night culture of BAC-targeted bacteria cells (e.g. EL350) is added to 10 ml YENB medium and grown at 32°C for 2-3 h until the OD_{600} reached 0.5. Then 100 µl 10% L(+) arabinose are added to the culture (final concentration, 0.1%) and incubated at 32°C for 1 h, in which the Cre-induction should take place. The culture is diluted 10^4 to 10^6 to obtain single colonies and streaked on plates containing the appropriate antibiotics.

If a plasmid is used instead of a BAC, the targeted plasmid has to be transformed to electrocompetent cells in which the Cre recombinase is already induced. Inducing Cre expression in cells which already contain the plasmid will lead to a complete loss of the plasmid.

3.6 Immunohistochemistry

For immunohistochemistry of brain slices and heart tissue the mouse has to be fixed by perfusion with paraformaldehyde (PFA) infusion. Mice are anaesthetized by intra-peritoneal injection of ketamine hydrochloride and xylazine hydrochloride. The thorax is opened to expose the heart. A canula is introduced into the heart and the mouse is perfused through the ascending aorta with Sörensen buffer for 3 min to flush out the blood and subsequently 4% paraformaldehyde fixative for ~ 10 min. The brain is removed from the skull, postfixed for 24-36 h in 4% PFA at 4°C and stored in 0,2% PFA in phosphate buffer at 4°C until use. The tissues are sliced with a vibratome in 50µm thick sections.

3.6.1 DAB Method

The DAB staining is based on a peroxidase system with an enhanced sensitivity without increased background staining. This technique employs an unlabeled primary antibody, followed by biotinylated secondary antibody and then a preformed **A**vidin and **B**iotinylated horsereadish peroxidise macromolecule **C**omplex (ABC technique), which amplifies the signal (Vectastain ABC Kit, Vector Laboratories). Tissue sections are permeabilised in 1% H_2O_2 in 1x PBS for 10 min at room temperature and washed with 1xPBS three times for 10

min. For blocking unspecific binding sites sections are incubated in 2% normal goat serum in 1% BSA/0.3% Triton X-100/1x PBS (day 1 buffer) for 1h at room temperature. The primary antibody anti-GFP (Molecular Probes Invitrogen) is 1:5000 diluted in day 1 buffer and the slices are incubated at 4°C over night. After two times washing in 0.3% BSA/0.1% Triton X-100/1x PBS (day 2 buffer) slices are incubated for 1h at room temperature in the secondary antibody for the DAB staining: biotinylated anti-rabbit IgG (H+L) (Vector Laboratories) 1:600 diluted in day 2 buffer. Slices are again washed twice in day 2 buffer. To enhance the staining reaction, sections are incubated with an avidin-biotin complex for 1 h followed by 1x washing in day 2 buffer and two washing steps with 1xPBS. The sections are incubated in DAB solution (0.4 mg/ml) in 20 mM Tris-HCL solution with 0.012% H2O2 until a staining is observed. The reaction is stopped by washing three times with 1x PBS. The stained slices are mounted on glass slides and cover-slipped with Eukitt. Slices are imaged with the stereoscope Stemi 2000-C (Zeiss).

3.6.2 Immune Fluorescence

For permeabilisation, sections are incubated in 0.1% Triton X-100 for 30 min at 4°C and washed with 1x PBS three times for 10 min. Blocking is achieved by incubation in 10% normal goat serum (NGS) in 1x PBS for 1h at room temperature. The slices are incubated in 10% NGS with the primary antibody over night at 4°C. After the sections are washed three times in 1% NGS they are incubated with the second antibody in 10% NGS for 1h at room temperature to visualize the first antibody. The slices are washed three to four times with 1x PBS and mounted on glass slides with Dako fluorescent mounting medium.
For imaging the fluorescence microscope Axioscop 2 plus (Zeiss) and the Nikon A1R 4 laser line confocal microscope at the Nikon Center are used.

3.7 Cultivation of Mammalian Cells

All tissue culture described is carried out under sterile conditions using sterile plastic ware, media and solution. All work is done under a sterile cell culture hood. All cell lines are incubated at 37°C in humidified cell culture incubators with 5% $C0_2$.

3.7.1 Hela Cells

Hela cells are grown in DMEM medium (Gibco) substituted with 10% FCS and 100 µg/ml (1x) Penicillin/Streptomycin (Gibco) to prevent bacterial contamination.

The cells are passaged by aspirating of the culture medium and by washing the cells with PBS. PBS-EDTA without magnesium and calcium is added and the solution is incubated for ~10 min until the cells start to detach from the bottom of the culture dish. The cell suspension is pipetted gently up and down and is transferred to a 15 ml Falcon tube. The cells are pelleted by centrifugation at 270xg for 5 minutes. The supernatant is aspirated and the cells are resuspended in an appropriate volume of Hela medium to dilute the cells.

3.8 DNA Transfer in Mammalian Cells

The analysis of gene expression and regulation requires a methodology to transfer foreign DNA into cells. This can be done by several chemical or by physical methods.

3.8.1 Transient Transfection by Lipofection

Transient transfection is done with the cationic lipid based transfection reagent Lipofectamin 2000 from Invitrogen. In this method the DNA molecules are enclosed by lipid-like vacuoles, which can easily merge with the cell membrane.

Prior to transfection, cells are growing at 90-95% confluence. Both Lipofectamine 2000 and DNA are mixed with serum-free Opti-MEM media. The quantity of each is dependant on the type of culture dish. After 5 min incubation in OPTI-MEM, the Lipofectamine 2000 and DNA are combined and incubated for 20 minutes at room temperature. 500 µl mixture of DNA:Lipofectamine 2000 complexes are then added to the cells, which are already covered by 1.5 ml of normal DMEM medium and the cells are incubated overnight.

3.9 Generation of Genetically Modified Mice

3.9.1 Preparation of Mouse Embryonic Fibroblasts (MEFs)

To maintain ES cells in a proliferative, undifferentiated state *in vitro* they should be cultured on a monolayer of mitotically inactivated embryonic fibroblast cells. For preparation of MEF cell stocks, pregnant mice are sacrificed 13.5 days post-coitus. The uterus is isolated and

transferred into a 10 mm dish containing PBS. The embryos are dissected away from the uterus and the membranes and transferred into a new dish with PBS. All internal organs and the heads are removed. The carcasses are again washed in PBS to remove as much blood as possible. The carcasses are then transferred into dry dish and cut into pieces of ~1 mm in diameter with scissors and forceps. The pieces are resuspended by adding 2 x 5 ml of 0.05%.

3.9.2 Cultivation of Embryonic Stem Cells (ES cells)

Embryonic stem cells are pluripotent cells derived from the inner cell mass (ICM) of blastocyst-stage embryos. ES cells can be maintained in an undifferentiated stage for many passages *in vitro* by using stringent culture conditions. Permanent mouse carrying genetic alterations introduced into ES cells can be obtained by transmitting the mutation through the germline by generating ES cell chimeras.

A number of different ES cell lines are available. For this project the 129/Sv-derived R1 cell line (A. Nagy) was used.

All ES cell culture procedures described must be carried out under sterile conditions using sterile materials, media and solutions. All work is done in a laminar flow hood. ES cells are cultured in a humidified incubator (5% CO_2, 95% rH) at 36.4°C.

3.9.2.1 Growth and passaging of ES Cells

ES cells are cultured on monolayers of mitotically inactivated feeder cells or on gelatinized tissue culture plated in the presence of leukemia inhibitory factor (LIF). When cells reach sub-confluence, they are passaged at a dilution which will permit them to be cultured for 48h until this density is reached again. To trypsinize the ES cells, the medium is aspirated and the cells are washed twice with 1x PBS and 2 ml of trypsin/EDTA are added. After incubation of ~5 min at 37°C cells begin to detach from the plate as small clumps. To stop trypsination, 5 ml of ES cell medium are added and the suspention is pipeted up and down to break the cell clumps. The cells are transferred into a 15 ml tube and pelleted by centrifugation for 5 min at 270 *g*. The cells are resuspended in an appropriate volume of fresh ES cell medium for a dilution of 1:5 to 1:7, depending on their growth rate. The ES cell medium is changed every day until the cells reach sub-confluence.

3.9.2.2 Freezing and of thawing of ES Cells

ES cells can be frozen in freezing medium containing 25% FBS and 10% DMSO at a density of 5-10 x 10^6 cells/ml. Cells are trypsinized from a 10 mm dish as described before. The pellet is resuspended in 3 ml of freezing medium. 1 ml of the cell suspension is aliquoted into freezing vials on ice. For slow freezing, the vials are transferred to a Styrofoam box or a slow-cool container, and then into a -80°C freezer. For longer storage cells are transferred to liquid nitrogen.

For thawing it is important to thaw the cells quickly and to remove the DMSO-containing medium as soon as possible. Frozen cells are thawed in a 37°C water bath and transferred into a 15 ml tube containing 10 ml of pre-warmed feeder cell medium. After centrifugation at 270 *g* for 5 min the supernatant is aspirated and the pellet resuspended in 10 ml of ES cell medium and plated on a 10 mm dish with feeder-layer or gelatine-coated. The medium is changed the next day to remove any debris.

3.9.3 Homologous recombination in ES cells

3.9.3.1 Preparation of DNA

A large scale preparation of the gene targeting vector DNA is prepared (30-40 µg DNA for one electroporation). After restriction digest to linearize the gene targeting vector, the DNA is purified over a low-melting agarose gel as described before to separate the genomic DNA from the BAC DNA. To purify the DNA from the agarose, the gel piece is melted and digested by agarase. The DNA is ethanol precipitated, washed twice in 70% ethanol and resuspended in an appropriated volume of sterile PBS.

3.9.3.2 Electroporation of ES cells

This method is used to introduce DNA into ES cells for gene targeting experiments. Technically this method is relatively simple compared to others. DNA can be electroporated into ES cells by application of a high voltage electrical pulse to the suspension of cells and DNA. After this pulse the DNA enters the cell through pores in the cell membrane.

The R1 ES cells (Passage #16 from A. Nagy, Toronto, Canada) are freshly thawed and cultured for at least two passages on feeder cells as described previously. Then a sub-confluent 10 cm dish (60-80 % confluence) is trypsinized and pre-plated 20-25 min in the

incubator to separate the feeder cells from the ES cells. The ES cells are collected, resuspended, counted in a Neubauer chamber and are kept on ice. The cell concentration is adjusted to 1x 10^7 cells/ml with sterile PBS.

For electroporation 800 µl of ES cells (1x10^7/ml) are mixed with 30-40µg of digested and purified gene targeting DNA. The mixture is transferred to a pre-cooled 4 mm gap electroporation cuvette and electroporated at 240 V, 500 µF and 0 Ω in the BTX ECM 630 electroporator. The cuvettes are removed from the cuvette holder and put on ice for 20 minutes. The cells from the cuvette are diluted in an appropriate volume of ES medium (normally 30 ml of medium for three gelatinized 10 cm dishes). The cells are incubated overnight and the next morning the medium was changed.

3.9.3.3 Selection and isolation of drug-resistant clones

Two days after electroporation, 200 µg/ml G418 and one day delayed 2 µM Gancyclovir is added to the medium to select for recombinant ES cells. The medium is changed every day since Gancyclovir can brake down and become toxic. After 3 days of selection, widespread cell death appears. After about 8 to 10 days of selection individual drug-resistant colonies appear and are large enough for picking (0.5-2 mm).

For picking, the drug-resistant ES cell colonies are marked on the bottom of the plate. The ES cell containing plates are washed twice with PBS and left in PBS during picking. Under a dissection microscope drug-resistant colonies of approximately the same size and shape are picked up with a Gilson P20 pipette adjusted to a volume of 6 µl with yellow tips. Each colony in PBS is transferred into one well of a 96-well V-shaped plate containing 35 µl of Trypsin/EDTA at room temperature. After picking 24 clones the plate is incubated for ~10 min at 37°C in the incubator until cell clumps break up. The reaction is stopped by adding 100 µl of medium to each well. The cells are mixed by pipetting up and down and transferred to a 96-well plate containing feeder cells. Each V-well is washed again with 100µl of medium and added to the same well of the 96-well plate with feeders. The plate is incubated at 37°C in the incubator and the medium was changed daily. In two to three days the cells should have reached ~80% confluence and are passaged, frozen and replicated for analysis. If the colonies have not grown to confluence in 2-3 days, the cells are 'tryplated' as followed: the cells are washed with PBS and trypsinized with 35 µl for 5 minutes at 37°C. 200 µl of medium is added and the cell clumps are broken up by pipetting up and down. 12-

24 hours later the medium is changed. The procedure of expansion and freezing of the ES cell clones is depicted in Fig. 6.

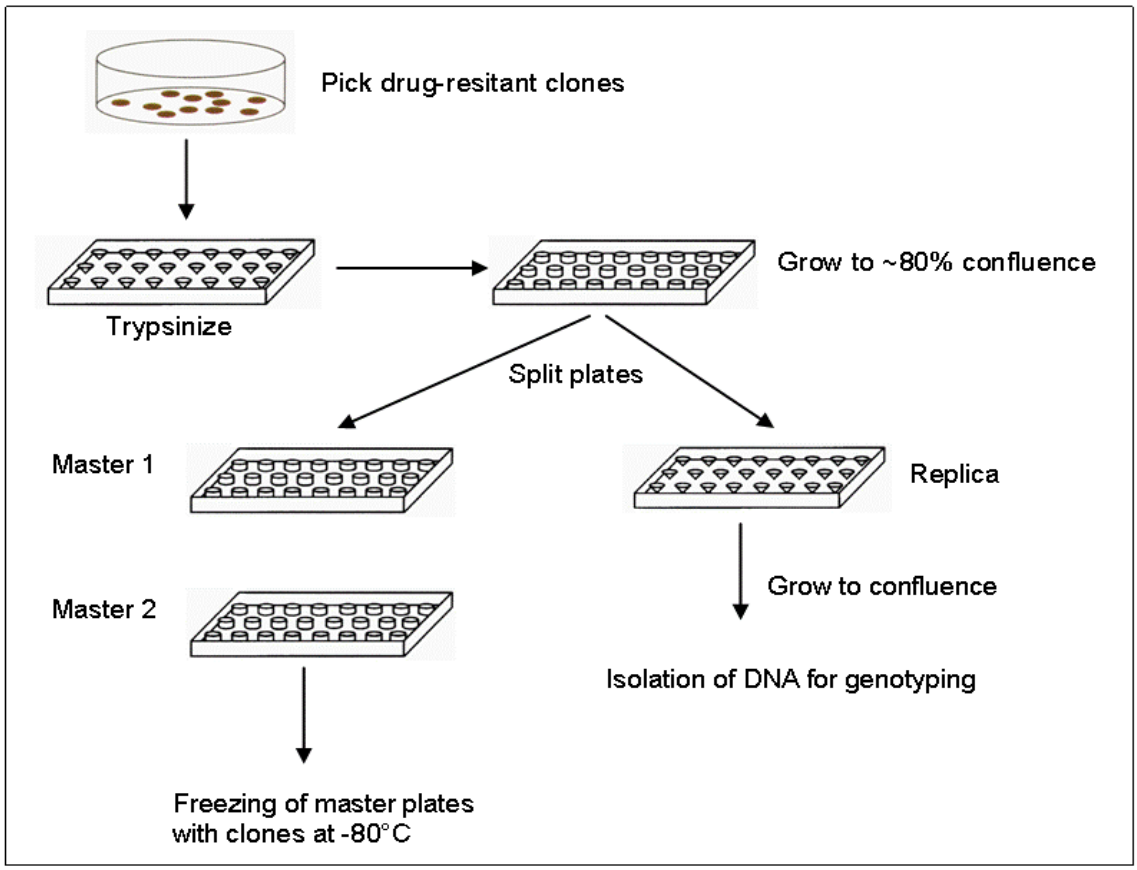

Fig. 6: Expansion and freezing of drug-resistant clones.

3.9.3.4 Freezing drug-resistant clones and preparation of replica plates

One set of gelatinized 96-well plate containing 200 µl medium and two sets of V-shaped master plates containing 60µl cold 2x freezing medium are prepared and kept on ice. The medium is aspirated from the growing ES cells and they are washed twice with 200 µl PBS. The cells are trypsinized with 50 µl of Trypsin/EDTA and incubated for 10 minutes at 37°C in the incubator. After cells have detached, the reaction is stopped by adding 120 µl of medium. 60 µl of the cell suspension is transferred in each V-shaped master plate containing 60 µl of pre-cooled 2x freezing medium in each well and mixed by pipetting up and down. 100 µl of mineral oil is layered on top of each well containing ES cells in freezing medium. The plate is completely sealed with Parafilm, wrapped into aluminum foil and was transferred into a pre-cooled Styrofoam box to a -80°C freezer. The remaining cell suspension (~50 µl) is transferred into the 96-well replica plate containing 200 µl of medium per well and returned

into the incubator. When confluent the cells are transferred into a 24-well plate to obtain more cells for the following DNA isolation. The ES cells are kept in culture until cells are grown overly confluent for DNA isolation.

3.9.4 Identification of Genetically Modified ES cells

3.9.4.1 Isolation of DNA from ES cell colonies

The genomic DNA of the drug-resistant ES colonies is extracted from over-confluent cells of the replica plates. The medium is aspirated from each well and the cells are washed twice with PBS and trypsinized with 35µl of Trypsin/EDTA. When cells have detached they are transferred into a reaction tube and centrifuged. For DNA isolation the DNeasy Tissue Kit (Qiagen) is used according to the manufacturer´s instructions. The DNesay Tissue Kit uses advanced silica-gel membrane technology for fast and efficient purification of total cellular DNA. The purified DNA is free of contaminants and enzyme inhibitors and is ready to use for PCR and Southern blotting.

The general procedure is fulfilled as follows:

- After centrifugation for 5 min at 300 x g, the cells are resuspended in 200 µl PBS.
- For lysation of the cells 20 µl Proteinase K and 200 µl buffer AL are added to each sample, mixed and incubated at 55°C for 1 h.
- To precipitate the DNA 200 µl ethanol (96-100%) are added and mixed.
- The mixture is transferred into a DNeasy Mini Spin Column and centrifuged at 8000 rpm for 1 min.
- To wash the DNA, 500 µl buffer AW1 is added and centrifuged at 8000 rpm for 1 min.
- 500 µl washing buffer AW2 is added and centrifuged at 13,200 rpm for 3 min to dry the DNeasy membrane.
- For elution the DNeasy column is placed in a clean 1.5 ml reaction tube and 100 µl elution buffer AE are pipetted onto the membrane.
- The membrane is incubated at room temperature for 1 min and then centrifuged for 1 min at 8000 rpm.
- The eluted DNA is stored at -20°C.

3.9.4.2 PCR genotyping of ES cell clones

After the selection of single resistant clones and DNA isolation the clones were genotyped by PCR. To demonstrate the correct site-directed integration by homologous recombination into the genomic locus, two primers were designed; one which binds in the inserted DNA sequence of the targeting vector, e.g. the *neo* cassette, and the other one which binds outside of the homology arm. For amplification of the long PCR fragment specific to correct integration the Expand Long Range dNTPack from Roche was used.

3.9.4.3 Expansion and freezing of targeted ES cell clones

The 96-well plate with the positive targeted ES cell clones is removed from the -80°C freezer and unwrapped. The plate is quickly warmed at 37°C in the incubator until the ice crystals disappear (~ 5 minutes) and the outside of the plate is cleaned with 70% EtOH. When the mineral oil has thawed, 100 µl of pre-warmed ES medium is added under the oil to each well containing a targeted positive clone and the cells are transferred to a 6-well plate with feeders in 2 ml of ES medium. The original 96-well is rinsed again with 200 µl of ES medium and added to the same well in the 6-well plate. The positive cells are incubated at 37°C in the incubator and the medium is changed after 6 hours to remove residual DMSO and mineral oil. When the cells reach semi-confluence after two days, the cells are passaged to a 10 cm plate with feeders. If the cells do not reach semi-confluence they are tryplated as described previously. When cells reach semi-confluence, the cells from one 10 cm plated in freezed in 3 cryo vials as described before.

3.9.5 Cre-mediated Recombination in ES Cells

The *loxP*- or *FRT*-flanked heterozygous positive targeted ES cell clones can be analyzed for their functionality by *in vitro* recombinase-mediated deletion. Therefore the ES cells are transiently transfected with a *Cre* expressing plasmid in cell culture.

The targeted ES cells are grown for at least two passages in G418 (150-250 µg/ml) to eliminate any cell clones that have randomly lost the *neo* resistant gene. 0.5-1 x 10^7 G418-resistent ES cells are electroporated with 20-30 µg supercoiled recombinase vector (pMC1-Cre) and plated at a low density of 0.5x10^7 cells per 10 cm dish on feeder in ES medium without G418. Two days after electroporation, the cells are trypsinized to obtain single cells

and plated at 10^3 cells/ 10 cm dish. Approximately five days after re-plating at low density, when colonies have established, colonies are picked as described before. Following trypsination half of the cells are transferred to a master 48 well plate containing feeders and ES medium and the other half is transferred to a gelatinized 48 well plate with ES medium containing G418. Cre-mediated recombination should transfer G418-sensitivity to the colonies. After 3-5 days the desired G418-sensitive clones are identified and the sibling G418-sensitive clones from the master plate are expanded, frozen and genomic DNA is purified for later analysis.

3.9.6 Preparation of positive ES cells for blastocyst injection

R1 ES cells are derived from the 129/Sv mouse strain, which have an agouti coat colour. These cells are injected into blastocysts derived from black C57Bl/6 mice.

Four days prior to injection, mitomycin treated feeder cells are thawed at 37°C and plated onto three 6 cm plates. 3 days before injection a vial containing the correctly targeted ES cell clone is thawed and plated onto the 6 cm plate. Two days before injection the subconfluent cells are split onto two 10 cm dishes with a ratio of 1/3 and 2/3. 7 am on the injection day, the plate with the optimal cell density is chosen (when the colonies are grown to dense the quality of the ES cells is affected; when there are too few ES cells on the plate the enrichment for injection is difficult. The medium is changed 2 hours before collecting the cells. 9 am on the injection day, the plate is washed twice with PBS and trypsinized with 2 ml of Trypsin/EDTA. After ~5 minutes the cells are resuspended by gently pipetting up and down with a polished Pasteur pipette. The reaction is stopped by adding 2 ml of medium and pipetted again to get a single cell suspension. 8 ml of medium is added and the cells are centrifuged at 270 x *g* for 5 minutes. The supernatant is aspirated and the cells are resuspended in 10 ml of medium. To separate the ES cells from the feeder cells, the cells are pre-plated on a new gelatinized 10 cm plate and incubated at 37°C. After 20-30 min the feeder cells attach to the bottom of the plate whereas the ES cells float in the supernatant. The supernatant is collected and plated onto a new gelatinized 10 cm plate. The incubation is repeated and if there are still too many feeder cells present, the cells are pre-plated for a third time. Then the supernatant with the ES cells is centrifuged at 270 x *g* for 5 minutes and the pellet is resuspended with a polished Pasteur pipette in 1 ml of ES medium plus 20µl/ml 1 M

HEPES buffer (final concentration 20 mM). The cells in the 15 ml falcon tube are put on wet ice and are ready for blastocyst injection.

3.9.7 Germ line transmission of chimeric mice

The offspring generated through injection of the targeted ES cells into the blasocysts are called chimeras. These chimeras are animals with two different populations of genetically distinct cells. They harbour a cell population of agouti-coloured R1 ES cells from the 129/SvJ mouse strain and a cell population of cells from the blastocyst donor, the black-coloured C57Bl6 mouse strain. On the basis of coat colour the contribution of the agouti-coloured ES cells to the chimeras can be easily seen and they usually have a more or less speckled coat colour of black and agouti.

The mutant allele of the chimera has to be transmitted through the germ line in order to get a genetically modified mouse line. In general the degree of coat colour chimerism of a particular animal correlates with the degree of germ line contribution. Therefore male chimeras with a high percentage of agouti-coloured coats (> 60%) are mated with female C57/BL6 mice. As the agouti colour is genetically dominant over the black coat colour, the genetically modified gene can not be transmitted to the offspring with black coats. In contrast, the agouty-coloured offspring are heterozygous (129/Sv / C57Bl6), they harbour one allele from the 129/Sv and one from the C57Bl6 genome. In these animals either the mutant or the wildtype agouti allele can be transmitted, so every agouti offspring mouse has to be genotyped.

For the analysis of the agouti coloured-offspring DNA is prepared from tail biopsies and analyzed by PCR or Southern Blot. The animals which are PCR positive for the genetic modification become the founders of the mutant mouse line and are backcrossed on the C57BL6 strain to get a pure genetic background of C57BL6 for the behavioral analysis of the mutant animals.

3.9.8 Animal husbandry and breeding

The animals are housed in the animal facility of the Central Institute for Mental Health, approved by the Regierungspräsidium Karlsruhe for animal husbandry and breeding. The animals are maintained under standard housing conditions in line with the guidelines of the

FELASA (Federation of European Laboratory Animal Science Association) and the GV-SOLAS (Society of Laboratory Animal Science). The animal rooms are constantly air-conditioned with a temperature range of 20-22°C and a humidity of ~50%. A constant biorhythm for the animals is guaranteed by fixed light and dark phases (day from 6 am to 6 pm). The animals are maintained according to their size and the experiment in clear Makrolon cages of type II and III and food and water is provided *ad libidum.*

4 Results

4.1 Generation of the $Ca_V1.3$-GFP^{flex} Mouse Line

A conditional knockout mouse line of the Cav1.3α1 subunit was generated using the phage P1 derived *Cre*/*loxP* system for temporal and local restriction of the knockout. Additionally, the FLEX system was used (Schnutgen et al., 2003), leading to inactivation of the floxed exon by an irreversible inversion between different *lox* sites after *Cre* expression, whereas the reporter gene eGFP is switched on. Exon 2 was chosen to be flanked by *loxP* sites, as the ubiquitous knockout of Cav1.3α1 showed a complete silencing of the gene by interrupting this exon (Platzer et al., 2000). To design a targeting vector for homologous recombination in embryonic stem (ES) cells, a genomic fragment containing exon 2 of *Cacna1d* was obtained. We used the mouse genomic DNA clone J14279Q4 (RZPD Berlin), containing the required DNA sequence. The vector was a cosmid isolated from a LAWRIST7 129 mouse strain genomic library. The genomic insert of the cosmid was tested by restriction digests and sequencing to verify the correct genomic DNA fragment containing the required exon 2.

4.1.1 Construction of the Targeting Vector BAC.Cav1.3-GFP^{flex}

A targeting vector is designed to recombine with and mutate a specific chromosomal locus. Here a replacement vector was used which replaced the coding region of the target in the genome by the mutated region. The fundamental elements for this vector were the homology to the target locus, a positive selection marker and a linearization site outside of the homology arm of the vector. Additionally, a negative selection marker was used to enrich the populations of transfected cells for targeted homologous integration events.

4.1.1.1 Cloning Strategy of the $Ca_V1.3$-GFP^{flex} Vector

For this knockout a new strategy was used, monitoring the *Cre*-mediated recombination in the transgenic mouse at the level of individual cells (Schnutgen et al., 2003). The so called FLEX switch allows a *Cre*-dependent genetic switch where the expression of a reporter gene like eGFP is switched on, while the expression of the Cav1.3α1 gene is turned off. Prerequisite for this switch is the availability of wild-type *loxP* and non-compatible mutant

lox sites, which differ in the spacer region, thus illegitimate recombination between these different sites can not occur (Wong et al., 2005). The exon 2 of *Cacna1d* was flanked by one pair of WT *loxP* sites and one pair of mutant *L3* sites, with an alternate organization and head-to-head orientation within each pair, leading to inversion of the floxed cassette after *Cre* expression. Next to the exon 2 an exon trapping cassette was inserted in inverted orientation. The exon trapping cassette consists of a promoterless reporter gene eGFP with an upstream general adenovirus splice acceptor and a downstream transcriptional termination sequence (polyadenylation sequence) (Schnutgen et al., 2005). As positive selection marker the construct contained a *FRT*-flanked neomycin resistance gene (*neo*). The 2.6 kb 5′ homology arm, containing exon 1a and the 5.6 kb 3′ homology arm, containing exon 3, served for homologous recombination. Downstream to the 3′ homology arm a thymidine kinase (TK) from Herpes simplex virus was introduced as a negative selection marker (Fig. 7).

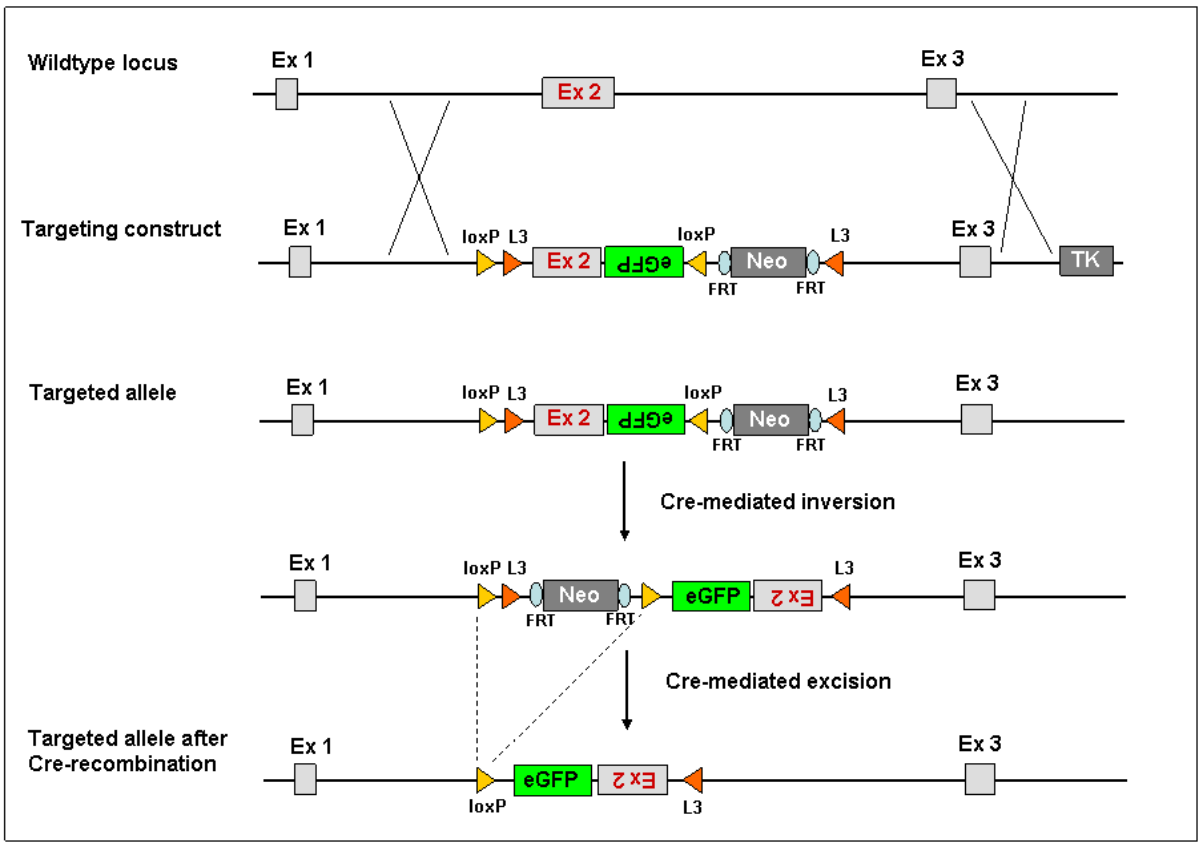

Fig. 7: Targeting strategy of the conditional knockout Cav1.3-GFP^{flex}. After *Cre*-expression the targeting can be tracked and visualized by the reporter gene eGFP.

The protocol for creating the targeting construct was adopted from Neal G. Copeland (Liu et al., 2003). Since it may be difficult to insert DNA fragments into large genomic DNAs due to the lack of unique restriction enzymes, a system based on phage recombination was used in some cloning steps. This homologous recombination system enables genomic DNA in BACs to be modified and subcloned, without the need of restriction enzymes and DNA ligase (Copeland et al., 2001). This new form of chromosome engineering is called recombineering.

4.1.1.2 Subcloning DNA into a Plasmid

Modifications of large constructs like BACs or cosmids using restriction enzymes is difficult as they are low-copy vectors with low yield. In addition, large DNAs can be unstable and break easily during purification. Subcloning a large genomic DNA fragment from a BAC or cosmid into a high-copy plasmid can circumvent some of these problems. The DNA fragment containing Cav1.3α1 exon 2 was cut out of the cosmid due to the presence of unique restriction enzyme sites 2.95 kb upstream (*NotI*) and 5.8 kb downstream (*FseI*) of *Cav1.3α1* exon 2, respectively. This fragment was sticky cloned into the high-copy plasmid pMCS-5 that is further referred to as pMCS-5.Ex2.

4.1.1.3 Targeting the First loxP and L3 site into the Subcloned Plasmid DNA

The first *loxP* and *L3* site were introduced into the subcloned DNA upstream of *Cacna1d* exon 2. This was achieved by inserting a *L3* site and a *loxP*-flanked *Neo* resistant cassette via recombineering into the subcloned plasmid DNA, and by subsequent removing of the *Neo* cassette via *Cre* recombination in E.coli. Therefore a minitargeting vector was cloned using the pL452 plasmid. pL452 contains a floxed *neo* gene which is driven by a hybrid PGK-EM7 promoter. PGK permits efficient *neo* expression in mammalian cells, whereas EM7 allows *neo* to be expressed in bacterial cells. Removing the *neo* cassette by expression of the *Cre* recombinase leaves behind a single *loxP* site at the target locus. Downstream of the floxed *neo* cassette the *L3* site was cloned using the *BamHI* restriction site. The *L3* site was generated by annealing oligonucleotides, containing a *BamHI* restriction site at both ends. The correct orientation of *L3* was confirmed by sequencing. To introduce the floxed *neo* gene and the *L3* site into the subcloned genomic DNA, it was flanked by two arms of 100-300 bp DNA

homologous to the targeting site. These homology arms were generated by PCR amplification, using the subcloned genomic DNA in the pMCS-5 plasmid as template. For this purpose, primer pairs were designed containing *SalI* and *EcoRI* (for homology arm CD, 180 bp) or *NotI* and *SacII* (for homology arm EF, 120 bp). These restriction sites allow for the direct cloning of the homology arms into pL452. Following PCR amplification, the products were restriction digested and ligated to the pL452 vector, flanking the *L3* site and the floxed *neo* cassette. This plasmid was referred to as minitargeting vector (Fig. 8).

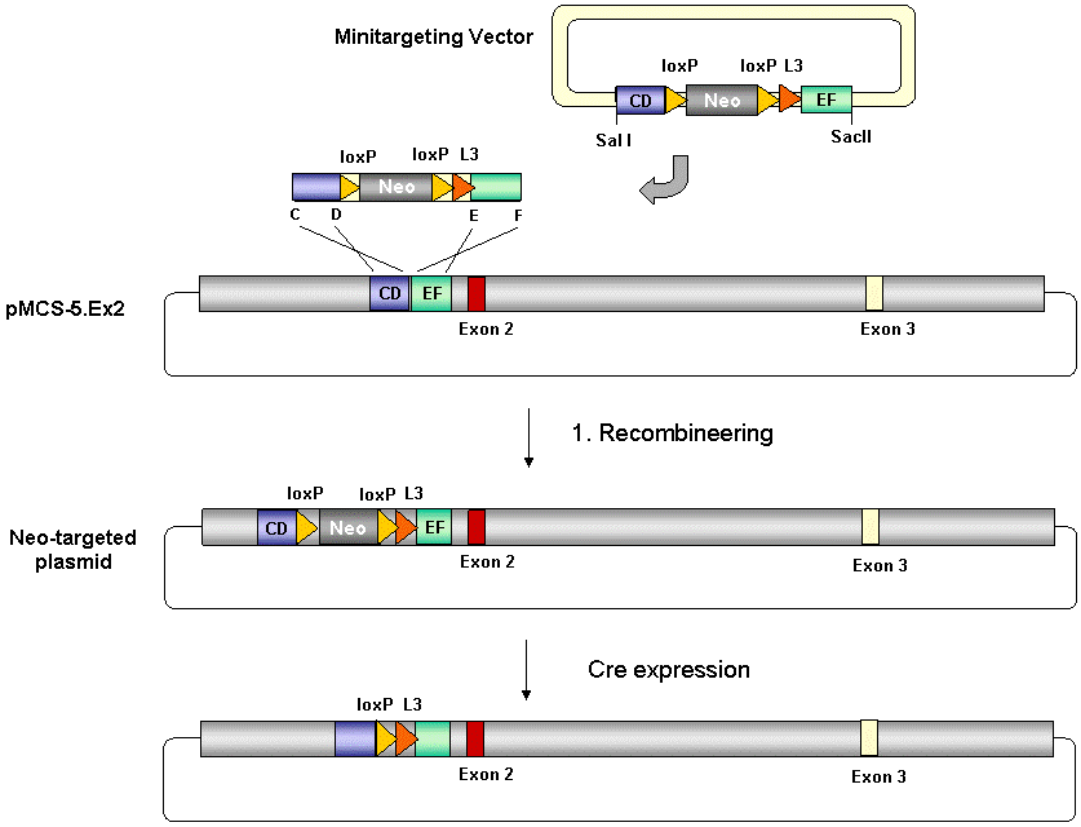

Fig. 8: Targeting of the first *loxP* and *L3* site into the subcloned genomic DNA in pMCS-5. The first targeting cassette including a floxed Neo cassette and a downstream L3 site was introduced upstream of *Cav1.3α1* exon2. Cre-mediated excision between the two loxP sites leaves behind a single *loxP* and a *L3* site.

The recombination was achieved in E.coli EL350 cells. Therefore the floxed *neo* gene and *L3*, together with both homology arms, were excised from the vector backbone by *SalI* and *SacII* for recombination. 150 ng of the purified cassette was electroporated into EL350 cells which were already transfected with pMCS-5.Ex2. In E.coli EL350 cells, the homologous recombination functions encoded by the *red* genes can be controlled by temperature (Lee et

al., 2001). Furthermore, these cells contain the *Cre* recombinase which is under the control of an arabinose-inducible promoter. The transfected EL350 cells had been induced for *Red* recombination functions by prior growth at 42°C for 15 min. Transformed cells were selected by their kanamycin resistance which were conferred by *neo*. Six of the resistant colonies were picked and examined by restriction enzyme digestion. All six colonies had the correct integration.

Next the floxed *neo* cassette had to be removed which will lead to a single *loxP* site. This was accomplished by inducing the *Cre* recombinase in the transfected EL350 cells by prior growth in arabinose-containing media for 1h. The cells were plated on ampicillin plates and, as control, on kanamycin plates. As *Cre*-mediated recombination is highly efficient, the kanamycin plates should have no or little colonies. The ampicillin plate was full of colonies, whereas the kanamycin plate showed only a few colonies. Ampicillin-resistant (Amp^r) colonies were checked for their kanamycin sensitivity and restriction digestion pattern to make sure that the floxed *neo* gene was properly excised. All picked Amp^r colonies were kanamycin sensitive and contained a single *loxP* site at the targeted locus.

4.1.1.4 Insertion of a Second Targeting Vector Downstream of Exon2

The next step was to introduce the eGFP reporter gene and the second *L3* and *loxP* site into the subcloned DNA downstream of *Cav1.3α1* exon 2. This was obtained by cloning a second targeting vector, using the plasmid pBluescript as backbone. A *FRT*-flanked *neo* cassette with an additional *loxP* site was cut out of pL451 and cloned via *EcoRI* and *BamHI* into pBluescript in that way, that the first and the second *loxP* site were in head-to-head orientation. Similar to the *neo* cassette used for the first targeting, this *neo* gene works also efficiently in both *E. coli* and mouse ES cells. *FRT* is the DNA recognition site for *Flp* recombinase which catalyzes the excision of DNA between these two *FRT* sites. The second *L3* site was cloned via *BamHI* downstream of the *FRT*-flanked *neo* cassette, also in head-to-head orientation to the first *L3* site. Next the pA-eGFP-SA was introduced via the *XhoI* restriction site downstream of exon 2 and upstream of the second *loxP* site. The *eGFP* gene was inserted in an inverted way, so that the polyadenylation site (pA) was 5′ and the splice acceptor (SA) 3′ of the gene. This ensures that *eGFP* was not expressed before *Cre* expression and the resulting switch. The last step of generating the second targeting vector was to introduce the two homology arms. Therefore,

the primer pairs G and H, containing the restriction sites *KpnI* and *ApaI*, respectively, and the primer I and J which contain *NotI* and *SacII* were generated. With these primers the two arms were amplified that are homologue to the targeting locus downstream of exon 2 (Fig. 9).

Since a plasmid like pMCS-5 would not tolerate such a large insert and become instable, the subcloned DNA fragment containing *Cav1.3α1* exon 2 and the first *loxP* and *L3* site was cloned into a BAC with an already inserted HSV-TK for subsequent negative selection in ES cell targeting.

The cassette with the second *loxP* and *L3* site, eGFP and the *FRT*-flanked *neo* gene was introduced into the subcloned DNA downstream of exon 2 in the same manner used to introduce the first *lox* sites. This conditional knockout targeting vector was named BAC.Cav1.3-GFP^{flex}.

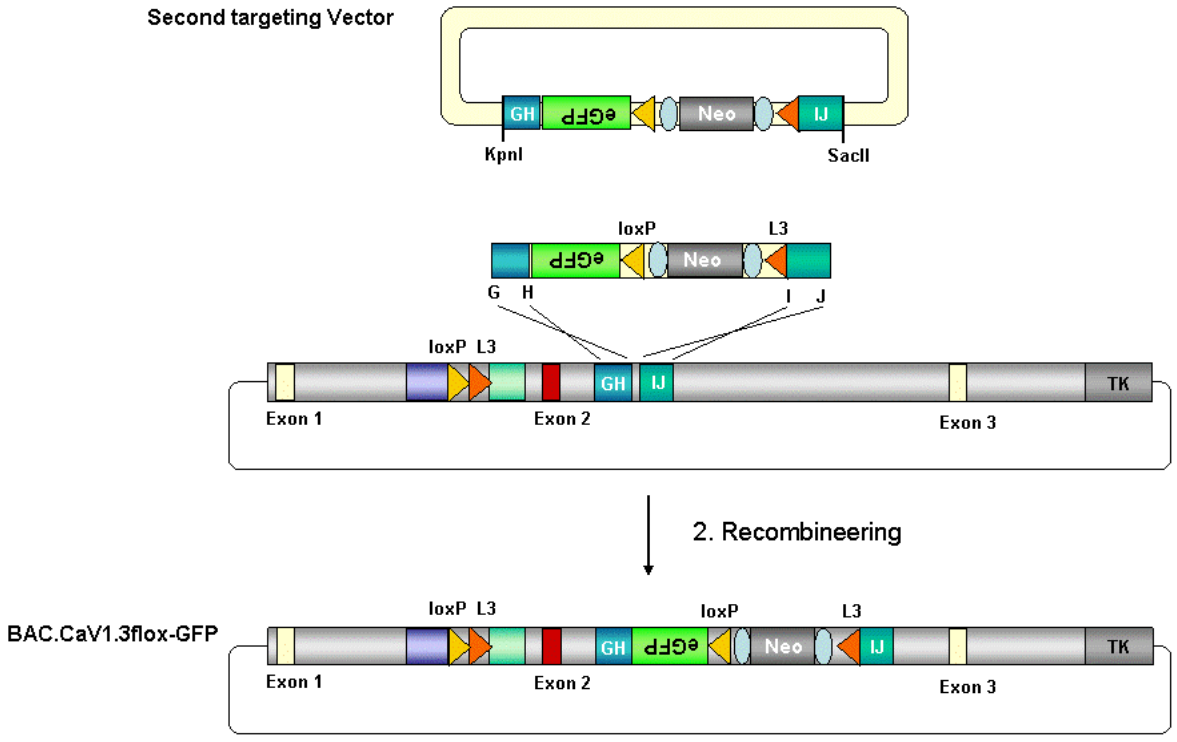

Fig. 9: Insertion of the second targeting cassette downstream of *Cav1.3α1* exon 2. The second targeting cassette contains a promoterless reporter gene eGFP with a universal splice acceptor and a polyadenylation site in inverted direction, a reverse *loxP* and *L3* site and a *FRT*-flanked *neo* cassette.

To functionally test the *loxP* and *L3* sites, the BAC was transformed into E.coli EL350 cells and the expression of the *Cre* recombinase gene was induced by arabinose. This led to an inversion of exon 2 and eGFP between the *lox* sites, whereby the *FRT*-flanked *neo* cassette

was excised. The *Cre*-mediated inversion was confirmed by restriction analysis, PCR and sequencing. The PCR strategy to test the switch is shown in Fig. 10.

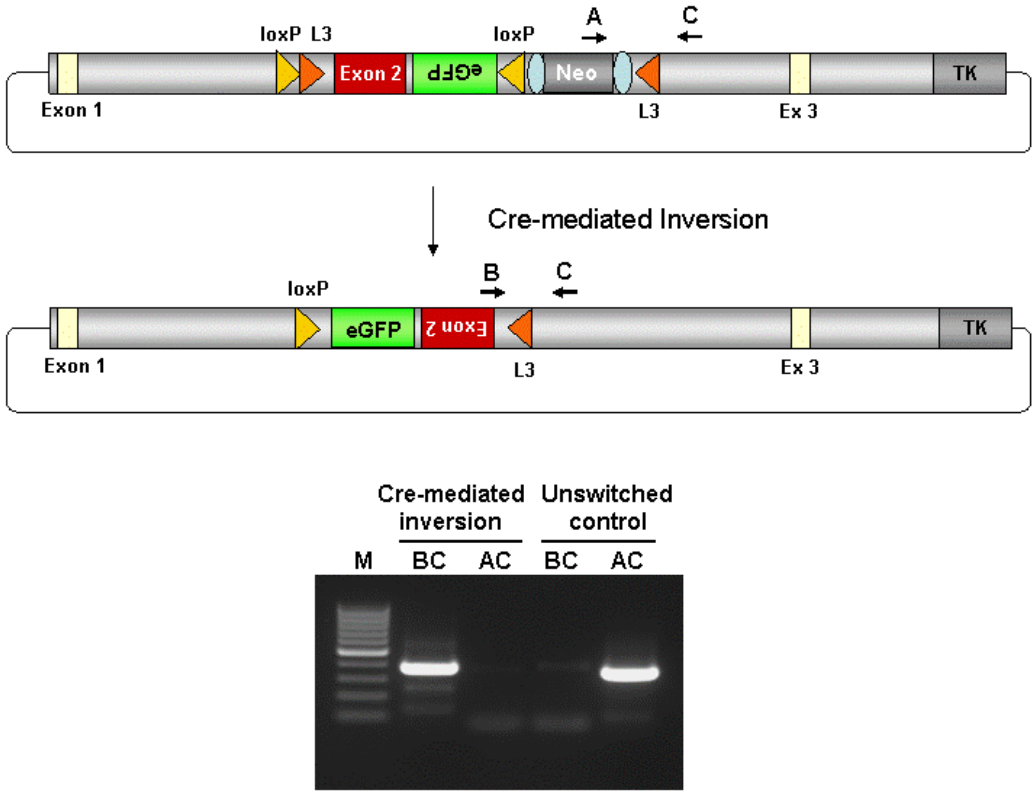

Fig. 10: ***Cre*-mediated inversion and subsequent excision between the *loxP* and *L3* sites in the targeting vector BAC.Cav1.3-GFP^{flex}.** After transformation in EL350 cells, expression of Cre recombinase led to a switch of the *lox* sites. Primers A and C amplify a product in the unswitched but not in the switched version of BAC.Cav1.3-GFP^{flex}. The primer combination B and C amplifies a fragment in the inverted version of the BAC.

4.1.2 Functionality of the Targeting Construct BAC.Cav1.3-GFP^{flex} *in vitro*

Before ES cell targeting, the functionality of the targeting vector was tested *in vitro*, to examine whether the *Cre*-mediated switch occurred and the *eGFP* gene was expressed. In the mouse genome the conditional knockout BAC is exchanged with the Cav1.3α1 locus by homologous recombination, whereby the endogenous exon 2 is replaced by the targeting construct. After *Cre*-mediated inversion the SA-eGFP-pA is placed in sense orientation and forms a fusion transcript with exon 1a, driven by the endogenous Cav1.3α1 promoter. This situation is not given when the targeting construct is brought into HeLa cells, since no integration into Cav1.3 locus followed by eGFP expression will take place. Furthermore, the endogenous Cav1.3α1 promoter is not active in cervical cancer cell-derived HeLa cells.

Therefore, a strong eukaryotic promoter with a splice donor, the Caggs promoter (chicken beta-actin promoter with CMV enhancer), was cloned into the 5′ homology arm 2 kb upstream of eGFP (Fig. 11 A).

The vector BAC.Cav1.3-GFP^{flex} containing the Caggs promoter was electroporated into HeLa cells together with a plasmid containing the *MC1-Cre*-recombinase. The transfected cells displayed a strong green fluorescence, pointing out that the *Cre*-mediated inversion following eGFP expression occurred (Fig. 11 B). As a control the targeting vector was transfected into HeLa cells without the *Cre*-plasmid. As expected no specific fluorescence could be detected (Fig. 11 C).

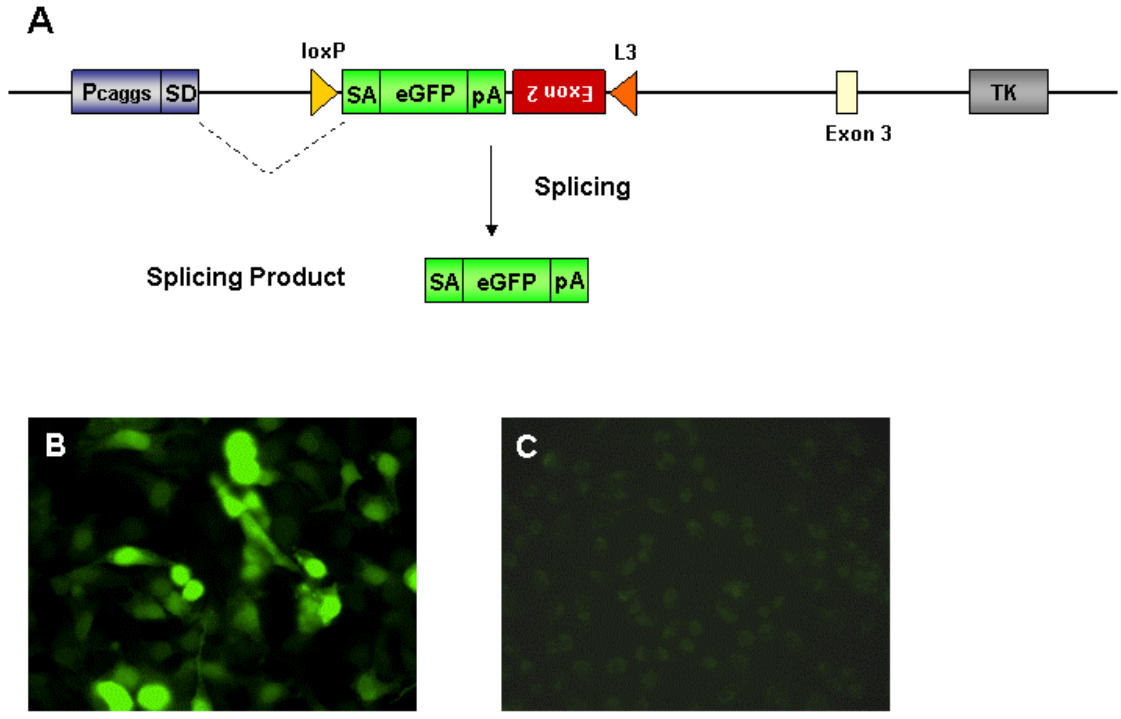

Fig. 11: Functionality of targeting construct *in vitro*. (A) Schematic drawing of the switched construct Cav1.3-GFP^{switch} in which eGFP expression is driven by the eukaryotic Caggs promoter. **(B)** After *Cre*-mediated switch, eGFP is driven by the eukaryotic Caggs promoter which leads to a strong expression of eGFP in HeLa cells. **(C)** As control the BAC.CaV1.3-GFP^{flex} construct was transfected into HeLa cells without *Cre* expression.

4.1.3 Production of Cav1.3-GFP^{flex} -Targeted of ES Cell Clones

For gene targeting the recombinant DNA was introduced into the ES cells to integrate in a specific locus via homologous recombination. Therefore, the targeting construct BAC.Cav1.3-GFP^{flex} was linearized with *AscI* and 60 µg of the linearized and purified BAC was

electroporated into R1 ES cells (Nagy et al., 1993) which are derived from agouti-coloured 129/SvJ mice. Since homologous recombination is a rare event (< 1:5000), G418 (200 µg/ml) for positive and Ganciclovir (2 µM) for negative selection were used to select for colonies with homologous integration. After 8-10 days of drug selection 18 drug-resistant colonies appeared and were picked into 96 well plates with feeder cells.

The isolated ES cell clones were analyzed by long-range PCR for specific integration into the genome. A specific primer pair was used to amplify a DNA fragment only if the recombinant construct was integrated into the targeted locus, not in wildtype allele or with random integration outside of the targeted locus. The primers used for this PCR were designed in that way that one primer anneals to the *neo* cassette and the other primer to the region directly downstream of the 3' homology arm of the targeting vector within the endogenous locus (Fig. 12). Only ES cell clones in which the endogenous exon 2 of Cav1.3α1 is replaced by the targeting construct via homologous recombination should reveal a 5.85 kb long amplicon. Primarily, we tried to amplify a fragment in the short homology arm with primers binding to a region outside the 5' homologous arm and to the first *loxP* site, but due to the very high GC content of this sequence the amplification was not possible.

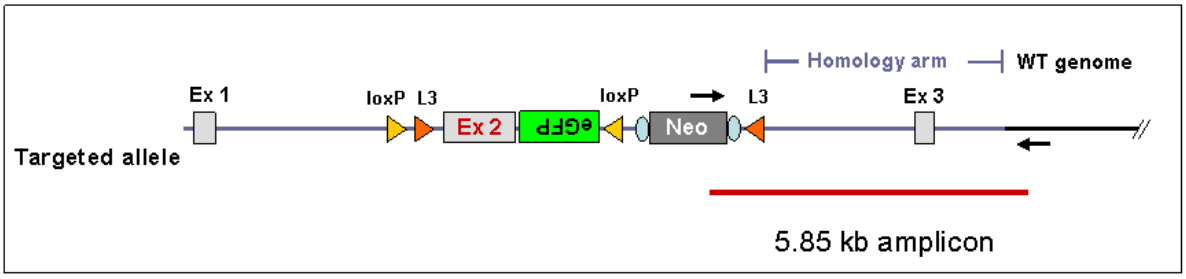

Fig. 12: Screening strategy by long-range PCR for identification of ES cells with locus specific Cav1.3-GFP^{flex} integration after homologous recombination. The forward primer NeoES_for binds within the *neo* cassette and the reverse primer 3'HAext_rev2 just outside of the 3' homologous arm (blue line) within the endogenous locus. The 5.85 kb fragment was amplified only in ES cells clones, in which the construct was inserted via homologous recombination.

From the 18 drug-resistant ES cell clones 6 were positive for the PCR reaction. The clones #7, #8, #10, #11, #12 and #15 showed a 5.85 kb fragment amplified with the primers NeoES_for and 3'HAext_rev2 (Fig. 13). As negative controls genomic DNA from wildtype R1 ES cells and the targeting vector were used to exclude an unspecific amplicon. In addition, the amplified PCR product was purified and sequenced to verify the specificity of the

amplification. From all six positive clones the amplified PCR product had the correct targeted sequence.

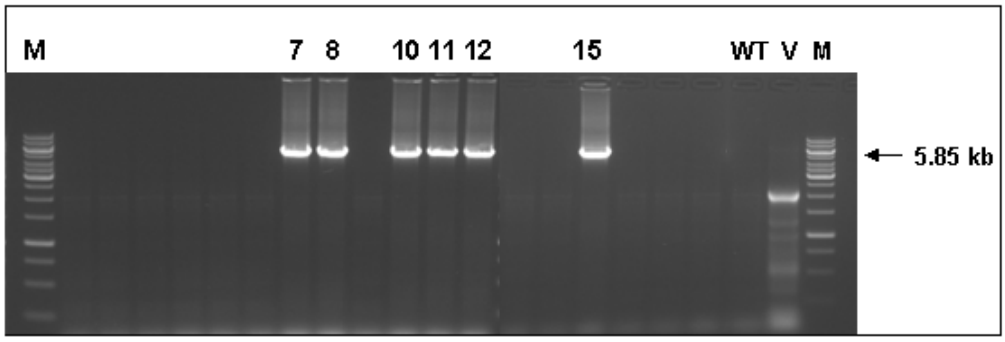

Fig. 13: PCR screening for the targeting construct Cav1.3-GFP^{flex} in the *Cav1.3α1* locus in ES cells. Long-range PCR over the 3′ homology arm confirmed the correct integration of the CaV1.3-GFP^{flex} construct with the presence of the specific 5.85 kb amplicon in 6 ES cell clones.

4.1.4 Generation of the Mouse Line Cav1.3-GFP^{flex}

All 6 positive ES cell clones were expanded and prepared for microinjection into blastocysts. The microinjection of the manipulated ES cell clones was done by Ariana Frömmig, a laboratory technician. Three independent injections were performed, with two positive ES cell clones in each injection session. For injection the clones were prepared following the protocol from Frank Zimmermann (ZTL Heidelberg), whereby the ES cells were preplated to remove the feeder cells and separated into single cells. The prepared ES cells were injected into blastocysts derived from the mouse strain C57Bl6 since the chimeras arised from the ES cells will be backcrossed to the C57Bl6 background. The blastocysts with the genetically modified ES cells were implanted into the uterus of pseudo-pregnant foster mothers from the strain B6D2F1, which gave birth to chimeric offspring. In general the degree of coat colour chimerism of a particular animal correlates with the degree of germ line contribution by ES cells since the coat colour of the mouse strain from which the R1 ES cells were derived (129/SvJ / agouti) differs from the coat colour of the mouse strain for the blastocysts (Fig. 14). Seven highly chimeric males where born (F0 generation) which were completely agouti-coloured. These offspring were generated from the ES cell clones #10, #12 and #15. From each clone two agouti-coloured male chimeras were bred with wildtype C57Bl/6N females to examine them for germ line transmission. Only male chimeras were bred since the R1 ES cells were derived from male embryos and thus a bias towards the male gender can be

observed that is reflected by a phenotypic male chimera with a female genotype (Joyner, 1993). Agouti-coloured progeny (F1 generation) showed successful germ line transmission. The mutated allele was not transmitted to F1 offspring with black coats, since the agouti colour is genetically dominant over the black coat colour. Table 1 shows the summery of chimeric offspring and their contribution to the germ line.

Fig. 14: Chimeric CaV1.3-GFP^{flex} mice. Since the coat colour of the mouse strain from which the R1 ES cells were derived (129/SvJ / agouti) differs from the coat colour of the mouse strain for the blastocysts, the coat colour of the chimeras can be used to determine the level of chimerism. The higher the amount of agouti coat colour the higher the degree of germ line contribution by ES cells.

ES Cell Clone	*Offspring (male)*	*Male Chimeras*	*Agouti (born)*	*PCR- pos (GFP+Neo)*	**Mouse line TierBase #0140**
# 10	12 (6)	5	28 (29)	no	CaV1.3-GFP ^{flox}
# 12	11 (6)	3	34 (46)	yes	CaV1.3-GFP ^{flox}
# 15	5 (4)	3	30 (30)	yes	CaV1.3-GFP ^{flox}

Table 1: Summery of chimeric CaV1.3-GFP^{flex} offspring from the ES cell injection and their germ line transmission. From each ES cell clone (#10, #12, #15) 2 or 3 highly chimeric males were backcrossed with C57Bl/6 females and tested for their contribution to the germ line by agouti-coloured fur and PCR.

Chimeras from ES cell clone # 10 transmitted the agouti fur colour to almost all F1 offspring, 28 mice were agouti-coloured, and only one offspring was black. From clone #12 derived chimeras had F1 offspring with 34 agoutis out of 46 litters. Chimeras from clone #15 thoroughly transmitted the agouti fur colour to all offspring.

4.1.5 Genotyping of Cav1.3-GFP^{flox} mice

The agouti-coloured progeny (F1 generation) was genotyped by PCR using DNA from tail tissue. The targeted ES cells were heterozygous for the introduced mutation; the wildtype allele or the mutant allele was transmitted to the agouti mice in 50% of animals. To test whether the mutated or the wildtype allele was transmitted, the offspring were genotyped by PCR using primer pairs that recognize sequences specific to the mutated allele. One primer pair binds to the *neo* cassette (Neo 5′ and Neo 3′) and the other to e*GFP* (GFP 5′ and GFP 3′) (Fig. 15). Additionally, they were genotyped with the primers NeoES_for and 3′HAext_rev2 used for ES cells after homologous recombination, to ensure again the construct has integrated correctly.

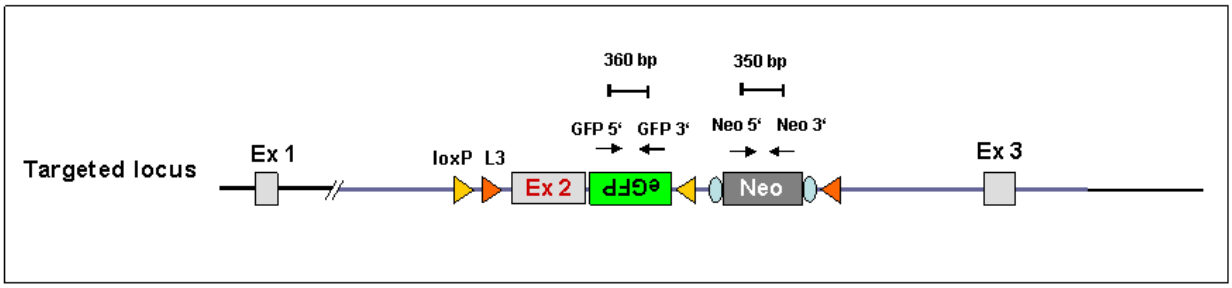

Fig. 15: PCR genotypic strategy for Cav1.3-GFP^{flex} mice. The agouti-coloured offspring were genotyped using internal GFP and neomycin primers which amplify 360 bp and a 350 bp fragment, respectively.

From 55 examined agoutis from 3 chimeras, 28 offspring showed germ line transmission as they were PCR-positive for both primer pairs. These 28 mice transmit the conditional knockout allele Cav1.3-GFP^{flox} through the germ line.

4.1.6 Removal of the Neomycin cassette by *Flpe*-recombination

The *neo* cassette is required for positive selection in ES cells. After transmission of the mutated Cav1.3-GFP^{flex} allele the neomycin cassette has to be removed to avoid gene

interference with silencing effects and influences on the phenotype of the genetically modified mice. In our case it has been shown that the removal of *neo* even was essential for *Cre*-mediated FLEX switch to occur (chapter 4.2). In order to remove the *FRT*-flanked neomycin resistance gene, the heterozygous Cav1.3-GFP$^{flex/+}$ mice were crossed with *Flpe*-deleter mice. In these mice the *Flpe* recombinase is driven by the promoter of the human ACTB gene which is active in almost all tissues, even in germ cells. This leads to transmission of the *neo* excision through the germline. Similar to the *Cre/loxP* system the *FRT*-flanked *neo* cassette is excised from the allele by *Flpe*-mediated recombination. The double transgenic offspring of the mating Cav1.3-GFP^{flex} x Flpe-deleter mice were analysed by PCR for the absence of the *neo* cassette (Fig. 16).

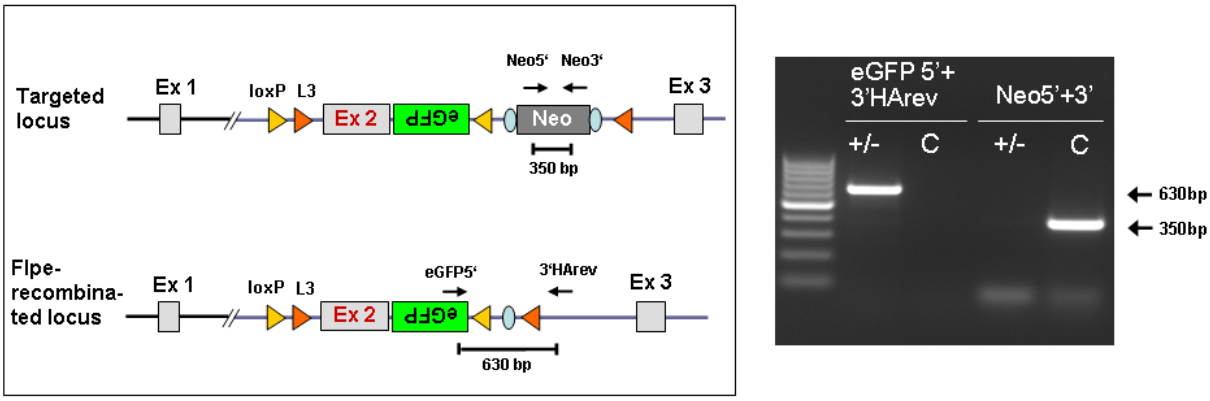

Fig. 16: PCR confirmed the Flpe-mediated excision of the *neo* cassette in CaV1.3-GFP^{flex} mice. Recombination in heterozygous mice was shown by the specific 630 bp PCR product and by the absence of the *neo*-specific PCR product. A littermate positive for the mutated allele but negative for the *Flpe*-recombinase served as control (C).

After excision of the neomycin resistance gene the primer pair eGFP 5′ and 3′HA_rev amplified a 630 bp PCR fragment. In single transgenic littermates which served as control (C) the fragment would be 2410 bp long and therefore not amplified under these PCR conditions. Furthermore, the absence of the *neo* cassette was confirmed by the absence of the *neo*-specific PCR band using the primer pair Neo 5′ + 3′.

In all analyzed offspring which harbour the Cav1.3-GFP^{flex} allele and the *Flpe*-recombinase the *neo* cassette was successfully excised by homologous recombination.

4.2 Conditional Knockout of the $Ca_V1.3\alpha1$ subunit via the FLEX Switch in $Ca_V1.3$-GFP^{flex} mice

The Cav1.3α1 subunit in the Cav1.3-GFP^{flex} mouse line can be inactivated by *Cre*-mediated recombination. By using the FLEX switch, the floxed exon 2 of *Cacna1d* will be irreversibly inverted and thus inactivated. Simultaneously, the reporter gene eGFP will be activated by the inversion, mirroring the expression pattern of the endogenous Cav1.3α1 gene *Cacna1d*. To confirm that we indeed generated a functional knockout of Cav1.3α1 we crossed heterozygous Cav1.3-GFP$^{flex/+}$ animals with Cre-deleter mice in which the *Cre* recombinase is driven by an adenovirus EIIa promoter in all tissues (Williams-Simons and Westphal, 1999). The EIIa promoter is already active in the ovum at the time of fertilization which leads to *Cre* recombination when the embryo is still at one-cell zygote stage. Thus, all cells of the developing animal, including germ line cells, will have the inverted DNA sequence and the mice will give the mutated allele to the next generation.

By crossing the Cav1.3-GFP$^{flex/+}$ animals with Cre-deleter mice, the expression of the Cav1.3 channels can be monitored by eGFP expression in all tissues in which the channel is located. Due to the lack of reliable antibodies against Cav1.3α1 for immunohistochemical detection the exact expression pattern of Cav1.3 can be determined. Furthermore we crossed the Cav1.3-GFP$^{flex/+}$ mice with CaMKIIa-Cre mice to obtain a tissue-specific deletion. In these mice the expression of the *Cre* recombinase is under the control of the calcium/calmodulin dependent protein kinase II alpha promoter. Hence, *Cre* recombinase is expressed postnatally in the forebrain.

Since the *neo* resistance cassette will be excised by the switch, we first used Cav1.3-GFP$^{flex/+}$ mice not yet crossed to Flpe-deleter mice. However, no inversion of the floxed allele could be detected when crossed to Cre-deleter or CaMKIIa-Cre mice, thus indicating inhibitory effects of the *neo* cassette on recombination. Therefore, all further breedings were done with Cav1.3-GFP$^{flex/+}$ mice in which *neo* was excised first.

4.2.1 PCR Analysis of Cav1.3-GFP^{flex} x Cre-deleter mice

The *Cre*-mediated switch of the floxed DNA sequence in the Cav1.3-GFP$^{flex/+}$ without *neo* x Cre-deleter can be determined with PCR from tail tissue. Therefore, primers were used which amplify a fragment specific for the inverted or non-inverted form of the mutant allele

(Fig. 17). In mice with the switched allele the primer combinations A/B and C/D amplified a fragment, respectively, that was specific for the *Cre*-mediated inversion. The primer combination F/D that gave a positive result for the mutated, non-inverted allele was negative for these animals (Fig. 18). As negative control in this PCR analysis served a mouse positive for the mutated allele but negative for Cre. This result showed that the floxed sequence in the mutated allele could be inverted by the *Cre* recombinase.

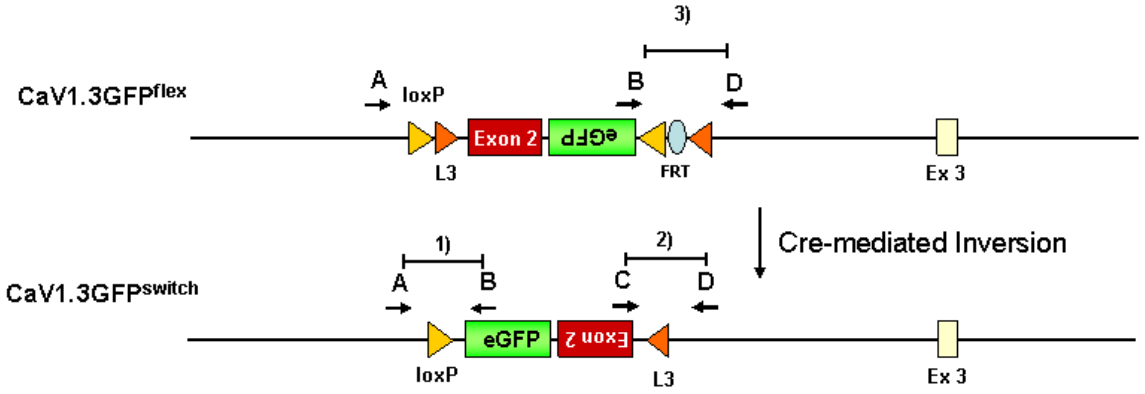

Fig. 17: PCR strategy for determination of the *Cre*-mediated inversion. To detect the inversion of the floxed sequence in the mutated Cav1.3-GFP^{flex} allele specific primer combinations were used. Primer A: 5'HAend_for, B: eGFP_rev, C: Ex2ES_rev, D: 3'HAbegin_rev.

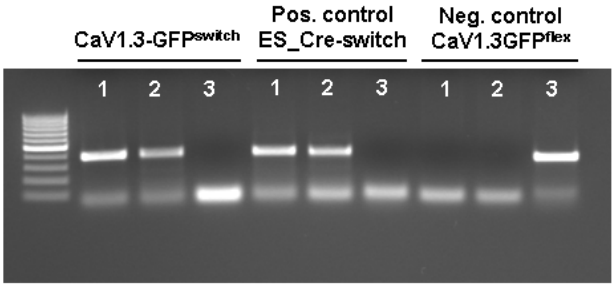

Primer combination	Cre-switch	CaV1.3-GFP^{flex}
1) Primer A + Primer B	+	-
2) Primer C + Primer D	+	-
3) Primer B + Primer D	-	+

Fig. 18: Genotyping PCR for detection of animals with an inverted Cav1.3-GFP^{flex} sequence. In heterozygous Cav1.3-GFP^{flex} x Cre-deleter mice positive for inversion, the primer combination A/B and C/D showed a positive result characteristic for *Cre*-mediated inversion.

4.2.2 Analysis of the mRNA Expression by RT-PCR

In double transgenic Cav1.3-GFP$^{flex/+}$ x Cre-deleter mice with the inverted allele the reporter gene eGFP with its universal splice acceptor (SA) should be spliced in frame to Cav1.3α1 exon 1 and subsequently be driven by the endogenous Cav1.3α1 promoter. Due to the transcriptional termination site pA (polyadenylation site) downstream to eGFP, Cav1.3α1

exon 3 is not transcribed. This leads to an expression of a truncated mRNA and protein. In WT mice and single transgenic Cav1.3-GFP$^{flex/+}$ mice exon 1 is spliced regularly to exon 2 resulting in a normal expression of the channel Cav1.3α1. To determine the switch on the level of mRNA expression, brain RNA from of Cav1.3-GFP$^{switch/+}$ mice heterozygous for the switch was analyzed by reverse transcription-PCR (RT-PCR). Therefore the brain of these animals was divided into two parts. One part was fixated and kept stored for later protein analysis. From the second part of the brain, the olfactory bulb and cortex were dissected for mRNA analysis. Total RNA of these tissues was isolated and reverse transcribed into single stranded cDNA. With PCRs of the cDNA the expression of the activated eGFP spliced in the switched Cav1.3α1 allele could be detected.

For analysis, a primer pair was used with the forward primer binding to *Cacna1d* exon 1 and the reverse primer binding to eGFP (Fig. 19 A). In the case of the switched allele a specific PCR fragment of 220 bp was amplified. As negative control littermates with the mutated Cav1.3α1 allele but negative for the *Cre* recombinase (Cav1.3-GFP$^{flex/+}$) were used. For a positive control PCR the forward primer Ex1_for and the reverse primer Exon2_rev specific to exon 2 were used which give rise to a 160 bp PCR fragment (Fig. 19 B). In heterozygous Cav1.3-GFP$^{switch/+}$ mice which still harbour one WT allele this control primer combination should always be positive.

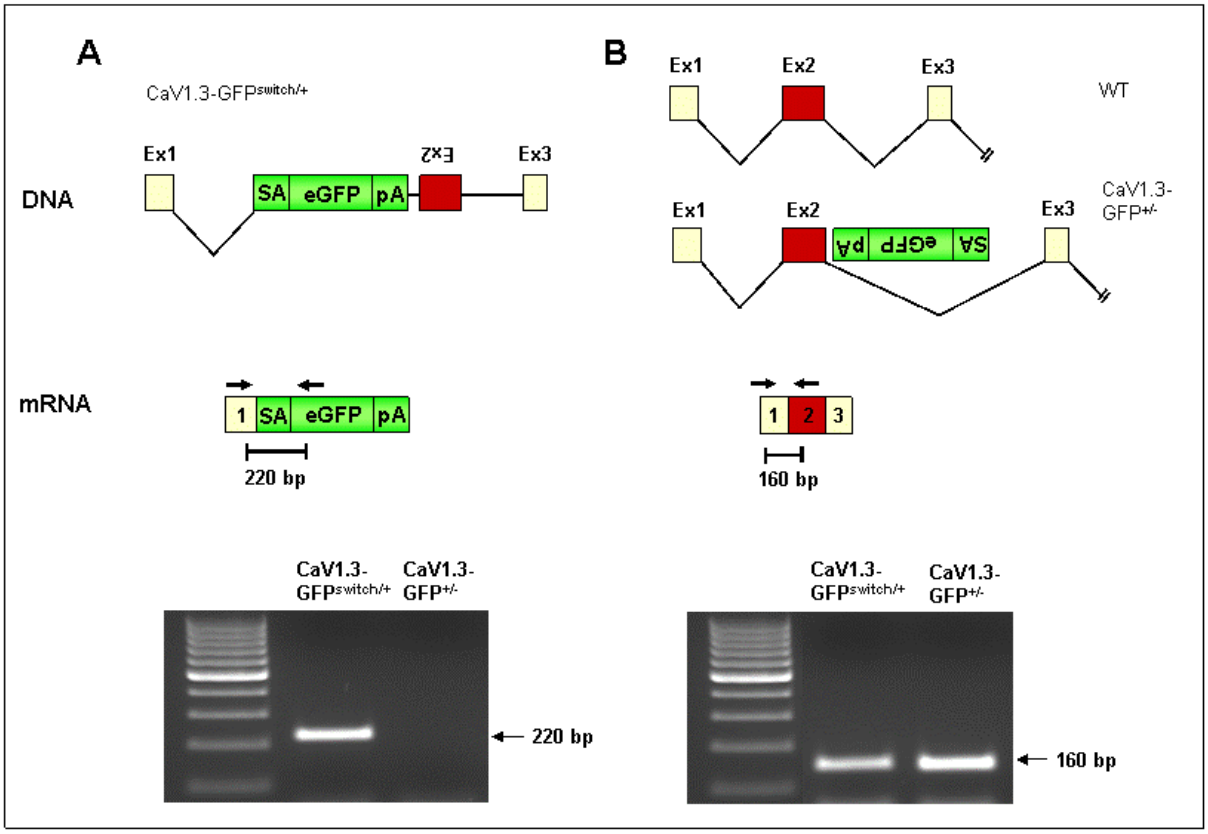

Fig. 19: RT-PCR analysis of Cav1.3-GFP^{switch} mice. Schematic drawing of the DNA and mRNA structure and RT-PCR of mRNA prepared from olfactory bulb. **(A)** Structure of the mutated and switched Cav1.3α1 locus (Cav1.3-GFP$^{switch/+}$) with *eGFP* with its universal splice acceptor (SA) and poly A site and the inverted *Cacna1d* Exon2. The arrows on the mRNA indicate the binding site of the primers Ex1_for and eGFP_rev which give a specific 220bp fragment after RT-PCR. **(B)** In wildtype mice (WT) and in Cav1.3-GFP$^{flex/+}$ mice exon 1 is regularly spliced to exon 2. As control PCR the primers Ex1_for and Ex2_rev were used which gave also a positive result in the heterozygous CaV1.3-GFP$^{switch/-}$ mice due to one WT allele.

As showed in Fig. 25 the RT-PCR analysis of Cav1.3-GFP$^{switch/+}$ mice indicated that the reporter gene eGFP was spliced to exon 1 of Cav1.3α1. The reporter gene eGFP was now driven by the endogenous Cav1.3α1 promoter.

4.2.3 Expression of eGFP Protein in Cav1.3-GFP^{switch} Mice

After the correct splicing of exon 1 and *eGFP* in heterozygous Cav1.3-GFP$^{switch/+}$ mice could be verified by RT-PCR analysis, we wanted to analyse the expression of the eGFP protein. To test this, the second part of the brain was sagittaly sectioned with a Vibratome and slices were analysed by immunohistochemistry with antibodies against eGFP. In addition to the analysis of the brain, heart tissue of Cav1.3-GFP^{flex} x Cre-deleter mice was sliced and stained

since it has been shown previously that the channel is also expressed in heart. The staining of eGFP should represent the endogenous expression pattern of the Cav1.3α1 gene.

Immunohistochemical DAB staining with antibodies against eGFP revealed a strong labelling in several brain regions (Fig. 20). The staining indicated that the eGFP protein was functional and could be used as a reporter for expression of the calcium channel. We detected a strong staining in the subventricular and periventricular zone (Fig. 20 B). This was surprising, since so far expression of the calcium channel in this region has not been reported. Strong eGFP-expression was also observed in the superior colliculus (SC), including the superficial gray layer and the optic nerve layer of the SC (Fig. 20 D). In the upper intermediate white layer of the superior colliculus a more moderate level of eGFP expression was observed. Adjacent to the superior colliculus stained cells were detected in the optic tract (OT) (Fig. 20 D). In the olfactory bulb (Fig. 20 A) a wide eGFP-expression was observed, including the glomerular layer, the mitral cells and the granular cell layer of the olfactory bulb. A slightly lower expression of eGFP was shown in the cortex through all layers (Fig. 20 B and C). Also in the thalamic regions eGFP-staining was detected (Fig. 20 A). In the cerebellum the molecular layer and, more weakly, the Purkinje cell layer was labelled (Fig. 20 E). In the CA1 and CA3 region of the hippocampus few cells located in the pyramidal cell layer and stratum oriens displayed a strong eGFP-expression (Fig. 20 C). Additionally, a moderate staining was observed in the whole stratum oriens and stratum radiatum. The dentate gyrus was only slightly stained in the stratum moleculare. As negative control a single transgenic littermate Cav1.3-GFP^{flex}, not expressing the *Cre* recombinase, was used that showed no staining for eGFP (Fig. 20 F).

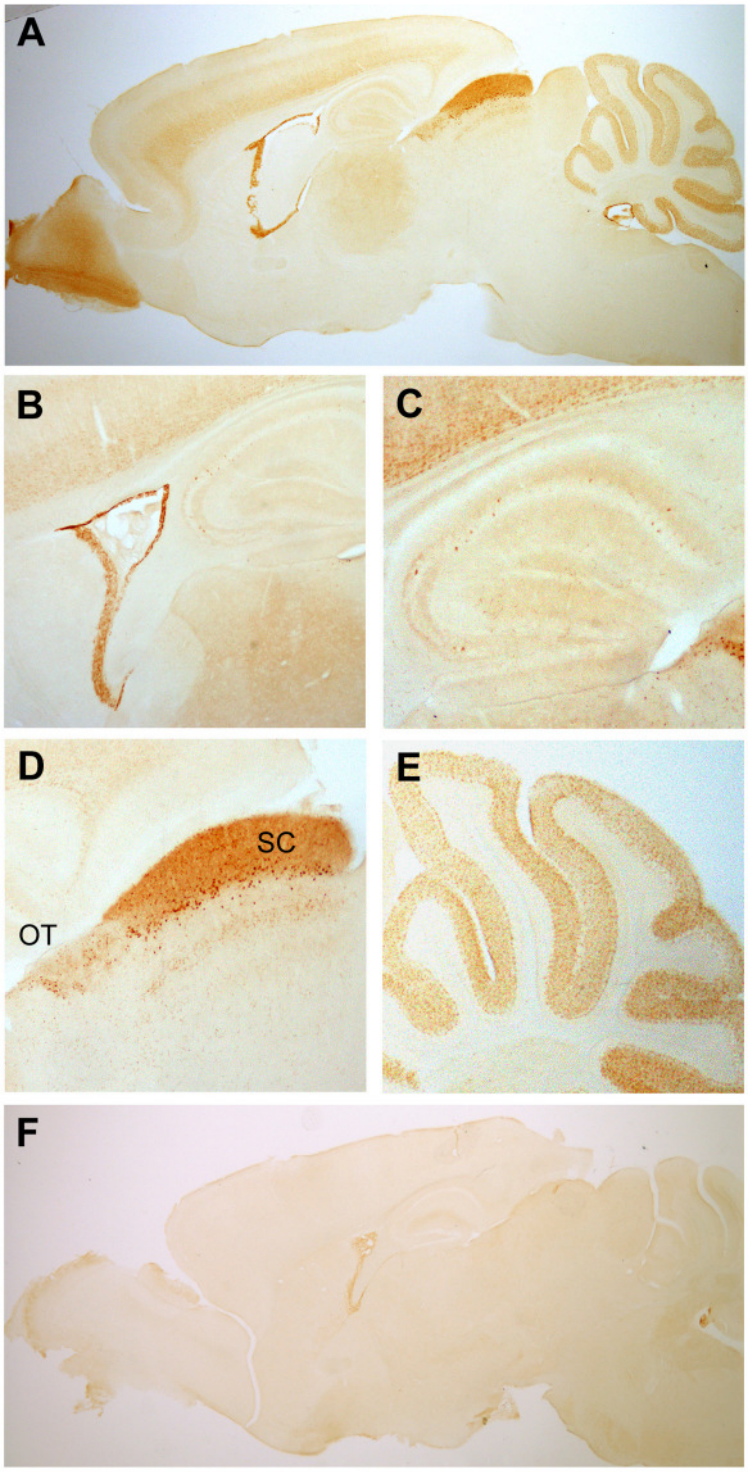

Fig. 20: Expression of eGFP protein in the brain of Cav1.3-GFP$^{switch/+}$ mice (DAB staining). Immunohistochemistry using antibodies against the reporter protein eGFP as an overview in a sagittaly sectioned brain. **(A)**. Magnification of eGFP expression in the lateral ventricle **(B)**, hippocampus **(C)**, superior colliculus (SC) and optic tract (OT) **(D)**, olfactory bulb **(A)** and cerebellum **(E)**. Immunohistochemistry on a brain section of a single transgenic littermate CaV1.3-GFP^{flex} served as negative control **(F)**.

Further analysis of the Cav1.3-GFP$^{switch/+}$ brain revealed eGFP expression in limbic, hypothalamic, thalamic and brainstem areas. Cav1.3-GFP^{switch} signal was found in several regions of the amygdala, like the lateral amygaloid nucleus (LA), the basolateral (BLA) and the central amygdaloid nucleus (CeA) (Fig. 21 A). The cells of the bed nucleus of accessory olfactory tract (BAOT) displayed a strong labelling (Fig. 21 B). In the brainstem eGFP expression was obtained in the facial nucleus (7N), the cuneate nucleus (Cu) and, slightly lower, in the locus coeruleus (LC) (Fig. 21 C). Around the third ventricle (3V) the ependymal cells were strongly stained (D). eGFP expression was also observed in the hypothalamic paraventricular nucleus (PVN) (Fig. 21 D) and the medial (MHb) and lateral habenular nuclei (LHb) (Fig. 21 E). Intensely labelled cells were detected in different thalamic regions (Fig. 21 F), namely the pregeniculate nucleus (PG), the dorsal lateral geniculate nucleus (DLG) and the lateral posterior thalamic nucleus (LP). Furthermore, eGFP expression was found in the optic tract (OT) and the medial pretectal nucleus (MPT) (Fig. 21 F).

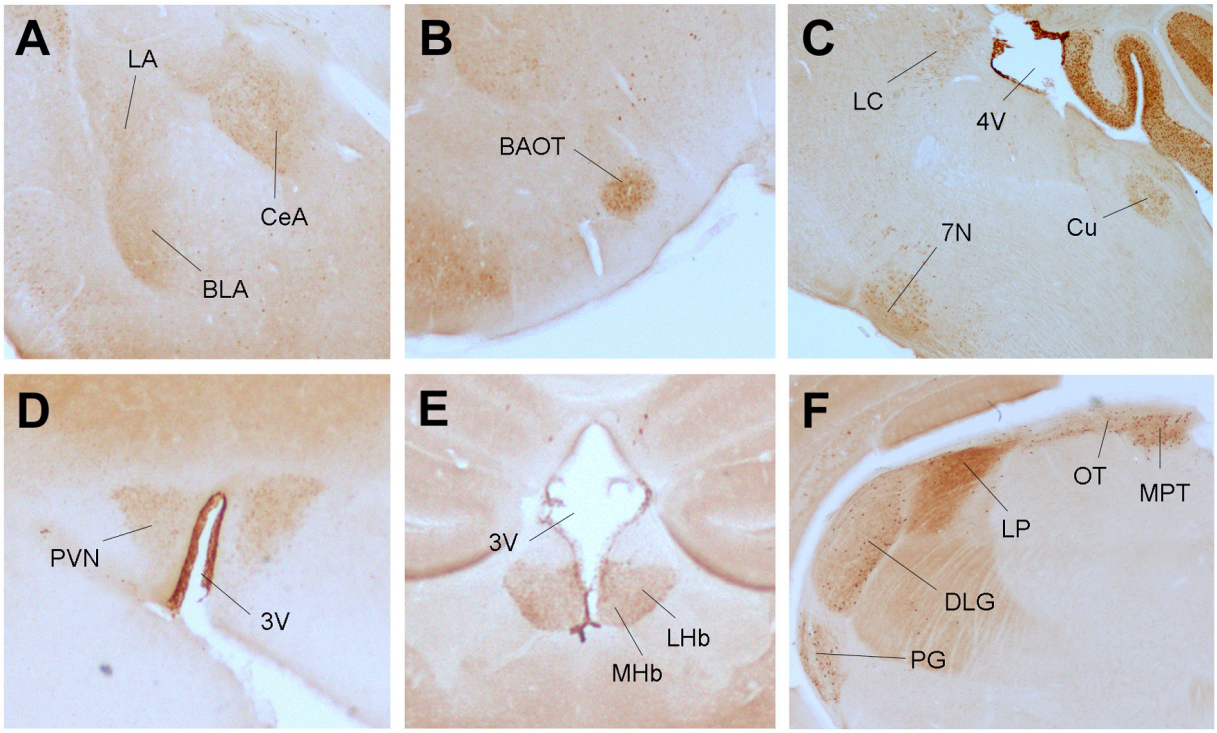

Fig. 21: DAB staining of eGFP expression in coronal (A,B,D-F) and sagittal brain sections (C) of Cav1.3-GFP^{switch} mice. Staining was observed **(A)** in the lateral amygdaloid nucleus (LA), in the basolateral part (BLA) and central amygdaloid nucleus (CeA), **(B)** in the bed nucleus of accessory olfactory tract (BAOT), **(C)** in the locus coeruleus (LC), the facial nucleus (7N) and the cuneate nucleus (Cu), **(D)** in the paraventricular nucleus (PVN), **(E)** in the medial (MHb) and lateral habenular nuclei (LHb) and **(F)** in the pregeniculate nucleus (PG), the dorsal lateral geniculate nucleus (DLG), the lateral posterior thalamic nucleus (LP), the optic tract (OP) and the medial pretectal nucleus (MPT).

Since previous studies revealed a role of Cav1.3α1 channels in sinoatrial pace making activity (Platzer et al., 2000; Zhang et al., 2005b), eGFP expression in the heart of Cav1.3-GFP^{switch} animals was examined. We found a strong eGFP staining in the septum of the heart (Fig. 26 G). Here the bundles of His are located which conduct the electrical impulse from the sinoatrial node and the atrioventricular node into the ventricles.

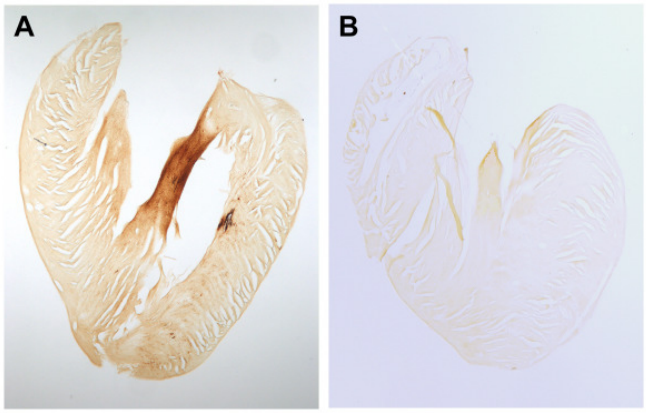

Fig. 22: eGFP expression in the heart of Cav1.3-GFP^{switch} mice. In the heart a strong staining in the septum was observed **(A)**. As negative control the heart from a single transgenic littermate was used **(B)**.

4.2.4 eGFP Expression in Cav1.3-GFP^{flex} x CaMKIIα-Cre mice

To verify that the expression pattern of eGFP in CaV1.3-GFP$^{flex/+}$ x Cre-deleter mice was specific to the CaV1.3-GFP^{flex} line, mice were paired with another Cre mouse line. Here we used the CaMKIIa-Cre mouse line which is the most-established the *Cre* line. Offspring of Cav1.3-GFP$^{flex/+}$ x CaMKII-Cre mice were analyzed by PCR to confirm the switch on DNA level. Since the *Cre* recombinase under the CaMKIIα promoter is active in the forebrain, parts of the forebrain were removed and DNA was isolated. The *Cre*-mediated inversion could be confirmed by PCR analysis in the same way as displayed above. The animals showed the same specific PCR pattern for the switch. For analysis of eGFP expression on mRNA level, RNA was isolated from the forebrain and reverse transcribed by RT-PCR. With PCRs on the cDNA with specific primers for exon 1 and *eGFP* as described above we could show that in these mice the *eGFP* gene was spliced to exon 1 of *Cav1.3α1* as expected (data not shown).
Immunolabelling in the mouse brain with antibodies against the eGFP protein revealed a similar expression pattern as in animals crossed with Cre-deleter mice. As displayed in Fig.

23 E, high eGFP expression was detected in the superior colliculus. Also the expression pattern in the cortical layers was the same compared to that in Cav1.3-GFP$^{flex/+}$ x Cre-deleter mice, even though here the staining was slightly stronger (Fig. 23 C). In the olfactory bulb a defined eGFP expression could be observed in the glomerular layer, the external plexiform layer, the mitral cells and the granular cell layer (Fig. 23 A). In the hippocampus very few strongly labelled cells were visible in the CA1 and CA3 region, besides a moderate staining in the stratum radiatum. The dentate gyrus displayed a slightly stronger staining, both in the granular cells and in the stratum moleculare (Fig. 23 D). Consistent with the CaMKIIα expression no eGFP labelling was observed in the periventricular zone of the lateral ventricle (Fig. 23 B). Also in the cerebellum the CaMKIIα promoter is inactive, even though in that brain region a very faint staining in the molecular layer could be noticed (Fig. 23 F). Single transgenic Cav1.3-GFP$^{flex/+}$ littermates served as negative control (Fig. 23 G).

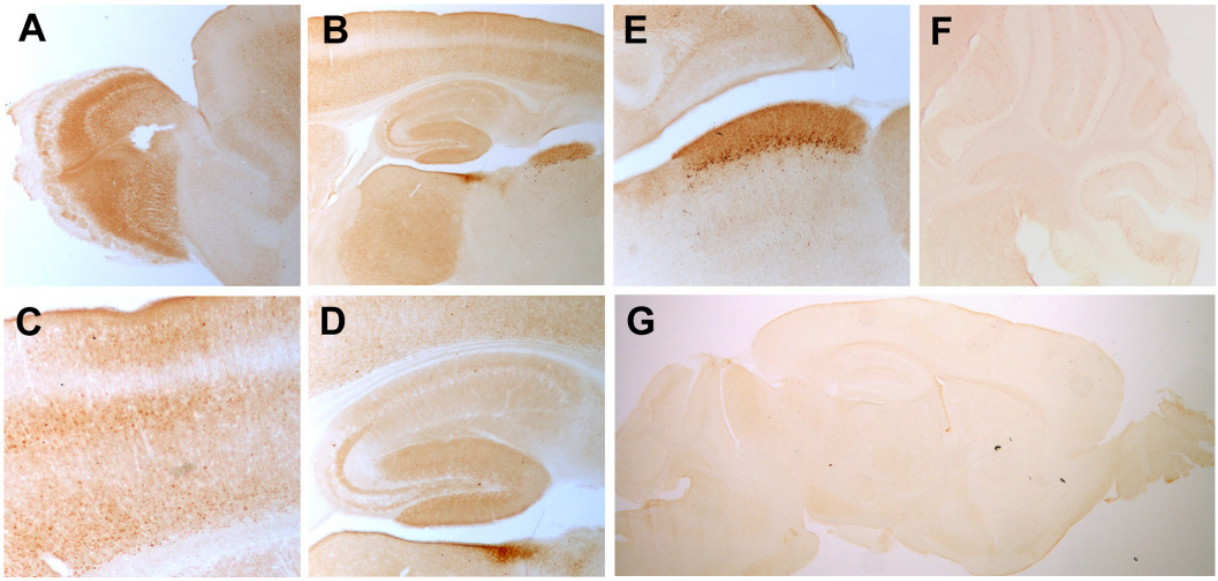

Fig. 23: Expression of eGFP protein in the brain of Cav1.3-GFP^{flex} x CaMKIIa-Cre mice. Brain of a double transgenic mouse was sagittaly sectioned and analyzed by immunohistochemistry using antibodies against the reporter gene eGFP and detection of antigen expression by HRP/DAB. **(A)** Olfactory bulb, **(B)** overview, **(C)** magnification of cortex, **(D)** hippocampus, **(E)** superior colliculus and **(F)** and cerebellum. **(G)** Negative control.

4.2.5 Analysis of eGFP Protein Expression by Double Immunofluorescence

Cav1.3α expression was previously described to be found in most brain regions (Hell et al., 1993). Nevertheless, detailed analysis of Cav1.3α expression in peri- and subventricular regions of the lateral ventricle was not described so far. Therefore we used a double fluorescence immunohistochemistry approach to determine the distribution and cell type of eGFP-labelled cells in brain sections of Cav1.3-GFP^{flex} x Cre-deleter mice.

Colocalization studies were performed on brain section by double-immunostaining using anti-eGFP antibody and following markers: neuronal nuclear antigen (NeuN), doublecortin (DCX), glial fibrillary acidic protein (GFAP), SOX2, GAD67 and tryptophan hydroxylase 1 (TPH1).

4.2.5.1 Localization of eGFP- and NeuN-positive cells

NeuN recognizes a neuron-specific nuclear protein in vertebrates (Mullen et al., 1992) which is considered as a marker for neuronal cells. To investigate whether the eGFP-expressing cells were NeuN-positive neurons, localization of eGFP and NeuN were compared. The eGFP-positive cells in the periventricular ependyma of the lateral ventricle and the subventricular zone were a non-neuronal cell type as they were immunonegative for NeuN (Fig. 24 A). In the cortex most of the eGFP-expressing cells were positive for NeuN even though in the cortical layer VI a small population remained only stained for eGFP (Fig. 24 B). Also in the olfactory bulb the majority of the cells were colabelled for the two markers (Fig. 24 C). In the CA1 and CA3 region of the hippocampus eGFP-expressing cells were of large shape and showed no colocalization with NeuN (Fig. 24 D-E). No eGFP-staining could be observed in the stratum oriens and radiatum and dentate gyrus as detected in the DAB staining. In the optic tract the eGFP-positive cell group was negative for the neuronal marker whereas in the superior colliculus the majority of the eGFP-expressing cells were colabelled wit NeuN (Fig. 24 F-G).

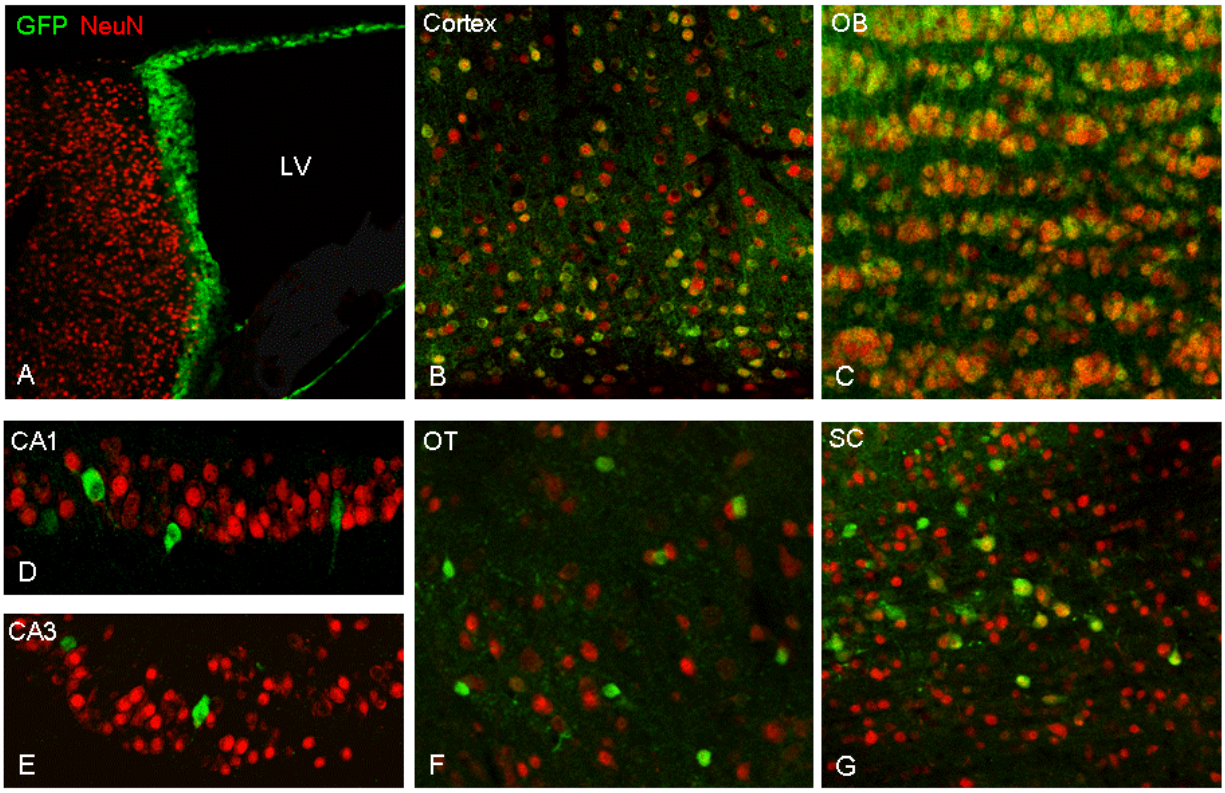

Fig. 24: Co-staining of eGFP and NeuN in brain sections of Cav1.3-GFP$^{switch/+}$ mice. (A) Double immunolabelling revealed that the eGFP-positive cells in the ependyma lining the lateral ventricle (LV) and the subventricular zone were not stained with the neuronal marker NeuN. **(B-C)** In the cortex and in the olfactory bulb (OB) the majority of the eGFP-expressing cells are immunopositive for NeuN. **(D-E)** In the hippocampal areas CA1 and CA3 no colabelling was detected. **(F-G)** In the optic tract (OT) eGFP-positive cells did not express NeuN whereas in the caudal located superior colliculus most of the eGFP-labelled cells colocalised with NeuN.

The positive colocalization of eGFP and NeuN in the cortex, the olfactory bulb and the superior colliculus indicate that the majority of the Cav1.3α-expressing cells were neurons in these brain regions whereas the eGFP-positive cells in the subventricular zone, hippocampus and optic tract represented another cell type.

4.2.5.2 Localization of eGFP- and GAD67-positive cells

It has been shown that Cav1.3α1 is expressed in various types of hippocampal GABAergic interneurons (Vinet and Sik, 2006). Since the eGFP-expressing cells in the hippocampus and the optic tract could not be characterized as NeuN-positive neurons, we wanted to analyze whether these cells could be inhibitory interneurons. Even though NeuN is known to stain also interneurons as well, NeuN-negative GABAergic interneurons were reported(Shechter et al., 2007). Here an anti-GAD67 antibody was used as marker for GABAergic interneurons.

GAD67 is the 67 kDA isoform of the enzyme glutamic acid decarboxylase which catalyzes the decarboxylation of glutamate to GABA. Double-immunostainings revealed that in the CA3 region of the hippocampus some cells displayed an eGFP/GAD67-colabelling (arrow), other eGFP-expressing cells were negative to GAD67 staining (asterisk) (Fig. 25 B1-3). In the optic tract a strong co-staining of GAD67 and eGFP was observed (Fig. 25 A1-3), indicating that Cav1.3α1 was expressed in GABAergic interneurons in a part of the visual system of the brain.

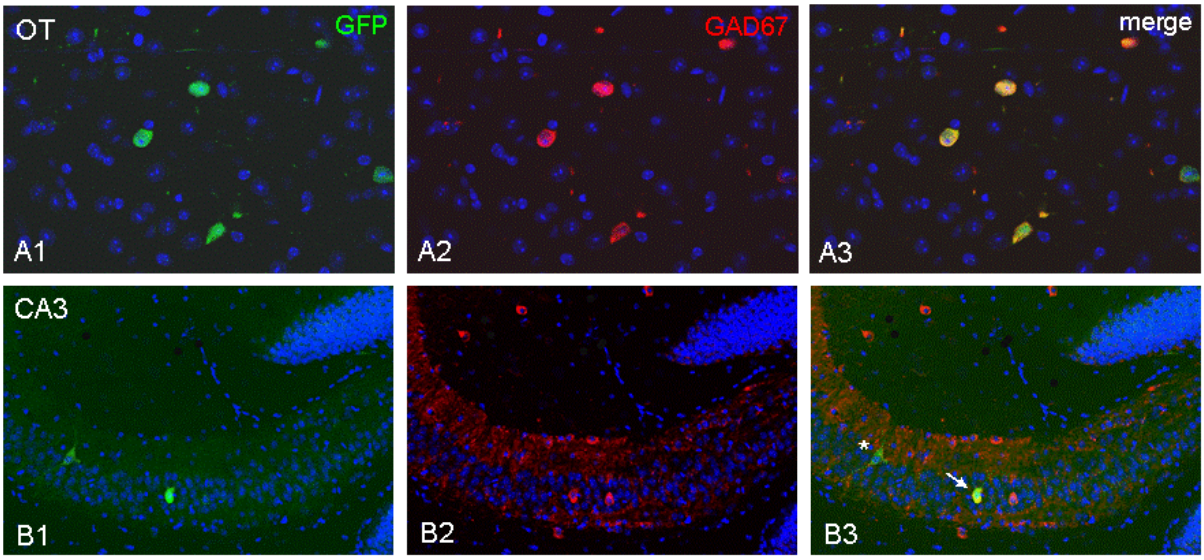

Fig. 25: Double immunofluorescence labelling of eGFP- and GAD67-positive cells in Cav1.3-GFP$^{switch/+}$ brain sections. (A1-3) Staining in the optic tract (OT) displayed an exact coexpression of eGFP- and GAD67-labelled cells. **(B1-3)** In the hippocampal region CA3 some of the eGFP-positive cells coexpress GAD67 (white arrow), whereas others are negative for the interneuron marker (asterisk).

4.2.5.3 Localization of eGFP- and DCX-positive cells

The most fascinating finding was the strong eGFP expression in the subventricular zone, known as one of the brain region in which adult neurogenesis is located. Therefore we analyzed the eGFP-stained cells with markers for neurogenesis. Doublecortin (DCX) is a microtubule-associated protein which is specifically expressed in immature neurons. DCX is necessary for the migration of neuronal precursor cells during the formation of the mammalian neocortex and is therefore used as one indicator for neurogenesis. As displayed in Fig. 26 (A) both cell types were present in the same brain area. However, eGFP-positive cells did not express DCX (B) in the subventricular zone in Cav1.3-GFP$^{switch/+}$ mice.

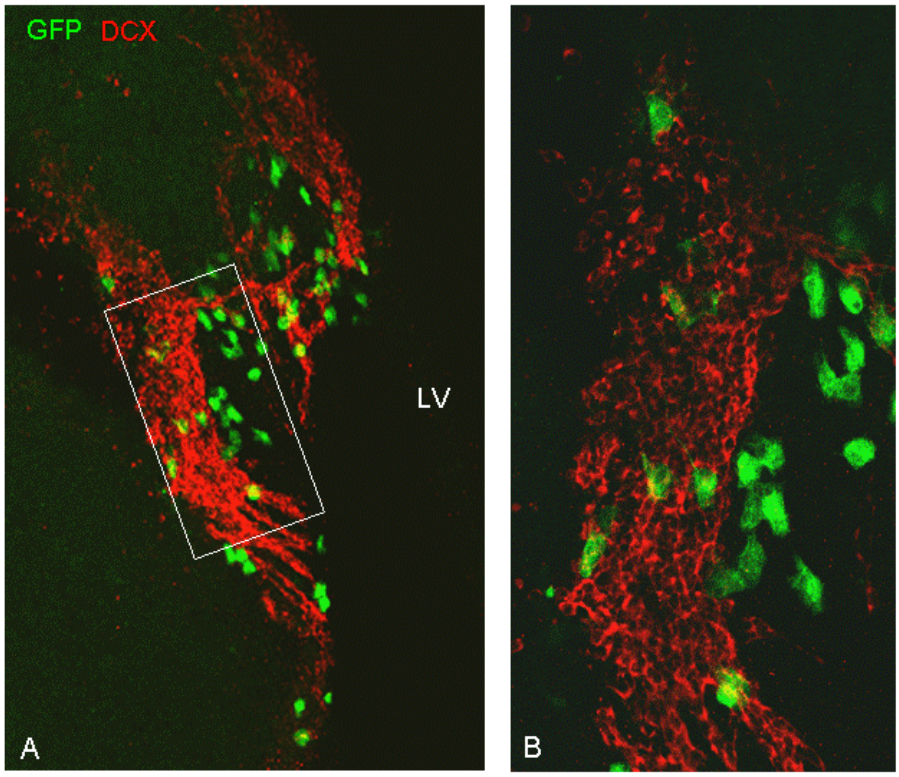

Fig. 26: Immunolabelling against eGFP and Doublecortin (DCX) in the subventricular zone. Cells positive for eGFP are located in the same brain region like DCX, nevertheless they do not express the neuronal precursor cell marker.

4.2.5.4 Localization of eGFP- and GFAP-positive cells

Immunostaining against the intermediate-filament protein GFAP (glial fibrillary acidic protein) strongly labels astrocytes. In addition, neural stem cells have been proposed to be part of a GFAP-positive astrocyte population located in the subependymal region of the brain which can divide to generate immature precursors and neuroblasts (Doetsch et al., 1999a). For characterization of eGFP-expressing cells in the subventricular zone and lateral ventricle ependyma of Cav1.3-GFP$^{flex/+}$ x Cre-deleter mice, we performed double immunostainings with anti-GFAP antibodies. The antibody against GFAP labelled the dendrites whereas eGFP was distributed mainly in the cell somata, which makes it challenging to point out a colocalization of the two markers.

In the lateral ventricle (LV) ependyma most, but not all, eGFP-positive cells expressed also GFAP (Fig. 27). The eGFP/GFAP-positive cells were observed in the ependymal cell layer directly lining the lateral ventricle (Fig. 27 A1-3) and in the top corner of the LV, where the

origin of the rostral migratory stream (RMS) is located (Fig. 27 B1-3). However, the RMS itself comprised GFAP-positive but eGFP-negative cells.

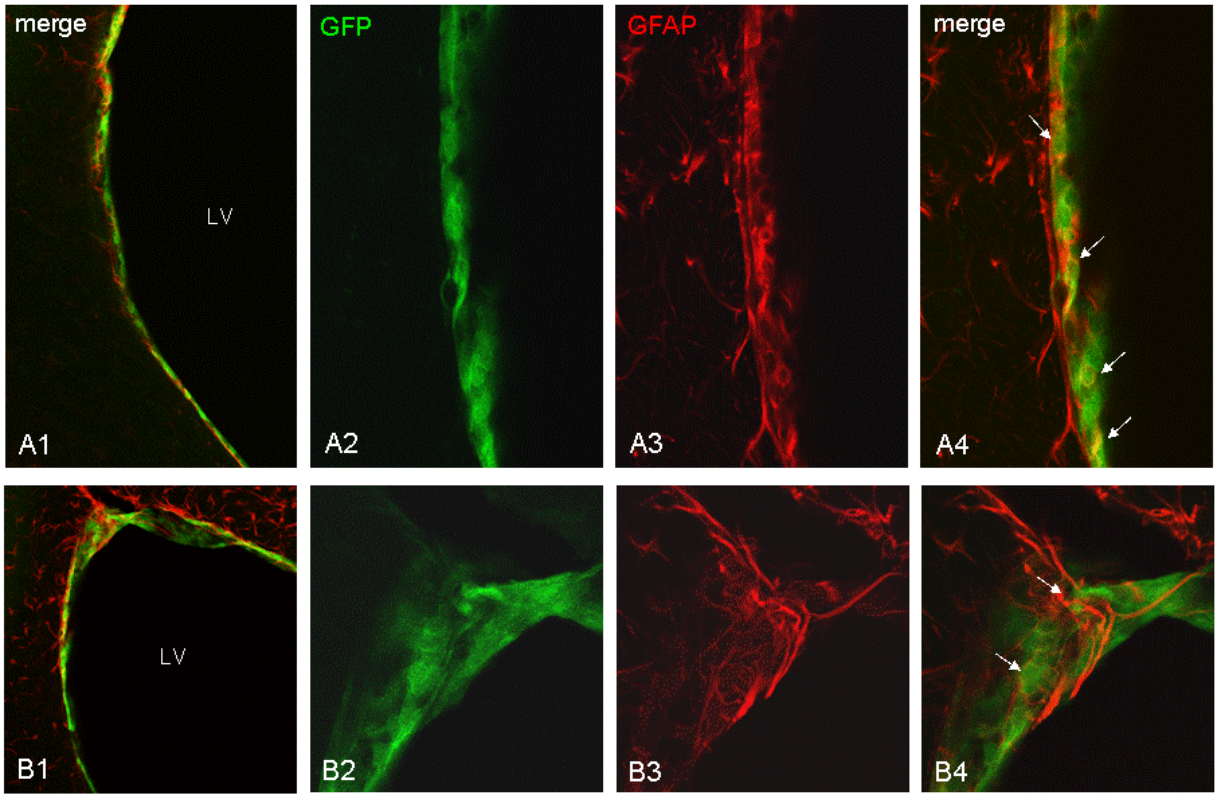

Fig. 27: Double immunofluorescence characterization of eGFP- and GFAP-expressing cells in the ventricular region. Sagittal brain sections of CaV1.3-GFP$^{switch/+}$ mice. **(A1-3)** In the ependymal cell layer lining the lateral ventricle (LV) eGFP-positive cells were colabelled with GFAP (white arrows). **(B1-3)** Colocalization of eGFP/GFAP-expressing cells in the top corner of the LV. The beginning rostral migratory stream, which is indicated by GFAP-positive cells, comprised no eGFP-expressing cells.

4.2.5.5 Localization of eGFP- and SOX2-positive cells

The transcription factor SOX2 (Sry-related HMG box 2) is a marker for embryonic neural stem cells and adult neural precursor cells. Additionally, it is required for the proliferation and maintenance of these cells. In the adult brain SOX2 is expressed within most proliferating neurogenic regions like the periventricular ependyma and subependyma (Ferri et al., 2004).

For better characterization of eGFP-expressing cells in these neurogenic regions, double-immunofluorescence experiments against eGFP and SOX2 were performed. A strong colabelling was detected in the ependymal cell layer lining the LV (Fig. 28 B) and in the

subventricular zone (Fig. 28 A and C). SOX2 was staining the cell nucleus whereas eGFP is labelled in the somata and, more weakly, in the dendrites.

These data suggest that Cav1.3α1 is expressed in the proliferating neuronal precursors in the neurogenic region at the lateral ventricle.

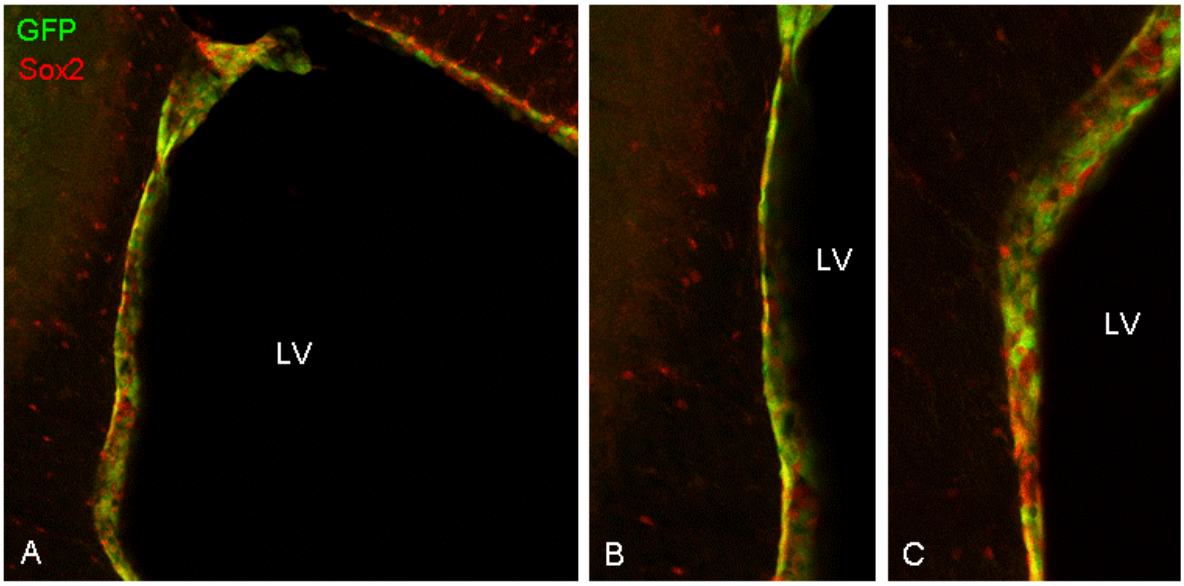

Fig. 28: Colocalization of eGFP and SOX2-positive cells in the lateral ventricle ependyma and subventricular zone. Double-immunofluorescence observed co-staining of eGFP and neuronal stem cell marker SOX2 in the ventricular zone.

4.2.5.6 Localization of eGFP- and TPH1-positive cells

A previous immunohistochemical study in the rat brain stem revealed a distinct Cav1.3 immunoreactivity in the caudal, median and dorsal raphe nuclei (Sukiasyan et al., 2009). To examine whether serotonergic neurons expressed eGFP in CaV1.3-GFP$^{switch/+}$ mice, double-immunostaining was carried out using antibodies against eGFP and TPH1. Tryptophan hydroxylase 1 is the rate limiting enzyme involved in the synthesis of the monoaminergic neurotransmitter 5-HT which marks all serotonergic cells in the central nervous system and in the periphery. Serotonergic raphe nuclei were analyzed in three different parts of the brain stem, the caudal nuclei in the medulla oblongata and the dorsal and median raphe nuclei in the pons and midbrain. As displayed in Fig. 29, eGFP-positive cells did not colocalise with TPH1-stained cells in all analysed raphe nuclei. These data indicate that the Cav1.3α1 channel was not expressed in 5-HT cells.

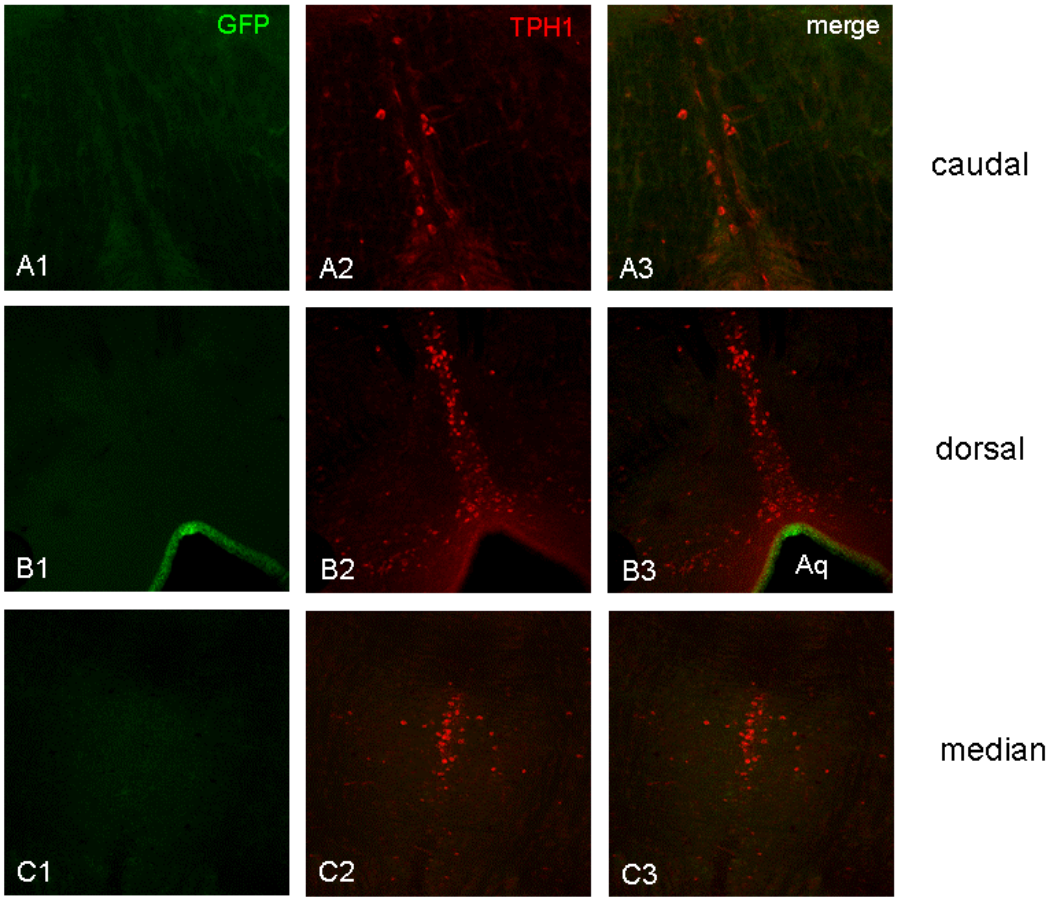

Fig. 29: Immunolabelling of eGFP- and TPH1-positive cells in coronal brain sections of Cav1.3-GFP$^{switch/+}$ mice. No coexpression of eGFP and TPH1 could be detected in the caudal **(A)**, dorsal **(B)** and median **(C)** serotonergic raphe nuclei.

5 Discussion

The neuronal L-type VGCCs $Ca_V1.2$ and $Ca_V1.3$ have been implicated in various physiological functions as heart development and cardiac pacemaking activity, behaviour, learning and memory, depressive-like behaviour, insulin secretion or inner ear development. The two isoforms have a similar expression pattern and are both sensitive to dihydropyridines (DHPs), a class of organic Ca^{2+} channel blockers and activators. Although pharmacological analyses have provided much insight into the regulation and function of L-type channels in neurons, all blockers have additional substantial input on the function of the CNS by affecting cardiovascular system functions. Moreover, available pharmacological tools do not allow the separation of the individual function of the isoforms $Ca_V1.2$ and $Ca_V1.3$.

Therefore, we used a genetic approach to get deeper insights into $Ca_V1.3$ expression and function. In recent years, several mouse models that target L-type channel genes were generated, including a conventional $Ca_V1.3$ knockout. However, limitations of the conventional gene targeting are the induction of compensatory gene expression, early embryonic lethality or the effect of peripheral phenotypes on the CNS. To circumvent these problems we have used the conditional *Cre/loxP* system as a technology for spatial and temporal control of gene inactivation. In our genetic approach, the $Ca_V1.3$-GFP^{flex} exon 2 of *Cacna1d* is inactivated using a *Cre*-dependent genetic switch (FLEX switch), representing an elegant way to monitor the cell with the inactivated channels after *Cre*-recombination. To investigate the functionality of the FLEX switch, the mouse line was analysed by breeding the conditional $Ca_V1.3$ mice with Cre-deleter mice and CamKIIa-Cre mice. Furthermore, the expression pattern of the $Ca_V1.3\alpha1$ subunit, mirrored by the expression of the reporter gene eGFP, was analysed by immunohistochemical methods.

5.1 Targeting Strategy of the $Ca_V1.3$-GFP^{flex} Construct

The strategy for the conditional mutation of the $Ca_V1.3$ channel was the FLEX (Flip Excision) switch, which is based on gene trap mutagenesis combined with site-specific recombination. Gene trapping was originally a high-throughput approach that can be used to introduce insertional mutations into the genome of mouse ES cells. It is performed with gene-trap

vectors whose principle element is a gene-trapping cassette consisting of an inverted promoterless reporter gene flanked by an upstream splice acceptor and a downstream transcriptional termination sequence polyA (polyadenylation site). Additionally, the cassette harbours a drug resistant gene as selection marker. When inserted into an intron of an expressed gene, the gene-trap cassette is transcribed from the endogenous promoter in form of a fusion transcript in which the exon upstream of the insertion site is spliced in frame to the reporter gene. However, these gene-trap vectors produce only null mutations which can cause embryonic lethal phenotypes. To address this limitation a site-specific recombination strategy termed Flip Excision (FLEX) was developed for conditional gene manipulation (Schnutgen et al., 2003). The FLEX switch uses two pairs of heterotypic, inversely oriented and alternately arranged *loxP*-type recombination sites. *Cre*-mediated recombination of either homotypic *loxP* site will cause inversion of the coding sequence (exon) and the reporter gene, followed by excision between the two homotypic *loxP* sites, leading to one of each heterotypic recombination sites oppositely oriented and incapable for further recombination. This results in inactivation of the coding sequence, while the expression of the reporter gene is turned on, and provides a rapid and precise identification of the disrupted gene on cellular level.

The Cav1.3-GFP^{flex} mouse line was generated by a "knock-in" of the FLEX switch vector performed by homologous recombination in ES cells. One of the first considerations when designing a targeting vector, is to determine the gene region which to delete. Since the Cav1.3α1 gene *Cacna1d* is large (~250 kDa) and distributed, depending on the transcript, to 47 - 49 exons and thereby spanning over 400 kb, we decided to inactivate an important exon close to the 5′ end. The conventional Cav1.3α1 knockout in mice was successfully accomplished by disrupting exon 2, by insertion of the *Neo* resistant cassette into the exon, resulting in the generation of a complete null allele (Platzer et al., 2000). For this reason we decided to target also exon 2 in the Cav1.3α1 gene. The FLEX-targeting vector was designed in that way that upstream of Cav1.3α1 exon 2 two heterotypic *loxP* sites were located and downstream the inverted reporter gene eGFP with the splice acceptor and polyA site, a *FRT*-flanked *neo* resistant gene and the second two *loxP* sites were introduced. The splice acceptor of the *eGFP* gene was chosen in the same open reading frame like Cav1.3α1 exon 2 so that eGFP is spliced in frame to the upstream exon 1 after *Cre*-mediated inversion.

In conditional gene knockouts, the gene has to be unaffected by modifications and must function normally like the endogenous one until recombined by *Cre* recombinase. Thus, when introducing the gene targeting elements into the genomic sequence, we had to consider that they were placed outside coding regions and did not interfere with regulatory intronic regions like splice acceptor and donor sites. When Cav1.3α1 exon 2 was flanked by the two heterotypic pairs of *loxP* sites and the exon-trap cassette, they were inserted 330 bp upstream and 230 bp downstream of the exon to do not interfere with regulatory elements surrounding the exon.

As mentioned above, prerequisite for the FLEX system was the availability of heterotypic *loxP* sites. The most commonly used combination of heterotypic *loxP* sites are WT *loxP* with *loxP511*, which differ by 1 bp in the core spacer region. Nevertheless, illegitimately recombination between them has been reported (Lee and Saito, 1998). Therefore, we used *lox257* (also referred to as *L3*), which differs by 3 nucleotides in the spacer sequence from the WT *loxP* site, thereby regarded to be less permissive as well as more efficient (Wong et al., 2005). When engineering FLEX switch vectors, it is also important to consider that the distance between homotypic *loxP* sites, once inversion has taken place, actually allows excision to occur. For successful excision the minimum distance between two homotypic recombination sites like two WT *loxP* or two *L3* must be at least 82 bp long (Hoess et al., 1985). In the Cav1.3-GFP^{flex} targeting construct the *loxP* sites were arranged in such a way that the distance between two homotypic sites after recombination was not closer than 100 bp, regardless whether the inversion occurred first via the recombination between WT *loxP* or *L3* sites.

By recombination in EL350 bacteria cells we could demonstrate the functionality of the *Cre*-mediated switch in the FLEX vector. The stable inversion of Cav1.3α1 exon 2 into the antisense direction and of eGFP into the sense orientation was successfully confirmed by restriction analysis and PCR. Since the reporter eGFP will, after targeting into the mouse genome, represent the expression of the Cav1.3α1 channel, we further verified the functionality of the eGFP protein in eukaryotic HeLa cells before proceeding to ES cell targeting. One difficulty was that in HeLa cells the promoterless reporter gene was not inserted into the genome by homologous recombination and therefore was not driven by the

endogenous Cav1.3α1 promoter. Moreover, the Cav1.3α1 promoter is presumably inactive in cervix carcinoma cells. For this reason we introduced a strong eukaryotic Caggs promoter, containing an additional 3' splice donor, into the intron upstream of exon 2. We could show that in the CaV1.3-GFP^{flex} construct, coelectroporated with a *MC1-Cre*-plasmid into HeLa cells, the inversion occurred and the reporter gene encoded for a functional fluorescent protein. Importantly, no eGFP fluorescence could be detected in control cells transfected without *Cre*, indicating that the eGFP cassette was fully silent before Cre-mediated rearrangement.

5.2 ES Cell Targeting of $Ca_V1.3$-GFP^{flex}

Homologous recombination of a targeting construct into the mouse ES cell genome is based on positive selection of a drug resistance in order to differentiate homologous recombination from random integration. In the targeting construct a neomycin resistant gene (*neo*) was used flanked by two *FRT* sites which allow later removing of the *neo* cassette. Additional, a negative selection marker (MC1-HSV-TK) was introduced downstream of the 5' homologous arm, that selected against random integration events into the genome. The combination of the two selection systems provided an efficient targeting of the Cav1.3α1 gene. Six ES cell clones out of 18 analysed clones (33%) were identified for correct homologous recombination, replacing the endogenous gene. Correctly targeted ES cell clones were injected into blastocysts and tested for germline transmission of the targeted Cav1.3α1 allele by backcrossing with C57Bl/6 mice. The high transmission to the next generation attested the high contribution of manipulated ES cells to the chimeras. Since the *loxP* sites, the reporter gene and *neo* were inserted into intronic regions flanking exon 2, Cav1.3α1 gene transcription should not be disturbed. Heterozygous Cav1.3-GFP$^{flex/+}$ mice were viable and displayed a phenotype comparable to WT.

Even though the *neo* resistance cassette was introduced into an intron, it can interfere with the expression of the targeted or neighbouring genes. In some cases, it has been determined that cryptic splice sites in *neo* interfere with normal splicing and therefore reduce WT mRNA levels or even lead to lethality (Pham et al., 1996; Ren et al., 2002). In Cav1.3-GFP$^{flex/+}$ mice the removal of *neo* was essential for efficient recombination of the targeted allele.

For these reasons *neo* was excised from the mouse genome by crossing Cav1.3-GFP^{flex} mice with *Flpe*-deleter mice, ubiquitously expressing the *Flpe* recombinase even in early development. After removal of the *neo* cassette Cav1.3-GFP^{flex} mice were backcrossed to C57Bl/6 mice, being the standard strain for genetic and behavioural analysis. Since the R1 ES cells were derived from a different mouse strain (129/SvJ) it is important to backcross the offspring of chimeric mice up to 10 times with C57Bl/6 mice to avoid genetic and phenotypic variation caused by mixed genetic backgrounds (Joyner, 1993). Particularly for future behavioural analysis it is essential to have a pure genetic background of at least 99.9%.

5.3 Conditional Knockout of $Ca_V1.3\alpha1$ by the Cre-mediated FLEX switch

Conditional gene knockout provides the ability to inactivate an endogenous gene in the mouse genome in a spatially and temporally controlled manner. It is not only useful to circumvent lethal phenotypes but also allows biological questions to be addressed with exquisite accuracy. In this study we used the FLEX switch, coupling conditional gene ablation to reporter gene activation after *Cre*-recombination.

The FLEX switch was first presented in 2003 by Schnütgen et al. presented as a directional strategy to detect *Cre*-dependent gene ablation at single cell level in the mouse genome (Schnutgen et al., 2003). He could show the complete *Cre*-mediated deletion of the retinoic acid receptor gene and the simultaneous expression of the reporter gene lacZ. Another study used the FLEX switch to target channelrhodopsin-2 for photostimulation of neurons (Atasoy et al., 2008). Just recently a study reported the generation of a FLEX switch-based reporter line for visualization of recombinase activity in zebra fish (Boniface et al., 2009). Even though only few studies are known using this system in animal models, these reports present the FLEX strategy as an elegant and efficient way to generate a conditional gene knockout.

When crossed to Cre-deleter mice we first used Cav1.3-GFP$^{flex/+}$ mice which still harboured the *neo* cassette, since after *Cre*-mediated inversion of the floxed sequence *neo* should be located between two homotypic recombination sites and subsequently be excised (Fig. 7). However, it required two successive breeding rounds with Cre-deleter mice until the switch with an inversion of exon 2 in antisense and eGFP in sense direction could be detected in

Cav1.3-GFP$^{flex/+}$ x Cre-deleter mice (Cav1.3-GFP$^{switch/+}$). One reason could be that the Cre recombinase must catalyse the recombination of four *loxP* sites. First the inversion between two homotypic *loxP* sites oriented head-to-head had to take place followed by an excision between the other pair of homotypic *loxP* sites. Possibly the E2a promoter, driving *Cre* in Cre-deleter mice, was too weak and offspring from the second breeding round were homozygous for the *Cre* gene, providing enough recombinase protein to promote the FLEX switch. Further PCR analysis revealed that in some animals the switch was stuck in an intermediate stage after inversion between *L3* sites, without further excision between the WT *loxP* sites (Fig. 5). Here, recombination between mutant *L3* sites seems to be more efficient than that between WT *loxP* sites. The *L3* site was developed by Wong et al. after the finding of illegitimate recombination between the commonly used combination of *lox*511 and the original *loxP* site (Wong et al., 2005). However, *L3* was never tested in the FLEX system before, so one has to consider that recombination between *L3* could be favoured over recombination between *loxP*.

Another possibility of the hindered switch was the presence of the *neo* cassette which may have an influenced on *Cre* recombination. For this reason Cav1.3-GFP$^{flex/+}$ mice in which the *neo* cassette was already removed were crossed to Cre-deleter mice. Here, the FLEX switch occurred immediately in the first mating round. DNA analysis from tail and brain DNA revealed a complete switch between the two pairs of heterotypic *loxP* sites. To confirm our results, Cav1.3-GFP$^{flex/+}$ mice with and without *neo* were additionally bred with CaMKII*α*-Cre mice, expressing *Cre* exclusively in the forebrain. Even though the CaMKII*α* promoter is well-established to be a very strong promoter the switch did not take place in Cav1.3-GFP$^{flex/+}$ mice which still harboured the *neo* cassette. After removal of *neo*, in contrast, also here the switch happened efficiently and completely in all Cav1.3-GFP$^{flex/+}$ x CaMKII*α*-Cre mice analyzed. These results demonstrate that the *Cre*-mediated FLEX switch occurred efficiently in Cav1.3-GFP$^{flex/+}$ mice if the *neo* cassette has previously been excised.

5.4 mRNA-Expression of $Ca_V1.3$

The reporter gene eGFP of the FLEX vector is promoterless and instead flanked by an upstream universal adenovirus splice acceptor (AdSA) and a downstream transcriptional termination sequence, the bovine growth hormone polyadenylation signal (pA). When introduced into the Cav1.3α1 locus and stable inverted by the *Cre*-mediated switch, eGFP expression will be driven by the endogenous Cav1.3α1 promoter. Prerequisite for a proper reporter gene expression is that exon 1 has to be spliced in frame to eGFP. Therefore it was essential to determine the correct open reading frame. The reporter gene was friendly provided by the group of Prof. Harald von Melchner from Frankfurt, with the SA in three different frames to be able to choose a frame matching the upstream exon. In the endogenous Cav1.3α1 gene exon 1 ends with G and exon 2 starts with AG which together form the triplett codon GAG coding for the amino acid glutamate. The AdSA with the splice site consensus AG was chosen in frame +2 which has two additional nucleotides TG upstream the translational start codon of eGFP. After splicing to exon 1, the two additional nucleotides from the SA together with G from exon 1 represent the codon GTG, followed by the reporter gene start codon ATG.

By mRNA analysis of Cav1.3-GFP$^{flex/+}$ mice crossed with Cre-deleter (Cav1.3-GFP$^{switch/+}$ mice) we could show the correct splicing of Cav1.3α1 exon 1 to the eGFP transcript. RT-PCR confirmed the exon1-eGFP transcript with a specific 220 bp amplification product. Contamination of genomic DNA can be excluded as exon 1 is located more than 1900 bp from the inverted locus which would result in a 2060 bp PCR fragment.

Because eGFP is further flanked by a downstream polyA sequence, transcription of Cav1.3α1 is terminated prematurely at this site, leading to a fusion transcript that encodes a functional reporter protein but a truncated, non-functional Cav1.3α1 protein. Additionally, the inversion of exon 2 inserts to several stop codons, which ensure translational termination in the case of the failure of polyA to terminated expression of Cav1.3α1. These RT-PCR experiments showed that, after stable inversion, eGFP is spliced to Cav1.3α1 exon 1, which leads to eGFP expression driven by the endogenous Cav1.3α1 promoter.

5.5 Expression pattern of $Ca_V1.3\alpha1$ mRNA represented by eGFP staining

The FLEX system allows monitoring the ablation of a gene of interest by simultaneous activation of a reporter gene. In this study, after the FLEX switch Cav1.3α1 exon 2 was replaced by eGFP. Thus, eGFP expression represents the expression pattern of the Cav1.3α1 calcium channel. As Cav1.3α1 is widely expressed in brain, brain slices of heterozygous Cav1.3-GFP$^{switch/+}$ mice were analysed for eGFP expression. Immunohistochemistry using antibodies against eGFP observed expression in many parts of the brain. However, the direct autofluorescence of eGFP was too weak to be detected under a fluorescent microscope. This may be due to the low protein concentration in heterozygous mice. Further examinations of homozygous Cav1.3-GFP$^{switch/switch}$ mice will elucidate this issue. In contrast, the Cav1.3-GFP^{flex}/*Cre*-transfected HeLa cells had displayed strong eGFP autofluorescence. Here, the HeLa cells contained both the Cav1.3-GFP^{flex} vector and the *Cre*-plasmid episomally in many copies which may lead to strong eGFP expression and fluorescence.
Taken together, the expression of the FLEX reporter gene in Cav1.3-GFP$^{flex/+}$ x Cre mice demonstrates the functionality of the conditional FLEX switch *in vivo* and that eGFP is functionally expressed and driven by the endogenous Cav1.3α1 promoter.

The FLEX switch mediated gene deletion of Cav1.3 which was visualised by eGFP expression. This feature can be utilised to examine the exact expression pattern and distribution of the inactivated gene. So far, most data of Cav1.3α1 localization in the brain were based on immunohistochemistry studies using Cav1.3α1 antibodies. However, no reliable Cav1.3 antibodies are available so far and potential cross-immunoreactivity with other proteins may influence the results. Moreover, the immunolabelling data are in many parts of the brain contradicting to in situ hybridization studies investigating localization and level of Cav1.3α1 gene expression (Tanaka et al., 1995). To address this problem, Cav1.3-GFP$^{flex/+}$ mice were crossed with Cre-deleters (CaV1.3-GFP$^{switch/+}$), which express *Cre* recombinase ubiquitously from early development on and generating germline deletion, thus providing an elegant tool for monitoring Cav1.3α1 in all tissues where the channel is normally expressed. Additionally, we crossed Cav1.3-GFP$^{flex/+}$ mice with CamKIIa–Cre mice to investigate Cav1.3 expression specific to the forebrain.

5.5.1 eGFP Expression in Neurons

Analysis of the distribution of eGFP stained cells exposed, in parts, a so far unknown expression pattern of the calcium channel. We observed eGFP labelling in mainly the cell bodies in all regions of the cerebral cortex, corresponding to the data of Hell et al. Co-staining with NeuN confirmed the neural cell type of these cells. In the olfactory bulb (OB) eGFP labelling was detected in the glomerular layer, in the granular layer and slightly in the mitral cells. L-type Ca^{2+} channel expression in the OB has been described controversially in the literature. Three different studies, using in situ hybridization and pharmacological studies as well as Ca^{2+} current recordings, provided evidence for the presence of L-type channels in olfactory bulb neurons (Davila et al., 2003; Tanaka et al., 1995; Wang et al., 1996), while other data argued against it (Yuan et al., 2004).

In the cerebellum of $Ca_V1.3$-$GFP^{switch/+}$ mice eGFP expression was observed in the Purkinje cells and in small cells in the molecular cell layer, whereas in the granular cell layer no eGFP-positive cells were found. In the literature, prominent expression of $Ca_V1.3$ in the cerebellum was reported in the cell bodies of the Purkinje cells and its dendrites projecting to the molecular layer, and a more moderate expression of small cells in the molecular and granular cell layer (Kim et al., 2004). Unlike our findings Hell et al. described intense staining in the granule layer (Hell et al., 1993). In contrast to our strategy to monitor $Ca_V1.3$ expression via reporter gene, thereby mirroring mRNA expression, the previous localization study was done by immunohistochemistry.

Previous findings observed intense $Ca_V1.3\alpha1$ expression in pyramidal neurons in the CA1-CA3 areas and granule cells in the dentate gyrus as well as in interneurons of the these regions (Hell et al., 1993). Several functions in the hippocampus have been accredited to $Ca_V1.3$ channels. It could be shown that working memory impairment is correlated with age-related increase in $Ca_V1.3\alpha1$ expression in area CA1 (Veng et al., 2003). Studies using conventional $Ca_V1.3$ knockout mice revealed that this channel mediates consolidation of contextually conditioned fear in mice (McKinney and Murphy, 2006). However, FOS expression studies as marker for neuronal activation observed only low contribution of $Ca_V1.3$ to c-Fos induction in area C1-C3 and the dentate gyrus (Hetzenauer et al., 2006). This is consistent with analysis of $Ca_V1.2$ and $Ca_V1.3$ knockout mice which suggested the $Ca_V1.2$

but not Cav1.3 isoform to play the prominent role in NMDA receptor-independent synaptic plasticity and memory formation (Clark et al., 2003; Moosmang et al., 2005).

Contrary to previous localization studies, we found only moderate expression of the eGFP reporter gene in the hippocampus of Cav1.3-GFP$^{flex/+}$ x Cre-deleter and CaMKIIa-Cre mice. In the stratum oriens and stratum radiatum in the CA1-CA3 region as well as the stratum moleculare and radiatum of the dentate gyrus a slight staining could be detected by DAB immunohistochemistry against eGFP. Though, this moderate staining could not be detected in direct immunofluorescence staining. This might be due to the more sensitive DAB staining, where the immunoreaction is amplified by the biotin-avidin system. It also has to be considered that the weak labelling might be background staining. However, the non-stained negative control of single-transgenic Cav1.3-GFP$^{flex/+}$ mice argues against it. Interestingly, some strongly stained large cells were observed in the pyramidal cell layer and stratum oriens. Double immunofluorescence indentified at least some eGFP-expressing cells as GABAergic interneurons. Also their large size and morphology argues for inhibitory neurons. Evidence for Cav1.3 expression in various GABAergic interneurons in the CA1 pyramidal cells and stratum oriens was provided by an immunohistochemical approach by Vinet et al. (Vinet and Sik, 2006).

We further found eGFP expression in several regions of the amygdala, the paraventricular nucleus (PVN), the locus coeruleus (LC) and different thalamic subregions like the lateral posterior thalamic nucleus, the dorsal lateral geniculate nucleus and the pregeniculate nucleus. These results are consistent with further observations measuring BayK-induced Cav1.3 mediated c-Fos activation in most of the described regions (Hetzenauer et al., 2006). In particular the amygdala, the locus coeruleus and the hypothalamic PVN are brain areas associated with emotion-related behaviour like anxiety- and depression-related behaviour and processing of stress (Millan, 2003). This is also conform with the findings that BayK-induced activation of these regions elicits increased depression-like behaviour (Sinnegger-Brauns et al., 2004) and that Cav1.3$^{-/-}$ null mutants display a suppressed anxiety-like behaviour (Nguyen et al., 2005). An interesting observation was the eGFP expression in the habenular nuclei. It has been proposed that the habenula is implicated in human major depressive episodes (Sartorius and Henn, 2007). The increased activation of the lateral

habenular nucleus leads to stimulation of the hypothalamic-pituitary-adrenal (HPA) axis and to the down regulation of the serotonergic, noradrenergic, dopaminergic systems.
Even though eGFP expression was found in regions involved in depression-like behaviour, no staining could be detected in the raphe nuclei, the brain regions from which the serotonergic fibres originate. Double-immunofluorescence studies revealed no coexpression of the 5-HT marker TPH1 and eGFP.

Apart from brain areas associated with cognitive behaviour, eGFP expression was noted in brain areas implicated in sensory processing. A specific staining was observed in the bed nucleus of accessory olfactory tract (BAOT), a vomeronasal system structure, which is involved in the maternal behaviour in female rats (Del Cerro et al., 1991). In the brainstem, the cuneate nucleus of the medulla and the facial nucleus of the pons were found to be eGFP-positive. This corresponds well to Cav1.3 immunoreactivity studies by Sukiasyan et al. who reported a strong labelling in the facial nucleus 7N and the cuneate nucleus (Sukiasyan et al., 2009). Furthermore, we detected an intense eGFP-staining in the superficial gray layer and the optic layer of the superior colliculus (SC) in Cav1.3-GFP$^{switch/+}$ mice. The superior colliculus plays an important role in the development of retinotopic maps. It receives retinal ganglion cell projections that form a precise point-to-point map of visual space. Consistent with our results, c-fos expression studies revealed Cav1.3-mediated Fos activation in the superficial gray layer and optic layer of the SC (Hetzenauer et al., 2006). Moreover, immunohistochemistry studies of Mize et al. showed expression of Cav1.2 in the SC, a channel with an expression pattern very similar to that of Cav1.3 (Mize et al., 2002). Several studies provided evidence for a role of L-type calcium channels in developmental synapse refinement of visual system structures by mediating long term potentiation (LTP) and long-term depression (LTD) in the SC (Cork et al., 2001; Lo and Mize, 2000, 2002). A recent study reported, that simultaneous activity of L-type channels and NMDA receptors are essential for induction of LTP in the juvenile superior colliculus in rodents (Zhao et al., 2006). This LPT was found to be activated by exceptionally low frequency of 20 Hz. That might argue for the involvement of Cav1.3 channels which have a relatively low activation threshold compared to Cav1.2. Further investigations will be necessary to clarify the function of Cav1.3 in retinotopic map formation.

5.5.2 eGFP Staining in the Periventricular zone

The most intense and at the same time unexpected eGFP expression in Cav1.3-GFP$^{flex/+}$ x Cre-deleter mice was observed in the peri- and subventricular zone of the lateral ventricle wall. The anterior part of the subventricular zone (SVZ) is, beside the dentate gyrus subgranular zone of the hippocampus, the brain region where adult neurogenesis is located (Taupin and Gage, 2002). The SVZ is the mitotically active region immediately adjacent to the lining of the lateral ventricle where neural stem cells and progenitor cells reside. These cells migrate to the olfactory bulb via the rostral migratory stream (RMS) where they differentiate into interneurons. The source of RMS neuroblasts are GFAP-positive neural stem cells (NSCs) adjacent to the ventricles (Ghashghaei et al., 2007). One attribute of NSC is that they express characteristic proteins which can be used for identification of these cells. Besides GFAP, neural stem/precursor cells (NPCs) also express SOX2, which is implicated in precursor-cell proliferation and NSC maintenance (Episkopou, 2005).

Double-immunohistochemistry analysis revealed eGFP/GFAP- and eGFP/SOX2- expressing cells in the layers adjacent to the lateral ventricle. It is difficult to distinguish whether these cells are ependymal cells directly lining the cells and/or cells in the subventricular zone as both cells types express the NPC markers GFAP and SOX2. Type B cells for example, the SVZ proliferating astrocytes, interact closely with ependymal cells and occasionally contact the ventricle lumen (Doetsch et al., 1999b). But also ependymal cells have been suggested to divide in vivo and function as stem cells (Johansson et al., 1999). Interestingly, whereas GFAP-expressing cells were labelled also in the RMS, eGFP-positive cells could not be detected to be migrating in Cav1.3-GFP$^{switch/+}$ mice. This can be explained that the endogenous Cav1.3 promoter might not be active anymore when the cells change their phenotype to migrating cells. The co-staining of eGFP with the NPC markers GFAP and SOX2 argue for an expression of the calcium channel Cav1.3α1 in the proliferating, neurogenic region.

It is well established that Ca^{2+} influx through neuronal L-type VGCCs results in signalling that affects the expression of genes involved in cell proliferation and neuronal differentiation (Hardingham et al., 1998; Weick et al., 2003). D'Ascenzo et al. hypothesized that these Ca^{2+} signals may also influence the differentiation of neural stem/progenitor cells toward the neural phenotype (D'Ascenzo et al., 2006). This neuronal differentiation from the NSCs derived from brain cortex of postnatal mice was strongly inhibited by the L-type channel

blocker nifedipine, and conversely, increased by the activator Bay K 8644. A similar study reported that exposure to extremely low-frequency electromagnetic fields promotes *in vitro* neurogenesis by upregulating the expression and activity of Cav1.2 and Cav1.3 (Piacentini et al., 2008). Also here the neuronal differentiation of NSCs was significantly increased by nifedipine.

Some studies also reported an implication of L-type VGCCs in adult neurogenesis. It has been shown that L-type channels are involved in ischemia-induced neurogenesis in the dentate gyrus and SVZ by upregulating inducible nitric oxide synthase expression in adult mice (Luo et al., 2005). Furthermore, Deisseroth et al. found that neurogenesis from adult NPCs promoted by excitation (excitation-neurogenesis coupling) is mediated by Cav1.2/Cav1.3 channels and NMDA receptors *in vivo* and *in vitro* (Deisseroth et al., 2004). Excitation through these channels acts to increase the expression of proneural phenotype genes and inhibit expression of glial fate genes. Neural precursors tent to have a more depolarized resting potential (in the -55 mV range) than mature neurons (Wang et al., 2003). This may lead to a partial opening of Cav1.2/Cav1.3 channels even in the resting, non-stimulated condition (Deisseroth et al., 2004). The relative resistance to inactivation at a more hyperpolarized state is characteristic for these channels, especially for Cav1.3, and makes them therefore well-suited to this type of chronic signalling.

Taken together, our findings of Cav1.3 expression in the peri- and subventricular zone together with previous observations suggest a role of Cav1.3α1 in adult neurogenesis and NSC proliferation. Further experiments using BrdU (bromodeoxyuridine) labelling will provide more information about the nature of eGFP expressing cells in the neurogenic subventricular zone.

5.5.3 eGFP Expression in Other Tissues

Besides neurons, Cav1.3 expression has been reported in several tissues like the heart, inner ear or pancreatic ß-cells. In the heart Cav1.3 is known to be located in the sinoatrial node (SAN), where it is required for cardiac pace making (Platzer et al., 2000). However, we have found eGFP expression also in the septum of the heart, which separates the right and left ventricle. This is conceivable as in the septum the bundles of His are located which conduct the electrical impulse from the sinoatrial node and the atrioventricular node into the

ventricles. Since the isolation and staining of the SAN requires specific skills, these analysis will be done by cooperation with Matteo Magnoni (University Montpellier) who is specialised on the mouse heart and this method.

Furthermore, Cav1.3 channels are expressed in the cochlea, where they are essential for the development of outer (OHC) and inner hear cells (IHC) and for almost all Ca^{2+} currents in the IHCs (Brandt et al., 2003; Platzer et al., 2000). To investigate eGFP expression in cochlear hair cells in Cav1.3-GFP^{flex} mice we have provided these mice to the group of Marlies Knipper in Tübingen. There the mice will be crossed to IHC/OHC-specific Cre mice which will result in a deletion of the channel restricted to the inner ear.

So far, the role of Cav1.3 VGCCs in the pancreas has been discussed controversially. However, recent findings revealed that, whereas Cav1.2 mediates the first high peak of insulin release, Cav1.3 is implicated in the maintenance of persistent insulin secretion (Eric Rennström, Lund University, personal communication). To gain more insights into pancreatic functions, ß-cells of Cav1.3-GFP^{flex} mice will be investigated by cooperation with this group.

5.6 Conclusion and Outlook

The Cav1.3-GFP^{flex} mice we have generated provide an important tool to inactivate Cav1.3 in specific tissues with simultaneous reporter gene expression, identifying cells with the gene ablation. This presents a new and interesting tool to elucidate the role of this calcium channel in living tissues *in vivo*. So far, existing immunoreactivity studies using anti-Cav1.3 antibodies and *in situ* hybridization studies reported partially inconsistent expression and distribution of Cav1.3 (Hell et al., 1993; Sukiasyan et al., 2009; Tanaka et al., 1995). Since in Cav1.3-GFP^{switch} mice eGFP is directly spliced to the upstream exon 1a and thereby driven by the endogenous Cav1.3 promoter, we propose that the labelling we observed represents the actual expression of the Cav1.3 mRNA.

However, in some brain areas like the hippocampus and the neurogenic region of the lateral ventricle the pattern we found differed from the previously published data. The eGFP expression reflects the activation state of the Cav1.3 promoter. This may explain that we found in some brain areas a remarkably high, in other areas an unexpected low expression.

Additionally, it has to be considered that the insertions of gene targeting elements into intronic sequences may have disturbed regulatory elements which may influence the expression pattern of the channel. Analysis of homozygous Cav1.3-GFP$^{flex/flex}$ will show whether the Cav1.3 channel is expressed normally like in wildtype mice. Another possibility could be the presence of an alternative splice form of exon 2 that we might have targeted. Homozygous Cav1.3-GFP$^{switch/switch}$ knockout mice will again clarify whether the Cav1.3α1 deletion is complete. Furthermore, *in situ* hybridisation studies using a probe for exon 2 sequence will be helpful.

Several studies have linked Cav1.3 channels to various diseases like cardiac arrhythmia and bradycardia, Parkinson's disease, anxiety- and depression-related behaviour and diabetes. Due to the lack of currently available selective L-type VGCC blockers, Cav1.3-GFP^{flex} mice will provide a new and useful tool to dissect the physiological role of L-type VGCCs. The mouse line may serve as basis for the development of specific calcium channel modulators for future therapeutic use.

6 Abbreviations

α	alpha
β	beta
µ	micro
A	Ampere
aa	amino acids
Ad	Adeno virus
Amp	ampicillin
AMPA	L-α-amino-3-hydroxy-5-methyl-isoxazolpropionic acid
ATP	Adenosine triphosphate
BAC	Bacterial artificial chromosome
bla	gene for the enzyme ß-Lactamase (ampicillin resistance)
bp	base pairs
BrDU	bromodeoxyuridine
BSA	bovine serum albumin
C	Celsius
Ca^{2+}	calcium
CA1-3	Cornus ammonis fields 1-3
CaMKIIa	Ca^{2+}/Calmodulin-dependent protein kinase II α
cAMP	Cyclic adenosine monophosphate
Carb	carbenicillin
C-terminal	Carboxy-terminal of a protein
cDNA	copy DNA
Cm	chloramphenicol
cre	gene for the Cre-recombinase
DA	Dalton
DAB	diaminobenzidine
DCX	doublecortin
DMSO	dimethylsulfoxide
DNA	deoxyribonucleic acid
DNAse	deoxyribonuclease
dNTP	2´-deoxyribonucleotide
dsDNA	double stranded DNA
E.coli	Escherichia coli
EDTA	ethylenediaminetetraacetic acid
eGFP	enhanced green fluorescent protein
ES	embryonic stem cells

et al.	et alii
EtBr	ethidium bromide
EtOH	ethanol
FBS	fetal bovine serum
FCS	fetal calf serum
fig.	figure
g	gram
G418	Geneticin
GAD	glutamic acid decarboxylase
GFAP	Glial fibrillary acidic protein
h	hours
HEPES	4-(2-hydroxyethyl)-1-piperazineethanesulfonic acid
HRP	horse radish peroxidise
HS	horse serum
IgG	immunoglobulin G
IHC	Inner hair cell
i.p.	intraperitoneal
k	kilo
KAc	potassium acetate
Kan	kanamycin
kb	kilo base pairs
l	liters
lacZ	gene for the ß-galactosidase of E.coli
LB	Luria broth
LIF	Leukemia inhibitory factor
loxP	locus of crossing over for phage P
LTP	long term potentiation
m	Meter(s)
m	milli
M	molar (mol/l)
min	Minute(s)
mRNA	messenger RNA
N-terminal	Amino-terminal of a protein
n	nano
NaAc	sodium acetate
neo	Neomycin resistance gene
NMDA	N-methyl-D-aspartate
NPC	Neural stem/precursor cell

nt	nucleotides
NTP	nucleoside triphosphate
OD	optical density
OHC	Outer hair cell
ori	origin of replication
P	promoter
p	plasmid
pA	polyadenylation signal
PFA	paraformaldehyde
PBS	phosphate buffered saline
PCR	polymerase chain reaction
pH	negative base-10 logarithm of H^+-ion concentration
PKA	Protein kinase A
r	resistant
RNA	ribonucleic acid
RNase	ribonuclease
rpm	Rounds per minute
RT	room temperature
SA	splice acceptor
SAP	shrimp alkaline phosphatase
sec	Second(s)
Sox2	Sry-related HMG box 2
ssDNA	single stranded DNA
SV40	simian virus 40
TAE	Tris-acetate-EDTA
Taq	thermos aquaticus
TBE	Tris-borate-EDTA
TE	Tris-EDTA
Tm	melting point
TPH1	tryptophane hydroxylase 1
Tris	tris-hydroxymethylaminomethane
U	Enzyme activity
UTR	untranslated region
V	Volt
VGCC	Voltage-gated calcium channel
WT	wildtype

7 References

Abremski, K., Hoess, R., and Sternberg, N. (1983). Studies on the properties of P1 site-specific recombination: evidence for topologically unlinked products following recombination. Cell *32*, 1301-1311.

Atasoy, D., Aponte, Y., Su, H.H., and Sternson, S.M. (2008). A FLEX switch targets Channelrhodopsin-2 to multiple cell types for imaging and long-range circuit mapping. J Neurosci *28*, 7025-7030.

Barg, S., Ma, X., Eliasson, L., Galvanovskis, J., Gopel, S.O., Obermuller, S., Platzer, J., Renstrom, E., Trus, M., Atlas, D., *et al.* (2001). Fast exocytosis with few Ca(2+) channels in insulin-secreting mouse pancreatic B cells. Biophys J *81*, 3308-3323.

Bauer, E.P., Schafe, G.E., and LeDoux, J.E. (2002). NMDA receptors and L-type voltage-gated calcium channels contribute to long-term potentiation and different components of fear memory formation in the lateral amygdala. J Neurosci *22*, 5239-5249.

Berjukow, S., Marksteiner, R., Gapp, F., Sinnegger, M.J., and Hering, S. (2000). Molecular mechanism of calcium channel block by isradipine. Role of a drug-induced inactivated channel conformation. J Biol Chem *275*, 22114-22120.

Bezanilla, F. (2002). Voltage sensor movements. J Gen Physiol *120*, 465-473.
Birnbaumer, L., Campbell, K.P., Catterall, W.A., Harpold, M.M., Hofmann, F., Horne, W.A., Mori, Y., Schwartz, A., Snutch, T.P., Tanabe, T., *et al.* (1994). The naming of voltage-gated calcium channels. Neuron *13*, 505-506.

Bito, H., Deisseroth, K., and Tsien, R.W. (1996). CREB phosphorylation and dephosphorylation: a Ca(2+)- and stimulus duration-dependent switch for hippocampal gene expression. Cell *87*, 1203-1214.

Blendy, J.A. (2006). The role of CREB in depression and antidepressant treatment. Biol Psychiatry *59*, 1144-1150.

Boniface, E.J., Lu, J., Victoroff, T., Zhu, M., and Chen, W. (2009). FlEx-based transgenic reporter lines for visualization of Cre and Flp activity in live zebrafish. Genesis.

Bootman, M.D., Berridge, M.J., and Roderick, H.L. (2002). Calcium signalling: more messengers, more channels, more complexity. Curr Biol *12*, R563-565.

Bootman, M.D., Collins, T.J., Peppiatt, C.M., Prothero, L.S., MacKenzie, L., De Smet, P., Travers, M., Tovey, S.C., Seo, J.T., Berridge, M.J., *et al.* (2001a). Calcium signalling--an overview. Semin Cell Dev Biol *12*, 3-10.

Bootman, M.D., Lipp, P., and Berridge, M.J. (2001b). The organisation and functions of local Ca(2+) signals. J Cell Sci *114*, 2213-2222.

Branda, C.S., and Dymecki, S.M. (2004). Talking about a revolution: The impact of site-specific recombinases on genetic analyses in mice. Dev Cell *6*, 7-28.

Brandt, A., Striessnig, J., and Moser, T. (2003). CaV1.3 channels are essential for development and presynaptic activity of cochlear inner hair cells. J Neurosci *23*, 10832-10840.

Calin-Jageman, I., Yu, K., Hall, R.A., Mei, L., and Lee, A. (2007). Erbin enhances voltage-dependent facilitation of Ca(v)1.3 Ca2+ channels through relief of an autoinhibitory domain in the Ca(v)1.3 alpha1 subunit. J Neurosci *27*, 1374-1385.

Capecchi, M.R. (1989). Altering the genome by homologous recombination. Science *244*, 1288-1292.

Carafoli, E., and Penniston, J.T. (1985). The calcium signal. Sci Am *253*, 70-78.

Cardenas, M.E., and Heitman, J. (1995). Role of calcium in T-lymphocyte activation. Adv Second Messenger Phosphoprotein Res *30*, 281-298.

Catterall, W.A. (2000). Structure and regulation of voltage-gated Ca2+ channels. Annu Rev Cell Dev Biol *16*, 521-555.

Catterall, W.A., Perez-Reyes, E., Snutch, T.P., and Striessnig, J. (2005). International Union of Pharmacology. XLVIII. Nomenclature and structure-function relationships of voltage-gated calcium channels. Pharmacol Rev *57*, 411-425.

Chan, C.S., Guzman, J.N., Ilijic, E., Mercer, J.N., Rick, C., Tkatch, T., Meredith, G.E., and Surmeier, D.J. (2007). 'Rejuvenation' protects neurons in mouse models of Parkinson's disease. Nature *447*, 1081-1086.

Chin, H.M., Kozak, C.A., Kim, H.L., Mock, B., and McBride, O.W. (1991). A brain L-type calcium channel alpha 1 subunit gene (CCHL1A2) maps to mouse chromosome 14 and human chromosome 3. Genomics *11*, 914-919.

Chrivia, J.C., Kwok, R.P., Lamb, N., Hagiwara, M., Montminy, M.R., and Goodman, R.H. (1993). Phosphorylated CREB binds specifically to the nuclear protein CBP. Nature *365*, 855-859.

Clark, N.C., Nagano, N., Kuenzi, F.M., Jarolimek, W., Huber, I., Walter, D., Wietzorrek, G., Boyce, S., Kullmann, D.M., Striessnig, J., *et al.* (2003). Neurological phenotype and synaptic function in mice lacking the CaV1.3 alpha subunit of neuronal L-type voltage-dependent Ca2+ channels. Neuroscience *120*, 435-442.

Copeland, N.G., Jenkins, N.A., and Court, D.L. (2001). Recombineering: a powerful new tool for mouse functional genomics. Nat Rev Genet *2*, 769-779.

Cork, R.J., Namkung, Y., Shin, H.S., and Mize, R.R. (2001). Development of the visual pathway is disrupted in mice with a targeted disruption of the calcium channel beta(3)-subunit gene. J Comp Neurol *440*, 177-191.

Curtis, B.M., and Catterall, W.A. (1984). Purification of the calcium antagonist receptor of the voltage-sensitive calcium channel from skeletal muscle transverse tubules. Biochemistry *23*, 2113-2118.

D'Ascenzo, M., Piacentini, R., Casalbore, P., Budoni, M., Pallini, R., Azzena, G.B., and Grassi, C. (2006). Role of L-type Ca2+ channels in neural stem/progenitor cell differentiation. Eur J Neurosci *23*, 935-944.

Davila, N.G., Blakemore, L.J., and Trombley, P.Q. (2003). Dopamine modulates synaptic transmission between rat olfactory bulb neurons in culture. J Neurophysiol *90*, 395-404.

Deisseroth, K., Bito, H., and Tsien, R.W. (1996). Signaling from synapse to nucleus: postsynaptic CREB phosphorylation during multiple forms of hippocampal synaptic plasticity. Neuron *16*, 89-101.

Deisseroth, K., Mermelstein, P.G., Xia, H., and Tsien, R.W. (2003). Signaling from synapse to nucleus: the logic behind the mechanisms. Curr Opin Neurobiol *13*, 354-365.

Deisseroth, K., Singla, S., Toda, H., Monje, M., Palmer, T.D., and Malenka, R.C. (2004). Excitation-neurogenesis coupling in adult neural stem/progenitor cells. Neuron *42*, 535-552.

Del Cerro, M.C., Izquierdo, M.A., Collado, P., Segovia, S., and Guillamon, A. (1991). Bilateral lesions of the bed nucleus of the accessory olfactory tract facilitate maternal behavior in virgin female rats. Physiol Behav *50*, 67-71.

Doetsch, F., Caille, I., Lim, D.A., Garcia-Verdugo, J.M., and Alvarez-Buylla, A. (1999a). Subventricular zone astrocytes are neural stem cells in the adult mammalian brain. Cell *97*, 703-716.

Doetsch, F., Garcia-Verdugo, J.M., and Alvarez-Buylla, A. (1999b). Regeneration of a germinal layer in the adult mammalian brain. Proc Natl Acad Sci U S A *96*, 11619-11624.

Dolmetsch, R.E., Pajvani, U., Fife, K., Spotts, J.M., and Greenberg, M.E. (2001). Signaling to the nucleus by an L-type calcium channel-calmodulin complex through the MAP kinase pathway. Science *294*, 333-339.

Dunlap, K., Luebke, J.I., and Turner, T.J. (1995). Exocytotic Ca2+ channels in mammalian central neurons. Trends Neurosci *18*, 89-98.

Eisenberg, E., and Hill, T.L. (1985). Muscle contraction and free energy transduction in biological systems. Science *227*, 999-1006.

Episkopou, V. (2005). SOX2 functions in adult neural stem cells. Trends Neurosci *28*, 219-221.

Ertel, E.A., Campbell, K.P., Harpold, M.M., Hofmann, F., Mori, Y., Perez-Reyes, E., Schwartz, A., Snutch, T.P., Tanabe, T., Birnbaumer, L., *et al.* (2000). Nomenclature of voltage-gated calcium channels. Neuron *25*, 533-535.

Evans, M.J., and Kaufman, M.H. (1981). Establishment in culture of pluripotential cells from mouse embryos. Nature *292*, 154-156.

Fabiato, A. (1983). Calcium-induced release of calcium from the cardiac sarcoplasmic reticulum. Am J Physiol *245*, C1-14.

Ferri, A.L., Cavallaro, M., Braida, D., Di Cristofano, A., Canta, A., Vezzani, A., Ottolenghi, S., Pandolfi, P.P., Sala, M., DeBiasi, S., *et al.* (2004). Sox2 deficiency causes neurodegeneration and impaired neurogenesis in the adult mouse brain. Development *131*, 3805-3819.

Geiger, J.R., Melcher, T., Koh, D.S., Sakmann, B., Seeburg, P.H., Jonas, P., and Monyer, H. (1995). Relative abundance of subunit mRNAs determines gating and Ca2+ permeability of AMPA receptors in principal neurons and interneurons in rat CNS. Neuron *15*, 193-204.

Ghashghaei, H.T., Lai, C., and Anton, E.S. (2007). Neuronal migration in the adult brain: are we there yet? Nat Rev Neurosci *8*, 141-151.

Ghosh, A., Ginty, D.D., Bading, H., and Greenberg, M.E. (1994). Calcium regulation of gene expression in neuronal cells. J Neurobiol *25*, 294-303.

Green, G.E., Khan, K.M., Beisel, D.W., Drescher, M.J., Hatfield, J.S., and Drescher, D.G. (1996). Calcium channel subunits in the mouse cochlea. J Neurochem *67*, 37-45.

Gurnett, C.A., Felix, R., and Campbell, K.P. (1997). Extracellular interaction of the voltage-dependent Ca2+ channel alpha2delta and alpha1 subunits. J Biol Chem *272*, 18508-18512.

Hardingham, G.E., Arnold, F.J., and Bading, H. (2001). Nuclear calcium signaling controls CREB-mediated gene expression triggered by synaptic activity. Nat Neurosci *4*, 261-267.

Hardingham, G.E., and Bading, H. (1998). Nuclear calcium: a key regulator of gene expression. Biometals *11*, 345-358.

Hardingham, G.E., Chawla, S., Cruzalegui, F.H., and Bading, H. (1999). Control of recruitment and transcription-activating function of CBP determines gene regulation by NMDA receptors and L-type calcium channels. Neuron *22*, 789-798.

Hardingham, G.E., Cruzalegui, F.H., Chawla, S., and Bading, H. (1998). Mechanisms controlling gene expression by nuclear calcium signals. Cell Calcium *23*, 131-134.

Hardingham, G.E., Fukunaga, Y., and Bading, H. (2002). Extrasynaptic NMDARs oppose synaptic NMDARs by triggering CREB shut-off and cell death pathways. Nat Neurosci *5*, 405-414.

Heilbrunn, L.V., and Wiercinski, F.J. (1947). The action of various cations on muscle protoplasm. J Cell Comp Physiol *29*, 15-32.

Hell, J.W., Westenbroek, R.E., Warner, C., Ahlijanian, M.K., Prystay, W., Gilbert, M.M., Snutch, T.P., and Catterall, W.A. (1993). Identification and differential subcellular localization of the neuronal class C and class D L-type calcium channel alpha 1 subunits. J Cell Biol *123*, 949-962.

Hetzenauer, A., Sinnegger-Brauns, M.J., Striessnig, J., and Singewald, N. (2006). Brain activation pattern induced by stimulation of L-type Ca2+-channels: contribution of Ca(V)1.3 and Ca(V)1.2 isoforms. Neuroscience *139*, 1005-1015.

Hockerman, G.H., Peterson, B.Z., Johnson, B.D., and Catterall, W.A. (1997). Molecular determinants of drug binding and action on L-type calcium channels. Annu Rev Pharmacol Toxicol *37*, 361-396.

Hoess, R., Wierzbicki, A., and Abremski, K. (1985). Formation of small circular DNA molecules via an in vitro site-specific recombination system. Gene *40*, 325-329.

Hofmann, F., Biel, M., and Flockerzi, V. (1994). Molecular basis for Ca2+ channel diversity. Annu Rev Neurosci *17*, 399-418.

Iwashima, Y., Pugh, W., Depaoli, A.M., Takeda, J., Seino, S., Bell, G.I., and Polonsky, K.S. (1993). Expression of calcium channel mRNAs in rat pancreatic islets and downregulation after glucose infusion. Diabetes *42*, 948-955.

Johansson, C.B., Momma, S., Clarke, D.L., Risling, M., Lendahl, U., and Frisen, J. (1999). Identification of a neural stem cell in the adult mammalian central nervous system. Cell *96*, 25-34.

Joyner, A.L., ed. (1993). Gene targeting- A Practical Approach (New York: Oxford University Press).

Kandel, E.R. (2001). The molecular biology of memory storage: a dialogue between genes and synapses. Science *294*, 1030-1038.

Kim, M.J., Chung, Y.H., Joo, K.M., Oh, G.T., Kim, J., Lee, B., and Cha, C.I. (2004). Immunohistochemical study of the distribution of neuronal voltage-gated calcium channels in the nNOS knock-out mouse cerebellum. Neurosci Lett *369*, 39-43.

Kim, S., Yun, H.M., Baik, J.H., Chung, K.C., Nah, S.Y., and Rhim, H. (2007). Functional interaction of neuronal Cav1.3 L-type calcium channel with ryanodine receptor type 2 in the rat hippocampus. J Biol Chem *282*, 32877-32889.

Klugbauer, N., Welling, A., Specht, V., Seisenberger, C., and Hofmann, F. (2002). L-type Ca2+ channels of the embryonic mouse heart. Eur J Pharmacol *447*, 279-284.

Kollmar, R., Fak, J., Montgomery, L.G., and Hudspeth, A.J. (1997). Hair cell-specific splicing of mRNA for the alpha1D subunit of voltage-gated Ca2+ channels in the chicken's cochlea. Proc Natl Acad Sci U S A *94*, 14889-14893.

Koschak, A., Reimer, D., Huber, I., Grabner, M., Glossmann, H., Engel, J., and Striessnig, J. (2001). alpha 1D (Cav1.3) subunits can form l-type Ca2+ channels activating at negative voltages. J Biol Chem *276*, 22100-22106.

Kurschner, C., Mermelstein, P.G., Holden, W.T., and Surmeier, D.J. (1998). CIPP, a novel multivalent PDZ domain protein, selectively interacts with Kir4.0 family members, NMDA receptor subunits, neurexins, and neuroligins. Mol Cell Neurosci *11*, 161-172.

Kurschner, C., and Yuzaki, M. (1999). Neuronal interleukin-16 (NIL-16): a dual function PDZ domain protein. J Neurosci *19*, 7770-7780.

Lee, E.C., Yu, D., Martinez de Velasco, J., Tessarollo, L., Swing, D.A., Court, D.L., Jenkins, N.A., and Copeland, N.G. (2001). A highly efficient Escherichia coli-based chromosome engineering system adapted for recombinogenic targeting and subcloning of BAC DNA. Genomics *73*, 56-65.

Lee, G., and Saito, I. (1998). Role of nucleotide sequences of loxP spacer region in Cre-mediated recombination. Gene *216*, 55-65.

Lipscombe, D., Helton, T.D., and Xu, W. (2004). L-type calcium channels: the low down. J Neurophysiol *92*, 2633-2641.

Lipscombe, D., Pan, J.Q., and Gray, A.C. (2002). Functional diversity in neuronal voltage-gated calcium channels by alternative splicing of Ca(v)alpha1. Mol Neurobiol *26*, 21-44.
Liu, P., Jenkins, N.A., and Copeland, N.G. (2003). A highly efficient recombineering-based method for generating conditional knockout mutations. Genome Res *13*, 476-484.

Llinas, R.R., Sugimori, M., and Cherksey, B. (1989). Voltage-dependent calcium conductances in mammalian neurons. The P channel. Ann N Y Acad Sci *560*, 103-111.

Lo, F.S., and Mize, R.R. (2000). Synaptic regulation of L-type Ca(2+) channel activity and long-term depression during refinement of the retinocollicular pathway in developing rodent superior colliculus. J Neurosci *20*, RC58.

Lo, F.S., and Mize, R.R. (2002). Properties of LTD and LTP of retinocollicular synaptic transmission in the developing rat superior colliculus. Eur J Neurosci *15*, 1421-1432.

Luo, C.X., Zhu, X.J., Zhang, A.X., Wang, W., Yang, X.M., Liu, S.H., Han, X., Sun, J., Zhang, S.G., Lu, Y., *et al.* (2005). Blockade of L-type voltage-gated Ca channel inhibits ischemia-induced neurogenesis by down-regulating iNOS expression in adult mouse. J Neurochem *94*, 1077-1086.

Mangoni, M.E., Couette, B., Bourinet, E., Platzer, J., Reimer, D., Striessnig, J., and Nargeot, J. (2003). Functional role of L-type Cav1.3 Ca2+ channels in cardiac pacemaker activity. Proc Natl Acad Sci U S A *100*, 5543-5548.

Manji, H.K., Drevets, W.C., and Charney, D.S. (2001). The cellular neurobiology of depression. Nat Med *7*, 541-547.

Martin, G.R. (1981). Isolation of a pluripotent cell line from early mouse embryos cultured in medium conditioned by teratocarcinoma stem cells. Proc Natl Acad Sci U S A *78*, 7634-7638.

McKinney, B.C., and Murphy, G.G. (2006). The L-Type voltage-gated calcium channel Cav1.3 mediates consolidation, but not extinction, of contextually conditioned fear in mice. Learn Mem *13*, 584-589.

Metzger, D., and Chambon, P. (2001). Site- and time-specific gene targeting in the mouse. Methods *24*, 71-80.

Michna, M., Knirsch, M., Hoda, J.C., Muenkner, S., Langer, P., Platzer, J., Striessnig, J., and Engel, J. (2003). Cav1.3 (alpha1D) Ca2+ currents in neonatal outer hair cells of mice. J Physiol *553*, 747-758.

Millan, M.J. (2003). The neurobiology and control of anxious states. Prog Neurobiol *70*, 83-244.

Miller, R.J. (1992). Voltage-sensitive Ca2+ channels. J Biol Chem *267*, 1403-1406.

Mize, R.R., Graham, S.K., and Cork, R.J. (2002). Expression of the L-type calcium channel in the developing mouse visual system by use of immunocytochemistry. Brain Res Dev Brain Res *136*, 185-195.

Moosmang, S., Haider, N., Klugbauer, N., Adelsberger, H., Langwieser, N., Muller, J., Stiess, M., Marais, E., Schulla, V., Lacinova, L., *et al.* (2005). Role of hippocampal Cav1.2 Ca2+ channels in NMDA receptor-independent synaptic plasticity and spatial memory. J Neurosci *25*, 9883-9892.

Mullen, R.J., Buck, C.R., and Smith, A.M. (1992). NeuN, a neuronal specific nuclear protein in vertebrates. Development *116*, 201-211.

Nagy, A., Rossant, J., Nagy, R., Abramow-Newerly, W., and Roder, J.C. (1993). Derivation of completely cell culture-derived mice from early-passage embryonic stem cells. Proc Natl Acad Sci U S A *90*, 8424-8428.

Namkung, Y., Skrypnyk, N., Jeong, M.J., Lee, T., Lee, M.S., Kim, H.L., Chin, H., Suh, P.G., Kim, S.S., and Shin, H.S. (2001). Requirement for the L-type Ca(2+) channel alpha(1D) subunit in postnatal pancreatic beta cell generation. J Clin Invest *108*, 1015-1022.

Neely, A., Wei, X., Olcese, R., Birnbaumer, L., and Stefani, E. (1993). Potentiation by the beta subunit of the ratio of the ionic current to the charge movement in the cardiac calcium channel. Science *262*, 575-578.

Nguyen, N.K., Striessnig, J., and Singewald, N. (2005). Role of CaV1.3 Calcium-Channels for Anxiety and Depression-like Behavior in Mice. Paper presented at: Neuroscience (Washington, DC).

Nowycky, M.C., Fox, A.P., and Tsien, R.W. (1985). Three types of neuronal calcium channel with different calcium agonist sensitivity. Nature *316*, 440-443.

O'Gorman, S., Fox, D.T., and Wahl, G.M. (1991). Recombinase-mediated gene activation and site-specific integration in mammalian cells. Science *251*, 1351-1355.

Olson, P.A., Tkatch, T., Hernandez-Lopez, S., Ulrich, S., Ilijic, E., Mugnaini, E., Zhang, H., Bezprozvanny, I., and Surmeier, D.J. (2005). G-protein-coupled receptor modulation of striatal CaV1.3 L-type Ca2+ channels is dependent on a Shank-binding domain. J Neurosci *25*, 1050-1062.

Pham, C.T., MacIvor, D.M., Hug, B.A., Heusel, J.W., and Ley, T.J. (1996). Long-range disruption of gene expression by a selectable marker cassette. Proc Natl Acad Sci U S A *93*, 13090-13095.

Piacentini, R., Ripoli, C., Mezzogori, D., Azzena, G.B., and Grassi, C. (2008). Extremely low-frequency electromagnetic fields promote in vitro neurogenesis via upregulation of Ca(v)1-channel activity. J Cell Physiol *215*, 129-139.

Platzer, J., Engel, J., Schrott-Fischer, A., Stephan, K., Bova, S., Chen, H., Zheng, H., and Striessnig, J. (2000). Congenital deafness and sinoatrial node dysfunction in mice lacking class D L-type Ca2+ channels. Cell *102*, 89-97.

Rajewsky, K., Gu, H., Kuhn, R., Betz, U.A., Muller, W., Roes, J., and Schwenk, F. (1996). Conditional gene targeting. J Clin Invest *98*, 600-603.

Ramakrishnan, N.A., Drescher, M.J., and Drescher, D.G. (2009). Direct interaction of otoferlin with syntaxin 1A, SNAP-25, and the L-type voltage-gated calcium channel Cav1.3. J Biol Chem *284*, 1364-1372.

Ramirez-Solis, R., Liu, P., and Bradley, A. (1995). Chromosome engineering in mice. Nature *378*, 720-724.

Randall, A., and Tsien, R.W. (1995). Pharmacological dissection of multiple types of Ca2+ channel currents in rat cerebellar granule neurons. J Neurosci *15*, 2995-3012.

Ren, S.Y., Angrand, P.O., and Rijli, F.M. (2002). Targeted insertion results in a rhombomere 2-specific Hoxa2 knockdown and ectopic activation of Hoxa1 expression. Dev Dyn *225*, 305-315.

Reuter, H. (1967). The dependence of slow inward current in Purkinje fibres on the extracellular calcium-concentration. J Physiol *192*, 479-492.

Reuter, H. (1983). Calcium channel modulation by neurotransmitters, enzymes and drugs. Nature *301*, 569-574.

Ringer, S. (1883). A further Contribution regarding the influence of the different Constituents of the Blood on the Contraction of the Heart. J Physiol *4*, 29-42 23.

Ringer, S. (1890). Concerning Experiments to test the Influence of Lime, Sodium and Potassium Salts on the Development of Ova and Growth of Tadpoles. J Physiol *11*, 79-84.

Safa, P., Boulter, J., and Hales, T.G. (2001). Functional properties of Cav1.3 (alpha1D) L-type Ca2+ channel splice variants expressed by rat brain and neuroendocrine GH3 cells. J Biol Chem *276*, 38727-38737.

Sandow, A. (1965). Excitation-contraction coupling in skeletal muscle. Pharmacol Rev *17*, 265-320.

Sartorius, A., and Henn, F.A. (2007). Deep brain stimulation of the lateral habenula in treatment resistant major depression. Med Hypotheses *69*, 1305-1308.

Sauer, B., and Henderson, N. (1989). Cre-stimulated recombination at loxP-containing DNA sequences placed into the mammalian genome. Nucleic Acids Res *17*, 147-161.

Schnutgen, F., De-Zolt, S., Van Sloun, P., Hollatz, M., Floss, T., Hansen, J., Altschmied, J., Seisenberger, C., Ghyselinck, N.B., Ruiz, P., *et al.* (2005). Genomewide production of multipurpose alleles for the functional analysis of the mouse genome. Proc Natl Acad Sci U S A *102*, 7221-7226.

Schnutgen, F., Doerflinger, N., Calleja, C., Wendling, O., Chambon, P., and Ghyselinck, N.B. (2003). A directional strategy for monitoring Cre-mediated recombination at the cellular level in the mouse. Nat Biotechnol *21*, 562-565.

Schulla, V., Renstrom, E., Feil, R., Feil, S., Franklin, I., Gjinovci, A., Jing, X.J., Laux, D., Lundquist, I., Magnuson, M.A., *et al.* (2003). Impaired insulin secretion and glucose tolerance in beta cell-selective Ca(v)1.2 Ca2+ channel null mice. EMBO J *22*, 3844-3854.

Schwartzman, R.A., and Cidlowski, J.A. (1993). Apoptosis: the biochemistry and molecular biology of programmed cell death. Endocr Rev *14*, 133-151.

Seino, S., Yamada, Y., Espinosa, R., 3rd, Le Beau, M.M., and Bell, G.I. (1992). Assignment of the gene encoding the alpha 1 subunit of the neuroendocrine/brain-type calcium channel (CACNL1A2) to human chromosome 3, band p14.3. Genomics *13*, 1375-1377.

Shechter, R., Ziv, Y., and Schwartz, M. (2007). New GABAergic interneurons supported by myelin-specific T cells are formed in intact adult spinal cord. Stem Cells *25*, 2277-2282.

Shen, S.S. (1995). Mechanisms of calcium regulation in sea urchin eggs and their activities during fertilization. Curr Top Dev Biol *30*, 63-101.

Siegel, G., Agranoff, B., Albers, R., Fisher, S., and Uhler, M., eds. (1999). Basic Neurochemistry: Molecular, Cellular, and Medical Aspects (Lippincott, Williams & Wilkins).

Siegel, R.W., Jain, R., and Bradbury, A. (2001). Using an in vivo phagemid system to identify non-compatible loxP sequences. FEBS Lett *505*, 467-473.

Sinnegger-Brauns, M.J., Hetzenauer, A., Huber, I.G., Renstrom, E., Wietzorrek, G., Berjukov, S., Cavalli, M., Walter, D., Koschak, A., Waldschutz, R., *et al.* (2004). Isoform-specific regulation of mood behavior and pancreatic beta cell and cardiovascular function by L-type Ca 2+ channels. J Clin Invest *113*, 1430-1439.

Striessnig, J. (1999). Pharmacology, structure and function of cardiac L-type Ca(2+) channels. Cell Physiol Biochem *9*, 242-269.

Striessnig, J., Koschak, A., Sinnegger-Brauns, M.J., Hetzenauer, A., Nguyen, N.K., Busquet, P., Pelster, G., and Singewald, N. (2006). Role of voltage-gated L-type Ca2+ channel isoforms for brain function. Biochem Soc Trans *34*, 903-909.

Sukiasyan, N., Hultborn, H., and Zhang, M. (2009). Distribution of calcium channel Ca(V)1.3 immunoreactivity in the rat spinal cord and brain stem. Neuroscience *159*, 217-235.

Takimoto, K., Li, D., Nerbonne, J.M., and Levitan, E.S. (1997). Distribution, splicing and glucocorticoid-induced expression of cardiac alpha 1C and alpha 1D voltage-gated Ca2+ channel mRNAs. J Mol Cell Cardiol *29*, 3035-3042.

Tanaka, O., Sakagami, H., and Kondo, H. (1995). Localization of mRNAs of voltage-dependent Ca(2+)-channels: four subtypes of alpha 1- and beta-subunits in developing and mature rat brain. Brain Res Mol Brain Res *30*, 1-16.

Taupin, P., and Gage, F.H. (2002). Adult neurogenesis and neural stem cells of the central nervous system in mammals. J Neurosci Res *69*, 745-749.

Tsien, J.Z., Chen, D.F., Gerber, D., Tom, C., Mercer, E.H., Anderson, D.J., Mayford, M., Kandel, E.R., and Tonegawa, S. (1996). Subregion- and cell type-restricted gene knockout in mouse brain. Cell *87*, 1317-1326.

Veng, L.M., Mesches, M.H., and Browning, M.D. (2003). Age-related working memory impairment is correlated with increases in the L-type calcium channel protein alpha1D (Cav1.3) in area CA1 of the hippocampus and both are ameliorated by chronic nimodipine treatment. Brain Res Mol Brain Res *110*, 193-202.

Vinet, J., and Sik, A. (2006). Expression pattern of voltage-dependent calcium channel subunits in hippocampal inhibitory neurons in mice. Neuroscience *143*, 189-212.

Wang, D.D., Krueger, D.D., and Bordey, A. (2003). Biophysical properties and ionic signature of neuronal progenitors of the postnatal subventricular zone in situ. J Neurophysiol *90*, 2291-2302.

Wang, X., McKenzie, J.S., and Kemm, R.E. (1996). Whole cell calcium currents in acutely isolated olfactory bulb output neurons of the rat. J Neurophysiol *75*, 1138-1151.

Weick, J.P., Groth, R.D., Isaksen, A.L., and Mermelstein, P.G. (2003). Interactions with PDZ proteins are required for L-type calcium channels to activate cAMP response element-binding protein-dependent gene expression. J Neurosci *23*, 3446-3456.

Williams-Simons, L., and Westphal, H. (1999). EIIaCre -- utility of a general deleter strain. Transgenic Res *8*, 53-54.

Wong, E.T., Kolman, J.L., Li, Y.C., Mesner, L.D., Hillen, W., Berens, C., and Wahl, G.M. (2005). Reproducible doxycycline-inducible transgene expression at specific loci generated by Cre-recombinase mediated cassette exchange. Nucleic Acids Res *33*, e147.

Xu, W., and Lipscombe, D. (2001). Neuronal Ca(V)1.3alpha(1) L-type channels activate at relatively hyperpolarized membrane potentials and are incompletely inhibited by dihydropyridines. J Neurosci *21*, 5944-5951.

Yang, J., Ellinor, P.T., Sather, W.A., Zhang, J.F., and Tsien, R.W. (1993). Molecular determinants of Ca2+ selectivity and ion permeation in L-type Ca2+ channels. Nature *366*, 158-161.

Yang, S.N., Larsson, O., Branstrom, R., Bertorello, A.M., Leibiger, B., Leibiger, I.B., Moede, T., Kohler, M., Meister, B., and Berggren, P.O. (1999). Syntaxin 1 interacts with the L(D) subtype of voltage-gated Ca(2+) channels in pancreatic beta cells. Proc Natl Acad Sci U S A *96*, 10164-10169.

Yu, F.H., and Catterall, W.A. (2004). The VGL-chanome: a protein superfamily specialized for electrical signaling and ionic homeostasis. Sci STKE *2004*, re15.

Yuan, Q., Mutoh, H., Debarbieux, F., and Knopfel, T. (2004). Calcium signaling in mitral cell dendrites of olfactory bulbs of neonatal rats and mice during olfactory nerve Stimulation and beta-adrenoceptor activation. Learn Mem *11*, 406-411.

Zhang, H., Fu, Y., Altier, C., Platzer, J., Surmeier, D.J., and Bezprozvanny, I. (2006). Ca1.2 and CaV1.3 neuronal L-type calcium channels: differential targeting and signaling to pCREB. Eur J Neurosci *23*, 2297-2310.

Zhang, H., Maximov, A., Fu, Y., Xu, F., Tang, T.S., Tkatch, T., Surmeier, D.J., and Bezprozvanny, I. (2005a). Association of CaV1.3 L-type calcium channels with Shank. J Neurosci *25*, 1037-1049.

Zhang, Z., He, Y., Tuteja, D., Xu, D., Timofeyev, V., Zhang, Q., Glatter, K.A., Xu, Y., Shin, H.S., Low, R., *et al.* (2005b). Functional roles of Cav1.3(alpha1D) calcium channels in atria: insights gained from gene-targeted null mutant mice. Circulation *112*, 1936-1944.

Zhao, J.P., Phillips, M.A., and Constantine-Paton, M. (2006). Long-term potentiation in the juvenile superior colliculus requires simultaneous activation of NMDA receptors and L-type Ca2+ channels and reflects addition of newly functional synapses. J Neurosci *26*, 12647-12655.

Zhao, R., Liu, L., and Rittenhouse, A.R. (2007). Ca2+ influx through both L- and N-type Ca2+ channels increases c-fos expression by electrical stimulation of sympathetic neurons. Eur J Neurosci *25*, 1127-1135.